Aus dem UniversitätsCentrum für Orthopädie und Unfallchirurgie
Ärzticher Direktor: Prof. Dr. med. Hans Zwipp
Geschäftsführender Direktor: Prof. Dr. med. Klaus-Peter Günther

Monitoring the first stages of the regeneration of bone defects

Dissertationsschrift

zur Erlangung des akademischen Grades
Doctor of Philosophy (Ph.D.)
der Medizinischen Fakultät Carl Gustav Carus der
Technischen Universität Dresden
vorgelegt

von

Wenling Gao

aus Wuhan, China

Dresden, 2013

1. Gutachter:

2. Gutachter:

Tag der mündlichen Prüfung: (Verteidigungstermin)

gez.: ----------
Vorsitzender der Promotionskommission

I. Table of content

II. List of abbreviations

BMP	Bone morphogenetic protein
BM-MSCs	Bone marrow derived mesenchymal stem cells
BSA	Bovine serum albumin
C3	Complement component C3
$CaCl_2$	Calcium chloride
CAM	Cell adhesion molecule
CCL	(C-C motif) ligand
CRP	C-reactive protein
CX3CL	(C-XXX-C motif) ligand
CXCL	(C-X-C motif) ligand
ECM	Extracellular matrix
EDTA	Ethylenediaminetetraacetic acid disodium salt
EE	Extraction efficiency
ELISA	Enzyme-linked immunosorbent assay
Eq	Equation
FGF	Fibroblast growth factor
FX	Coagulation factors X
H&E	Hematoxylin and Eosin
HCl	Hydrochloric acid
HEPES	4-(2-Hydroxyethyl)-1-piperazineethanesulfonic acid
HPLC	High-performance liquid chromatography
ID	Identifier
IGF	Insulin-like growth factor-1
IL	Interleukin
IL-1R2	Interleukin-1 receptor type II
IL-1ra	Interleukin-1 receptor antagonist
IPI	International Protein Index
KCl	Potassium chloride
KH_2PO_4	Potassium dihydrogen phosphate
M-CSF	Macrophage colony-stimulating factor
MIF	Macrophage migration inhibitory factor
MMP	Matrix metalloproteinase

mRNA	Messenger ribonucleic acid
MS	Mass spectrometry
MSCs	Mesenchymal stem cells
MW	Molecular weight
MWCO	Molecular weight cut-off
Na_2HPO_4	Disodium hydrogen phosphate
NaCl	Sodium chloride
NaOH	Sodium hydroxide
NOS	Nitric oxide synthase
OPN	Osteopontin
Panther	Protein Analysis Through Evolutionary Relationships
PBS	Phosphate buffered saline
PD	Pixel density
PDGF	Platelet-derived growth factor
PEEK	Polyether ether ketone
PER	Perfusion fluid
pI	Isoelectric point
PMNs	Polymorphonuclear leukocytes
PTH	Parathyroid hormone
RoBo-1	Rodent bone protein
ROS	Reactive oxygen species
RR	Relative recovery
SD	Standard deviation
SDS-PAGE	Sodium dodecyl sulfate-polyacrylamide gel electrophoresis
TGF	Transforming growth factor
TNF	Tumor necrosis factor
UVB	Ultraviolet B
VEGF	Vascular endothelial growth factor
XCL	(C motif) ligand

Terminology of microdialysis

C_d	Concentration of analyte in microdialysate
C_e	Concentration of analyte in external fluid
C_i	Concentration of analyte in perfusate
D	Diffusion coefficient
L	Membrane's length
Q_d	Flow rate of the perfusate
R_d	Resistance to the microdialysate
R_e	Resistance to the external fluid
R_m	Resistance to the membrane
r_o	Radius of membrane surface
r_α	Radius of inner cannula,
r_β	Radius of inner side of membrane
$V_{microdialysate}$	Volume of collected microdialysate
V_{theory}.	Theoretical volume of microdialysate

1 Summary

The different strategies of tissue engineering for functional reconstruction of critical-size bone defects require a thorough knowledge of physiological mechanisms of bone repair. Bone healing is a complex process affected by various mediators. Several investigations have studied the gene expression 1 to 3 days after an acute or experimental fracture. Little is known about the humoral and cellular *in vivo* reaction in the early stages of bone healing. In contrast to other methods of molecule sampling and detection, which usually lead to the inhibition of the biological activity following complex sample preparation and quantification, microdialysis is a real-time monitoring technique which can be applied in living tissues providing a strong link between analytical methodology and biochemistry. In this study, the optimal conditions for microdialysis in a critical size rat long bone defect model for both *in vivo* and *in vitro* analyses were developed. Mediators and components of the extracellular matrix occurring in the first 24 to 48 hours of bone healing locally and systemically were monitored via microdialysis and blood sampling, respectively. Furthermore, novel proteins and their modulation were explored during this time frame.

In vitro microdialysis was used to optimize the condition for protein recovery. Addition of bovine serum albumin (BSA) resulted in an enhanced recovery of interleukin (IL)-6. The maximal relative recovery (RR) was from 15.0% without BSA and 23.6% with BSA, while the maximal RR of transforming growth factor (TGF)-β1 was 11.2% with BSA and the concentration of TGF-β1 was below the detection limit of enzyme-linked immunosorbent assay (ELISA) without BSA. Using *in vivo* microdialysis, total protein concentrations varied between 0.20±0.12 mg/mL and 0.44±0.18 mg/mL. Among the mediators produced in the fracture hematoma within 24 h after the injury, IL-6 was secreted with the highest concentration of 309.1 pg/mL between 12 and 15 h after creation of the critical size bone defect. Meanwhile, the detectable concentrations of TGF-β1 in microdialysates ranged from 3.6 to 44.0 pg/mL and in blood plasma TGF-β1 was constantly producted ranging from 656.3 to 8398.2 pg/mL for 24 h after bone defct. Moreover, another constant producted growth factor in blood plasma was PDGF-BB and the concentration ranged from 222.1 to 589.4 pg/mL for 8 h after bone defect. Using high performance liquid chromatography-tandem mass spectrometry (HPLC-MS/MS), 36 proteins were identified in the microdialysates over 8 h, and 884 proteins were identified on probes which were implanted into the bone defect over 24 h. Among the proteins identified in the hematoma, only a minority originated from the extracellular space. Protein analysis indicated five pathways associated with bone healing that were overrepresented after creating soft tissue and bone defects, of which FGF signaling was specific for bone defects. Furthermore, C-X-C motif ligands CXCL-1, CXCL-2, CXCL-3, CXCL-4, CXCL-5, CXCL-7, rodent bone protein (RoBo-1),

insulin-like growth factor (IGF)-I, and chitinase-3-like protein 1 were detected in the fracture hematoma. These proteins are potentially associated to early bone healing. As seen by histological analysis, polymorphonuclear leukocytes (PMNs) and lymphocytes penetrated into the fracture hematoma immediately after surgery and peaked at 24 h.

This study for the first time presents data from both the local and systemic acute response to bone and soft tissue injury in a small animal model. The results of mcrodialysis sampling may serve as a baseline for future investigations on different models and time frames. Several proteins and pathways have been identifeid as potentially important for early bone regeneration warranting in depth analysis in further studies.

Keywords: microdialysis, bone, critical-size defect, cytokine, growth factor, sampling

2 Introduction

2.1 The process of bone healing

Bone tissue has a hierarchical structure and is a complex and delicate biological system. Upon injury, bone tissue is able to undergo healing process with remarkable self-repairing capacity without fibrous scar formation. The fracture healing process consists of the following 4 natural stages: 1) inflammation, 2) soft callus, 3) hard callus, 4) remodeling (Fig. 1) (Kolar et al., 2010). These stages have been well summarized and characterized by histological investigation (Einhorn, 1998).

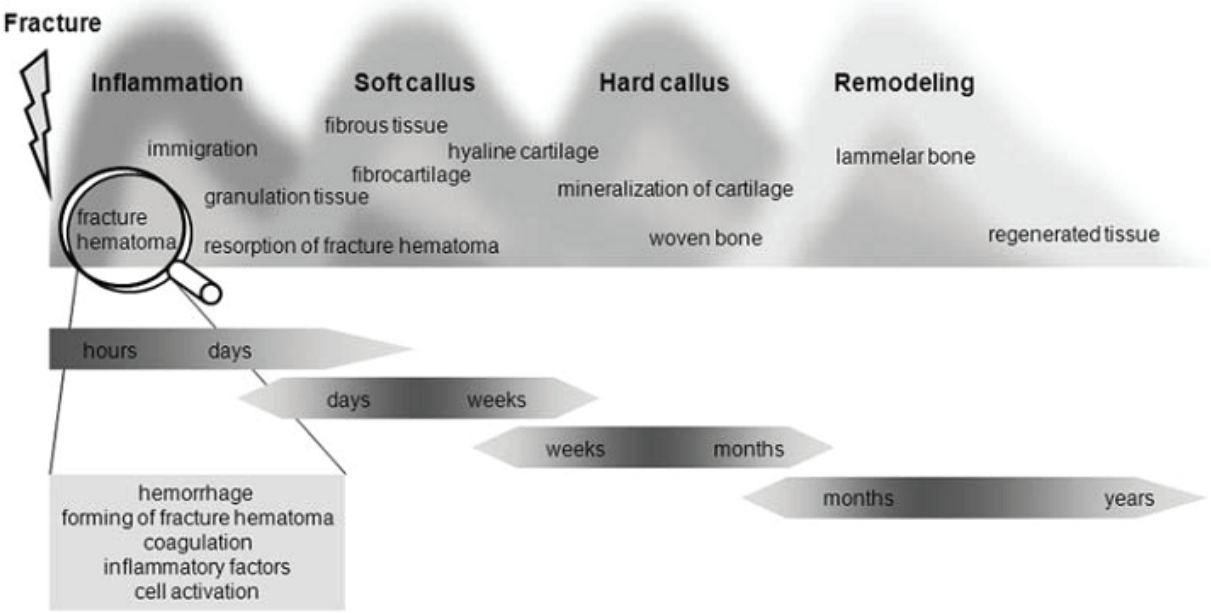

Fig. 1: The bone healing process with consecutive and overlapped stages (Kolar et al., 2010).

2.1.1 Stages of fracture healing

a) Inflammation

The inflammation stage includes the formation of a hematoma. The trauma leads to the injury of blood vessels at the fracture site. The gap of the fracture is soon occupied by the hematoma and hemostasis occurs immediately (Ozaki et al., 2000; Schmidt-Bleek et al., 2009). Following the formation of the hematoma, the inflammation response is initiated. The acute inflammation peaks within 24 h and can last for several days (Cho et al., 2002). The predominant phenomenon at this stage is infiltration of immune and inflammatory cells derived from bone marrow, surrounding soft tissues or leaking from the destructed vessels. Meanwhile, the mesenchymal stem cells (MSCs) or osteoprogenitors recruit to the local site and respond at fracture site from peripheral blood, bone marrow, endosteum, periosteum,

muscle or adipose tissue (Caplan, 1991; Kitaori et al., 2009; Beamer et al., 2010). Meanwhile, kinds of mediators are released from collapsed tissue and also secreted by activated cells. Via the interactions between cells and the mediators, a cascade of healing processes is activated. During this stage MSCs begin to differentiate into chondrogenitors/chondrocytes or osteoblasts (Einhorn, 1998; Phillips, 2005). On the other hand, the angiogenesis is initiated (Dimitriou et al., 2005). With the synthesis of a variety of collagen isotypes and fibrous tissue in the hematoma, granulation tissue gradually replaces the hematoma (Ozaki et al., 2000; Winn, 2005; Kolar et al., 2010).

b) Soft callus

Following inflammation, callus formation occurs. The kinetic of this process depends on the fracture site with the formation of compact bone being more slowly than cancellous bone (Frost, 1989). Endochondrogenesis and initial ossification are the predominant features during this stage. Transforming growth factor (TGF)-β is discussed to be involved in the initiation of callus formation (Bostrom, 1998). After removing granulation tissue by invading macrophages and giant cells, the cartilage is gradually formed by differentiating and proliferating chondrocytes (Einhorn, 1998). Due to the secretion of chondrocytes and their progenitors, the cartilage extracellular matrix (ECM) is abundant with proteoglycans such as aggrecan and collagen. Among the collagen, type II and type X collagen are regarded as ECM markers at this stage (Einhorn, 1998). With the process of chondrogenesis the fracture ends are bridged by formed cartilage (Barnes et al., 1999).

c) Hard callus

During the soft callus formation, proliferating and differentiating osteoblasts start to generate woven bone beneath the periosteum (Nakamura et al., 1998; Einhorn, 1998). When the soft callus becomes hypertrophic and the fracture stabilizes, the cartilage ECM gradually mineralizes via the hypertrophic chondrocytes and later osteoblasts. Osteocalcin as the marker of osteogenesis is initially detected (Einhorn, 1998). Then the cartilage is degraded by activated chondroclasts (Einhorn, 1998). With apoptosis of chondrocytes, osteoprogenitors and capillaries invade into the mineralized cartilage with the osteoprogenitors orienting along the neovessel (Einhorn, 1998; Barnes et al., 1999; Deschaseaux et al., 2009). Finally, the mineralized cartilage is replaced by woven bone and the bridged bone becomes rigid (Gerstenfeld et al., 2006).

d) Remodeling

The remodeling stage initiates approximately several weeks after fracture and can continue for years until the affected bone regains its original shape, structure and mechanical strength. Following the Wolff's law and the process of resorption by osteoclasts combining

with bone formation by osteoblasts, the external callus is absorbed and woven bone is slowly remodeled into lamellar bone which parallels to the longitudinal axis (Shapiro, 2008). In the meantime, the resorption of internal callus generates the medullary canal (Marzona & Pavolini, 2009).

2.1.2 Early stage of inflammation

During wound healing inflammation has profound physiological purposes such as host defense against infection, restoration of the homeostatic state, adaption to stress, tissue-repair response and restoration of function (Li et al., 2007a). The cellular actions and inflammatory signals following injury are critical in response to trigger and regulate bone regeneration and for successful bone repair (Mountziaris et al., 2008). When the inflammatory process is disturbed, bone healing will be impaired (Gerstenfeld et al., 2003; Phillips, 2005; Wallace et al., 2011).

1) Coagulation and complement system during bone healing

Before inflammation starts, the hemostasis and the hematoma formation are initiated first. The coagulation can be triggered by the extrinsic and intrinsic pathways or both (Fig. 2). The extrinsic pathway depends on the release of tissue factor, whereas the intrinsic pathway is activated when the ECM is exposed in the vascular wall (e.g. collagen) and activates the platelets due to the injury. Both pathways can activate coagulation factor X (FX) to FXa and subsequently generate thrombin that cleaves the soluble plasma fibrinogen into monomer fibrin (Baum & Arpey, 2005; Chu, 2010). The fibrin monomers covalently cross-link with FXIII which is released by activated platelets. Hence, a stable insoluble fibrin clot forms. In a rat ribs fracture model, the fibrin clot was formed at the end of fractured fragment 12 h after surgery (Brighton & Hunt, 1991). With the coagulation, the clot becomes the matrix for recruitment of migrating or resident cells and the reservoir of mediators (Kurkinen et al., 1980; Street et al., 2000). Many mediators derived from activated degranulating platelets can trigger chemotactic signals. The released mediators include fibroblast growth factor (FGF)-2, platelet-derived growth factor (PDGF), large quantities TGF-β1, epidermal growth factor, β-thromboglobulin, (C-X-C motif) ligand (CXCL)-4, histamine, serotonin and prostaglandins (Gruber et al., 2003; Broughton et al., 2006). Attributed to the powerful mediators, the platelets are involved in many processes during fracture healing beside coagulation. They are associated with the initiation and the modulation of immediate bone fracture due to the release of the growth factors PDGF and TGF-β1 (Bolander, 1992). Moreover, they can activate the complement system (Peerschke et al., 2006).

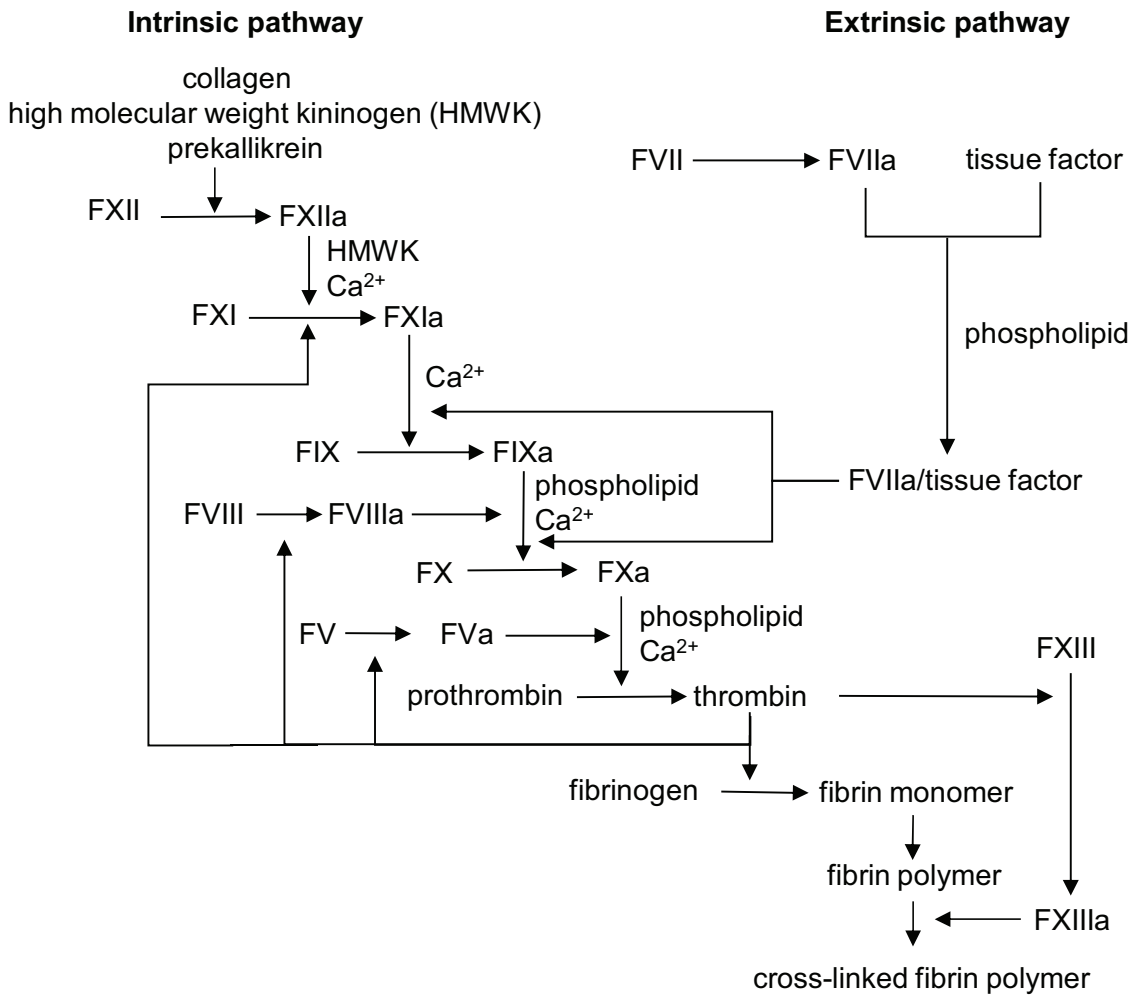

Fig. 2: Scheme of coagulation cascade.

Complement system plays an important role in the pathogenesis and removing damaged tissue. Furthermore, it is also involved in the processes of opsonization of pathogens, formation of anaphylatoxins or elimination of immune-complexes during inflammation (Ehrnthaller et al., 2011). The complement system is activated through 3 ways: the classical, the alternative, and the lectin pathway. All 3 ways can induce the complement components C3b and C5b from C3 and C5. C3b and C5b not only lead to the formation of membrane attack complex which causes the pathogens lysis, but can also bind with pathogens and promote phagocytosis by neutrophils and macrophages as opsonins. After bone is injured, they also function essentially for the bone regeneration (Schoengraf et al., 2013). Apart from the strong immune and inflammatory response induced by the complements, which influences fracture healing indirectly, the complements exert the potency in the aspects of osteoprogenitors (Recknagel et al., 2012; Schoengraf et al., 2013), The anaphylatoxins (C3a and C5a) cleaved from C3 and C5 act as powerful chemoattractants for human MSCs *in vitro* and the recruitment of osteoblasts during the rats fractured bone healed *in vivo*

(Schraufstatter et al., 2009; Ignatius et al., 2011). In addition, complements directly influence the osteoblast–osteoclast interaction and modulate the inflammatory response by osteoblasts (Recknagel et al., 2012; Schoengraf et al., 2013).

2) Inflammatory cell response

Coagulation and inflammation correlate tightly. During coagulation, the vasoconstriction, vasodilatation and elevation of vascular permeability occur due to effects of the vasoconstrictors that are produced by the activated platelets like histamine, serotonin and prostaglandins.

With the vasodilatation, the elevation of vascular permeability and the chemotactic gradient of chemoattractants, inflammatory cells and progenitors migrate towards the injured site. Among the inflammatory cells neutrophils, monocytes and macrophages are predominant (Hietbrink et al., 2006; Li et al., 2007a). The migration of these cells depends on the upregulaed expression of cell adhesion molecules (CAM) on endothelial cells (Beamer et al., 2010). Furthermore, they migrate to the injured site sequentially. Neutrophils, as the major part of polymorphonuclear leukocytes (PMNs), are known to be the first group of cells arriving at the site of injury. This might be due to the higher percentage of neutrophils in the blood compared to monocytes and to the kinetics of expression of leuko-endothelial adhesion molecules (Kaplanski et al., 2003). Moreover, cytokines and chemokines play a role for the migration of neutrophils. IL(interleukin)-1 and tumor necrosis factor (TNF)-α can promote the expression of vascular cell adhesion molecules (VCAM)-1 and endothelial leukocyte adhesion molecule (ELAM)-1 on blood vessels and enhance the neutrophil migration (Pohlman et al., 1986; Osborn et al., 1989; Bevilacqua et al., 1989). IL-6-sIL-6Rα complex can activate the vascular endothelial cell to secrete CXCL-8 which attracts neutrophils, and might favor the resolution of infiltration of neutrophils during acute inflammation (Romano et al., 1997; Kaplanski et al., 2003). .

(Lee et al., 2009b). On account of the potent mediators in the early injured site, the human fracture hematoma was found to enable an activation of neutrophils and result in an increased neutrophil infiltration due to the toxicity to vascular endothelial cell and disrupting the integrity of the endothelial barrier (Timlin et al., 2005). However, in a sheep tibia fracture model, the first arrived neutrophils declined with increasing lymphocytes within 4 h after surgery (Schmidt-Bleek et al., 2009). Generally, the peak of neutrophils infiltration came at 24 to 48 h after injury (Witte & Barbul, 1997). Apart from the effect of cytokines (IL-1 and TNF-α) and chemokines (CXCL-4 and CXCL-8), many other chemoattractants affect the migration of neutrophils, such as PDGF, TGF-β, CXCL-1, C5a and leucotriene B4 (Deuel et al., 1982; Shibata et al., 1996; Kaplanski et al., 2003). Among these chemoattractants, part of them are responded by the release from activated platelets (IL-1, TNF-α, CXCL-4, complement, PDGF

and TGF-β) (Broughton et al., 2006).

The main tasks of the infiltrated, activated neutrophils are the clearing from bacteria and cellular debris via reactive oxygen species (ROS) and proteolytic enzymes (Broughton et al., 2006). For human bone fracture, the production of ROS increases in PMN by using 48 h- to 5 day-old human fracture hematoma fluid (Hauser et al., 1999). Meanwhile, Timlin et al. found 48 to 72 h-old human fracture hematoma responded to the delay of neutrophil apoptosis. They considered that IL-6, granulocyte macrophage colony-stimulating factor and platelet-activating factor were associated with the biological foundation of the delay (Timlin et al., 2005). Many matrix metalloproteinases (MMP) produced by neutrophils such as MMP-8 and MMP-9 are a group of enzymes that degrade the collagen in damaged ECM and promote the tissue remodeling (Kjeldsen et al., 1992; Nwomeh et al., 1998; Broughton et al., 2006). Besides the effects of phagocytosis and ECM destruction, PMNs are the major producer of pro-inflammatory cytokines (IL-1α, IL-1β and TNF-α), which is very important during initiation of wound healing in mice (Hübner et al., 1996). Although neutrophils are believed to be inessential for tissues repair, their phagocytosis is taken over by the following macrophages especially in the case of absent bacterial contamination (Simpson & Ross, 1972; Witte & Barbul, 1997).

Following the infiltration of neutrophils the monocytes as the precursors of macrophages start to accumulate (Broughton et al., 2006). The transition from neutrophils to monocytes contributes to the shift of the subtype of chemokines via IL-6-sIL-6Rα complex (Kaplanski et al., 2003; Broughton et al., 2006). Chemokine superfamily as a subset of cytokines are mainly responsible for chemotaxis and were divided into 4 major groups according to the protein structure (Broughton et al., 2006):

a) CXC-subfamily: e.g. CXCL-1, CXCL-2, CXCL-3, CXCL-4, CXCL-8;
b) C-C-subfamily: e.g. (C-C motif) ligand (CCL)-2, CCL-4, and CCL-5,
c) C-subfamily: (C motif) ligand (XCL)-1 and XCL-2.
d) CX3C-subfamily: (C-XXX-C motif) ligand (CX3CL)-1.

The different cysteine patterns chemoattract different types of inflammatory cells. The CXC-subfamily chemokines with ELR motif, e.g. CXCL-1, CXCL-2, CXCL-3, chemoattract only neutrophils. Whereas without the ELR motif, e.g CXCL-9, only activated lymphocytes were chemoattracted (Shibata et al., 2002; Broughton et al., 2006). In addition, C-C-subfamily chemokines are chemotactic for lymphocytes, monocytes, eosinophils and basophils except neutrophils (Broughton et al., 2006).

Among these chemokines, CXCL-8 and CCL-2 are believed to be the most important for the recruitment of neutrophils and monocytes, respectively. Meanwhile CXCL-4 is also able to chemoattract monocytes (Deuel et al., 1981). Besides chemokines, PDGF, vascular endothelial growth factor (VEGF) and TGF-β are also able to chemoattract monocytes (Deuel

et al., 1982; Wahl et al., 1987; Clauss et al., 1990). Normally during wound healing monocytes are attracted around 48 to 96 h after injury with a peak after 48 h, and they transform into macrophages (Witte & Barbul, 1997; Broughton et al., 2006). In a mice tibia fracture model, the monocytes appeared in the hematoma within 24 h after surgery (Bourque et al., 1993). At the periphery of hematoma, few macrophages occurred within 24 h as well in the mice tibia fracture model (Bourque et al., 1993; Kon et al., 2001). The transformation of macrophages from monocytes only took few hours, and after 48 h the number of macrophages increased (Bourque et al., 1993). Moreover, the molecules that activate the coagulation can also activate monocytes and macrophages (Opal, 2000). They produce many important mediators. Monocytes produce and express IL-6, IL-1, TNF-α, FGF and PDGF (Wahl et al., 1987; Dimitriou et al., 2005). Among them IL-6 facilitate the differentiation of monocytes into macrophages (Kaplanski et al., 2003). Macrophages are essential for wound healing (Broughton et al., 2006). In a mice macrophages cell line study C5a was found to act as a strong chemoattractant for macrophages (Aksamit et al., 1981). During the inflammation, the major roles of macrophages are phagocytosis and the removal of the debris using enzymes (Witte & Barbul, 1997). Furthermore, macrophages are responsible for the production of IL-1α, IL-1β, IL-6, TNF-α, TGF-β, FGF-2, VEGF-A and insulin-like growth factor (IGF)-1 (Bourque et al., 1993; Kon et al., 2001; Werner & Grose, 2003). By producing MMPs, monocytes and macrophages can digest the ECM (Broughton et al., 2006; Beamer et al., 2010). In a model of mice tibia fracture macrophages also seem to initiate cell division at the fracture site via the production of PDGF (Bourque et al., 1993). In addition, the monocytes and macrophages lineages would transform into osteoclasts for the process of bone healing (Schoengraf et al., 2013).

Although lymphocytes were reported to be present in sheep fracture hematoma as early as 4 h after surgery, normally for wound healing they peaked at the end of inflammation (Witte & Barbul, 1997; Schmidt-Bleek et al., 2009).

With the infiltration of those inflammatory cells, degranulating platelets and activated endothelial cells, many cytokines and growth factors are regulated particularly within 24 h after fracture according to various *in vivo* studies. IL-6, IL-1β and TNF-α were strongly expressed and peaked at 24 h after bone fracture in mice model, then their level decreased at day 3 (Kon et al., 2001; Cho et al., 2002). Except for the effect of chemotaxis mentioned above, these cytokines responded for the enhancement of the ECM synthesis and angiogenesis (Kon et al., 2001). Moreover, cells affect the osteopregenitors during the early inflammation stage. In *in vitro* studies IL-1β and TNF-α were found to inhibit the proliferation or differentiation of MSCs (Lacey et al. 2009; Lange et al. 2010). Furthermore, TNF-α down-regulated the osteocalcin gene promoter in osteoblast-like cells, while IL-6 played a minor role *in vitro* (Li & Stashenko, 1992). Besides, immunosuppressive factor IL-10 was released

in the human hematoma within 24 h after fracture to modulate the immune response (Hauser et al., 1996).

3) Bone-related cellular response during fracture healing

In vitro studies showed that besides the complement components, bone morphological protein (BMP)-2, BMP-4 and PDGF-BB modulated the chemotaxis for human MSCs, nevertheless, the chemotactic ability of BMP-2 is still controversial (Fiedler et al., 2002; Bais et al., 2009). During the inflammatory stage of bone healing, the bone marrow derived MSC (BM-MSC)-like cells appeared in the 48 h human fracture hematoma (Oe et al., 2007). Although many researches considered that the MSCs originated from the surrounding soft tissues and bone marrow, the systemic derived MSCs in the injured site seem to be necessary for an optimal healing response (Kitaori et al., 2009; Marsell & Einhorn, 2011).

Many growth factors, such as TGF, VEGF and PDGF, are capable of enhancement of osteogenesis. As a member of the TGF-family, TGF-β1 is released from degranulating platelets and the destructed bone matrix after bone injury (Assoian et al., 1983; Janssens et al., 2005). It recruited osteoblast progenitors, stimulated their proliferation and differentiation and synthesis of ECM (Joyce et al., 1990; Janssens et al., 2005). TGF-β1 has a high basal level of expression in the intact mice tibias, and sharply rises as early as 12 h, and by day 1 after fracture the expression returned to the baseline level seen in the intact tibias (Ito et al., 1999; Cho et al., 2002). Besides, PDGF exhibited the ability of osteogenesis during bone healing. *In vitro* PDGF can induce osteoblasts to secrete osteopontin (OPN) (Tanaka & Liang, 1995). Within 2 days after mice tibia bone fracture PDGF that was produced by macrophages may act as a key to initiate the cell division in fibroblast-like MSCs and of cells in the cambial layer of the periosteum (Bourque et al., 1993). Nevertheless, because of the outstanding osteoinductive potential, the BMP family was investigated intensively in the context of bone healing during the years. Compared with other growth factors such as VEGF and PDGF-BB, BMP-2 exerted a stronger potential of osteogenesis based on a delayed-union rat model (Kaipel et al., 2012). In an *in vitro* study Bais et al. have demonstrated BMP-2 was essential for the differentiation of the MSCs (Bais et al., 2009). After bone fracture in a mice model, BMP-2 was found to be the earliest induced gene with strong expression that achieves maximum expression 24 h after surgery (Cho et al., 2002). At the protein level, BMP-2 was observed on day 2 in swelling periosteum which was distal and proximal to the fracture site (Bostrom et al., 1995). By blocking BMP-2 signaling, the bone formation will pause at very early stage (Tsuji et al., 2006).

During the inflammtion stage of fracture, some osteoclasts usually appear to resorbe the surface of the fracture (Frost, 1989). Horowitz et al. has summarized IL-1 and TNF can directly stimulate osteoclast formation *in vitro* (Horowitz & Lorenzo, 2008). The messenger

ribonucleic acid (mRNA) of osteoprotegerin (OPG), receptor activator of nuclear factor κB ligand (RANKL) and macrophage colony-stimulating factor (M-CSF), which were related to the osteoclast differentiation increased as early as 24 h after fracture in mice (Kon et al., 2001). Furthermore, VEGF that is involved in migration, survival and stimulation of monocytes and macrophages can indirectly influence the osteoclast formation (Nakagawa et al., 2000).

4) Angiogenesis during the inflammatory stage

Angiogenesis is important and essential for bone healing since it not only transports oxygen and nutrient for the cells but also MSCs for osteoblast differentiation (Beamer et al., 2010). Generally this process is initiated 3 days after bone injury (Dimitriou et al., 2005). Nevertheless, the concentration of PDGF and VEGF, two important related growth factors, elevated at high level in human fracture hematoma within 24 h after injury in comparison to plasma level (Street et al., 2000; Street et al., 2001). At genetic level, expression of VEGF was upregulated within 24 h after the tibia was fractured in a mice model which reflected the early response to the bone injury (Schmid et al., 2009). VEGF as a potent endothelial cell mitogen was able to attract myocytes *in vitro* (Grosskreutz et al., 1999). Some angiogenic genes like hypoxia-inducible factor 1-alpha (HIF-1α), which is associated with the production of VEGF, was upregulated in periosteum within 24 h after the sheep tibia was osteotomized (Schmidt-Bleek et al., 2012).

5) Other mediators during the early inflammation

IGF-1 is stored predominantly in the bone ECM of rodents and can also be released from platelets into the hematoma as a major signaling mediator to control the inflammatory cascade (Bautista et al., 1990; Phillips, 2005). It is induced by growth hormone and effected by parathyroid hormone protein (PTH) (Rosen & Niu, 2008). Furthermore, 24 h after limb fractures the mRNA of IGF-I and parathyroid hormone-related protein (PTHrP) which is a member of PTH family were expressed in periosteum both in the mice and the rat model (Ito et al., 1999; Okazaki et al., 2003). In Bourque's research, IGF-1 was only identified in young chondroblasts at the protein level after fracture in mice tibia, while the expression of PTHrP experienced for the entire healing period but at a low level (Bourque et al., 1993; Ito et al., 1999).

The members of the FGF family are critical during fracture repair. FGF-1 and FGF-2 are abundant in bone ECM (Barnes et al., 1999). During the inflammation stage FGF partially derives from platelets, and is partially expressed in macrophages or periosteal cells among the granulation tissue (Bolander, 1992). Bourque et al. found FGF-2 was initially stained in cells of the expanding cambial layer of the periosteum during soft callus stage (Bourque et al.,

1993). By gene analysis in mice with fractures, Schmid et al. found FGF-1, FGF-2 and FGF-5 were upregulated at 24 h after bone injury and played a redundant role during early response. Since the increasing expressions of FGF-1 and FGF-2 might partially contribute to the fixator-induced trauma, they suggested that FGF-5 was important for the early fracture healing comparing with FGF-1 and FGF-2 (Schmid et al., 2009).

Although the formation of soft and hard callus followed inflammation, many chondrogenic and osteogenic related genes were also expressed during the early inflammatory stage. Indian hedgehog (Ihh), smoothened (Smo) and patched (Ptc) which were involved in differentiation, proliferation and maturation of chondrocytes were upregulated from 8 to 12 h after mice tibias fractured (Ito et al., 1999). OPN and osteocalcin as markers of osteogenesis increased as early as 6 h after bone fracture and the high expression persisted over 24 h in mice tibiae (Ito et al., 1999; Kon et al., 2001; Cho et al., 2002). Furthermore, many researchers have found the expression of type I collagen which is the main component of the bone ECM elevated within 24 h after the mice tibia fractured (Gerstenfeld et al., 2001; Kon et al., 2001; Cho et al., 2002). Nevertheless, Schmid and his colleagues did not find an expression of any marker of chondrogenesis or osteogenesis within 24 h after mice fracture (Schmid et al., 2009).

2.2 Clinical challenges

Unfortunately, not every fractured bone is able to heal completely. In the clinic, many reasons such as serious trauma, tumor resection, inflammation, pathological degeneration or congenital malformations can induce critical-size bone defects. The severe destruction of tissue and loss of bone marrow and periosteum generate a loss of powerful osteoprogenitors and osteoconductive material. This causes disability of spontaneous bone healing, which subsequently induces pseudoarthrosis or nonunion that lead to severe impairment of lifestyle for the patient and become a great challenge in the clinic (Calori et al., 2007). Instead of bridging segmental bone, only loosen fibrous connective tissue, small amount of cancellous and woven bone were observed at the edge of defect towards the periosteum side, and then bone formation ceased (Chiba et al., 2001; Kirker-Head et al., 2007). To overcome the limitation of physiological healing, great efforts have been made during past decades to enhance bone healing. So far, the golden standard of treatment is autogenous bone graft. But it has many drawbacks, such as limitation of bone availability, significant morbidity at the donor site and continuous pain, extra surgery and the risk of virus infection, particularly when large grafts are required (Sutherland & Bostrom, 2005). Hence, developing an approach to accelerate bone regeneration is required. Considering the importance of the initial healing cascade in bone, to characterize the early physiological changes in bone defect might

contribute to understand the mechanism of bone defect healing and the improve the approach for future therapies.

2.3 Microdialysis

Microdialysis is a well-established powerful sampling technique to monitor target molecules in tissues or fluid compartments *in vitro* or *in vivo*. Originally, it was termed intracranial dialysis and applied to collect chemical information in rodent brain (Stenken, 2006). Other than in the brain this technique is now widely used in multiple organs such as skin, muscle, adipose tissue and eye (Louzada-Júnior et al., 1992; Rosdahl et al., 1998; Averbeck et al., 2006). However, few researches have applied this technique in bone tissue. Those studies mostly focused on the pharmacological metabolism, the mechanical response or the blood flow in ischemia in bone (Thorsen et al., 1996; Stolle et al., 2004; Bøgehøj et al., 2007). Only one study applied microdialysis on the analysis of TNF-α after muscle flap transposition during a canine tibia fracture (Brown et al., 2000).

2.3.1 The principle of microdialysis

The principle of microdialysis is based upon the diffusion of molecules through a semi-permeable membrane due to a concentration gradient (Fig. 3). The diffusion coefficient (*D*) is a parameter describing the efficiency of the molecular diffusion. Higher value of D indicates increasing amountS of molecules that diffuse within an interval. For small molecules e.g. inorganic ions and glucose, D ranges from 10^{-5}–10^{-6} cm^2/s whereas for large molecules e.g. proteins, D decreases to the grade of 10^{-6}–10^{-7} cm^2/s (Klein et al., 1979; Rosenbloom et al., 2005). The semi-permeable membrane controls the influx of molecule into the microdialysate according to the molecular weight cut-off (MWCO) of the membrane. The commercially available membrane MWCO ranges from 6–300 kDa. Only molecules whose molecular weights are smaller than the MWCO are able to pass through. Previously this technique was exclusively used to recover small hydrophilic molecules. But nowadays it is also extensively used for large biomolecule sampling such as proteins (Stenken, 2006; Wang et al., 2007).

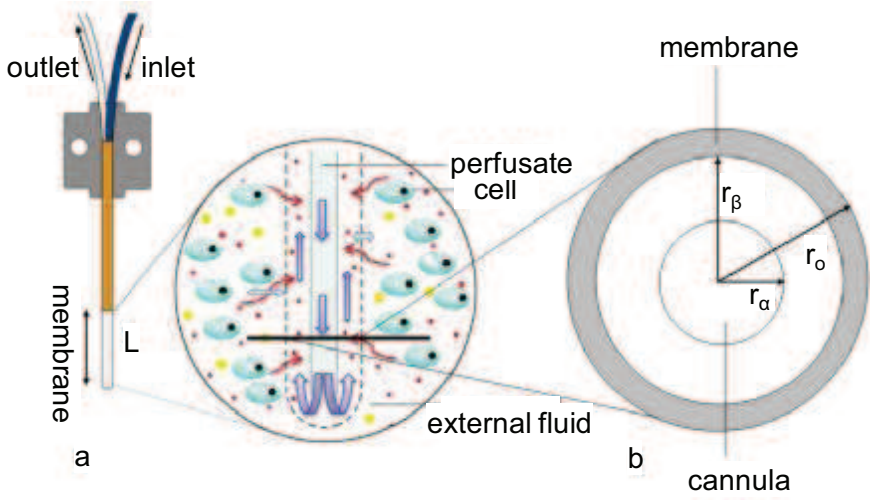

Fig. 3: Scheme of the microdialysis recovery process. a) Sagittal plane of the probe membrane area in tissues. Red, small molecules, Yellow, large molecules. **b)** Cross section of probe. r_α, r_β, r_o are the radius of inner cannula, inner side of membrane and outer membrane surface respectively and L is the length of the membrane.

The recovery efficiency is assigned to evaluate the efficiency of sampled molecules. Two parameters are commonly used: 1) the absolute recovery which represents the total amount of the target molecule recovered in a microdialysate, 2) the extraction efficiency (EE) which represents the percentage of the target molecule concentrations in a microdialysate to the concentrations of the target molecule that is in the external fluid (Nandi & Lunte, 2009). The EE is mostly used to evaluate the recovery efficiency and a mathematical equation is established to describe it (Eq.1) (Bungay et al., 1990).

$$EE=\frac{C_d - C_i}{C_e - C_i}\times 100\% = \left(1-\exp\left(-\frac{1}{Q_d\left(R_d+R_m+R_e\right)}\right)\right)\times 100\% \qquad \text{Eq. 1}$$

C_d, C_e and C_i are the concentrations of the molecules in the microdialysate, the external fluid and the perfusate, whereas Q_d is the flow rate of the perfusate; R_d, R_m and R_e the resistances to the microdialysate, the membrane and the external factors (such as a complex matrix). These three resistance parameters negatively correlate with D in the microdialysate, the external fluid and the perfusate. For the recovery mode which indicates C_i=0, the EE is known as the relative recovery (RR) and Eq.1 can be simplified as:

$$RR=\frac{C_d}{C_e}\times 100\% \qquad \text{Eq. 2}$$

Practically the equilibrium between the microdialysate and the external fluid is hard to obtain. Hence, the RR will never reach 100% and cannot reflect the absolute value in the

external fluid. In order to resolve this problem, diverse calibration methods have been proposed (Plock & Kloft, 2005). However, none of them are perfectly practicable. Although the concentration of the target molecule in the microdialysate is not the absolute value, the relative level which changes from baseline may be more effective in some cases (Clough, 2005). Once the microdialysis is attempted to set up, there are several factors which influence the recovery and should be taken into consideration.

2.3.2 Parameters influencing the recovery

1) Probe geometry and materials

The length and thus the extensive area of the probe membrane can increase the RR. The physical property e.g. the charge of the membrane also interferes the process of recovery (Zhao et al., 1995). Moreover, to enhance the RR the polymer membranes have been chemically or biologically modified (Huinink et al., 2010; Dahlin et al., 2010).

2) Molecular weight cut-off

The molecular weight is negatively associates with the RR (Helmy et al., 2009). Only the target molecules whose molecular weights are one-third to -fourth less than MWCO are readily recovered (Torto et al., 1998; Plock & Kloft, 2005). The tertiary-quaternary structure of proteins, the shape or the radius of the hydration shell of the molecules in the medium also affect the recovery (Ao et al., 2004; Rosenbloom et al., 2005). Although the higher MWCO permits more and larger molecules passing through, it conversely induces the fluid loss from the perfusate, which is harmful for large molecule recovery (Ao & Stenken, 2006).

3) Perfusate

Physiological solutions are normally used to perfuse, e.g. the Ringer´s solution, saline, phosphate buffered saline (PBS) or artificial cerebrospinal fluid (Stolle et al., 2004; Hillman et al., 2005; Takeda et al., 2011). The ion strength, the osmotic value and the pH of the perfusate also influence the recovery (Zhao et al., 1995; Trickler & Miller, 2003; Helmy et al., 2009). Addition of colloid to crystalloid perfusates can avoid perfusate loss and enhance the recovery through increasing the colloid pressure (Hamrin et al., 2002). Among the colloids, dextran and bovine serum albumin (BSA) are the mostly used. Beside the colloid, heparin-immobilized microspheres or antibody-coated microspheres also have been designed to enhance protein recovery of specific proteins (Ao et al., 2004; Duo & Stenken, 2011).

4) Flow rate

Theoretically, a lower flow rate induces a higher RR according to Eq.2. When the flow rate approaches zero, an equilibrium becomes accessible and the RR is close to 100%. However, the ultraslow flow rate implies smaller volume of collected microdialysate at an interval and requires a long time to collect adequate volume for analysis. Meanwhile, long

time and small volume of microdialysate induce a subsequently risk of evaporation (Menacherry et al., 1992). Routinely, flow rate ranges between 0.1–5.0 μL/min for protein recovery. On the other hand, a higher flow rate is beneficial for protein recovery, because the higher flow rate can diminish the binding of proteins to the inner surface of the membrane especially for hydrophobic proteins (Waelgaard et al., 2006).

5) Other factors

A higher temperature leads to a higher D of the molecules in terms of the thermal kinetic motion principle which indicates the higher RR. Nevertheless, in life science the body temperature is recommended for microdialysis studies (Plock & Kloft, 2005). The positions of the collection tubes for microdialysates induce different hydrostatic pressures which is associated with the amount of fluid loss (Hamrin et al., 2002). Then the properties of the membranes change over time especially for long-term implantation of the probe which might cause a foreign body reaction (Wang et al., 2007; Helmy et al., 2009).

Although the microdialysis is applied widely, so far, none has been applied to investigate the dynamic changes of mediators in a critical size bone defect during the early stage of healing.

2.4 Aim of this study

It is well known that the inflammation stage is critical for fracture healing. However, this process has not been thoroughly characterized at the site of injury so far. Therefore, microdialysis was established in rats with bone and soft tissue defects to identify and characterize the inflammatory reaction in the early stages of bone healing. The principal aims of this study were:

1) Establishing microdialysis a s a method to characterize the early stages of bone healing and creating a baseline for further observations
2) To identify and monitor the level of selected local cytokines and growth factors within 24 h after creating bone defects *in vivo*
3) To identify proteins present in bone and soft tissue defects *in vivo*
4) To identify and monitor the level of circulating cytokines and growth factors within 24 h after creating bone defects to characterize the systemic response to injury *in vivo*
5) To characterize the morphological features of the fracture hematoma with 48 h after creating bone defects *in vivo*.

3 Materials

3.1 Materials, devices and animals

BD Falcon® Tube (15 mL and 50 mL)	BD Biosciences, Bedford, USA
CMA 20 Microdialysis Probe	CMA Microdialysis AB, Solna, SWE
CMA 402 syringe pump	CMA Microdialysis AB, Solna, SWE
Dental micromotor including foot switch and handpiece	Eickemeyer Medizintechnik für Tierärzte KG, Tuttlingen, GER
Gigly wire saw 0.22 mm	RISystem AG, Davos, SUI
Hand drill	RISystem AG, Davos, SUI
HandyStep® electronic repetitive pipette	Brand GmbH & Co. KG, Wertheim, GER
Infinit M200 pro microplate reader	Tecan Group Ltd., Männedorf, SUI
Leica camera DC 300	Leica Microsystems CMS GmbH, Heerbrugg, SUI
Light microscopy	Leitz DMRBE, Leica Mikrosysteme Vertrieb GmbH, Wetzlar, GER
LTQ Orbitrap XL Mass Spectrometer	Thermo Fisher Scientific Inc., San Jose, CA, USA
MF-ChemiBIS 1.6	DNR Bio-Imaging Systems, Israel
Micotubes (1.5 mL and 2 mL)	Sarstedt AG & Co., Nümbrecht, GER
Microcentrifuge 5415 R	Eppendorf AG, Hamburg, GER
Microsyringe 1 mL	CMA Microdialysis AB, Solna, SWE
NanoAcquity Nanoflow HPLC system	Waters GmbH, Milford, MA, USA
NanoDrop ND-2000c Spectrophotometer	PEQLAB Biotechnologie GmbH, Erlangen, GER
Nunc 96-well plate	Thermo Fisher Scientific Inc., Roskilde, DEN
Precision Dispenser Tips (5 mL and 12 mL)	Brand GmbH & Co. KG, Wertheim, GER
RatFix drill- & saw guide 6 mm	RISystem AG, Davos, SUI
RatFix plate, 8 hole at 23 mm, Femur	RISystem AG, Davos, SUI
RatFix shoulder screw 0.7x5.7 mm	RISystem AG, Davos, SUI
Rotamax 120	Titramax, Heidolph, Schwabach, GER
Rotation microtome RM2055	Leica Mikrosysteme Vertrieb GmbH, Nussloch, GER

Semi-Micro Balance series 225SM-DR	Precisa Gravimetrics AG, Dietikon, SUI
Thermomixer® comfort 5355	Eppendorf AG, Hamburg, GER
Tissue Processor STP 420	Microm International GmbH, Merelbeke, BEL
TriVersa NanoMate Nano-electrospray ion source	Advion Inc., Ithaca, NY, USA
Vacuum concentrator plus	Eppendorf AG, Hamburg, GER
Wistar rat	Janvier, Le Genest-Saint-Isle, FRA

3.2 Chemicals

0.9% sodium chloride (0.9% NaCl)	Fresenius Kabi Deutschland GmbH, Bad Homburg, GER
1,4-Dithiothreitol	Carl Roth GmbH & Co., Karlsruhe, GER
10% Glucose	B. Braun Melsungen AG, Berlin, GER
2-Iodoacetamide	Merck KGaA, Darmstart, GER
4-(2-Hydroxyethyl)-1-piperazineethanesulfonic acid (HEPES)	Carl Roth GmbH & Co., Karlsruhe, GER
Acetonitril, ROTISOLV®, HPLC Gradient Grade, Methylcyanid, Cyanomethan	Carl Roth GmbH & Co., Karlsruhe, GER
Amersham™ ECL Plus Western Blotting Detection Reagents	GE Healthcare, Piscataway, NJ
Ammonium bicarbonate	Sigma-Aldrich Chemie GmbH, Taufkirchen, GER
BSA	Merck KGaA, Darmstadt, GER
Calcium chloride ($CaCl_2$)	Merck KGaA, Darmstadt, GER
Canada-balsam	Sigma-Aldrich Chemie GmbH, Taufkirchen, GER
Cutasept® G	BODE Chemie GmbH, Hamburg, GER
Dextran-70	Carl Roth GmbH & Co., Karlsruhe, GER
Eosin	Merck KGaA, Darmstadt, GER
Ethanol	Merck KGaA, Darmstadt, GER
Ethylenediaminetetraacetic acid disodium salt (EDTA)	Sigma-Aldrich Chemie GmbH, Taufkirchen, GER
Formic acid	Merck KGaA, Darmstadt, GER

Glycine	Carl Roth GmbH & Co., Karlsruhe, GER
Hematoxylin	Merck KGaA, Darmstadt, GER
Hydrochloric acid (HCl)	Merck KGaA, Darmstadt, GER
Ketamin 10%	Bela-pharm, Vechta, GER
Paraffin	Engelbrecht Medizin- und Labortechnik GmbH, Wien, AUT
Potassium chloride (KCl)	Merck KGaA, Darmstadt, GER
Potassium dihydrogen phosphate (KH_2PO_4)	Merck KGaA, Darmstadt, GER
Proteome profiler™ array, Rat Cytokine Array Panel A array	R&D Systems GmbH, Wiesbaden, GER
Quantikine® ELISA BMP-2 Immunoassay	R&D Systems GmbH, Wiesbaden, GER
Quantikine® ELISA Mouse/Rat PDGF-BB Immunoassay	R&D Systems GmbH, Wiesbaden, GER
Quantikine® ELISA Mouse/Rat/Porcine/Canine TGF-β1 Immunoassay	R&D Systems GmbH, Wiesbaden, GER
Quantikine® ELISA Rat IL-1β/IL-1F2 Imunoassay	R&D Systems GmbH, Wiesbaden, GER
Quantikine® ELISA Rat IL-6 Immunoassay	R&D Systems GmbH, Wiesbaden, GER
Quantikine® ELISA Rat TNF-α Immunoassay	R&D Systems GmbH, Wiesbaden, GER
Quantikine® ELISA Rat VEGF Immunoassay	R&D Systems GmbH, Wiesbaden, GER
NaCl	Merck KGaA, Darmstadt, GER
Sodium hydroxide (NaOH)	Carl Roth GmbH & Co., Karlsruhe, GER
Disodium hydrogen phosphate (Na_2HPO_4)	Merck KGaA, Darmstadt, GER
Trypsin	Roche Diagnostics GmbH, Mannheim, GER
Xylazine 20%	Riemser Arzneimittel, Greifswald, GER
Compute pI/Mw tool	http://web.expasy.org/compute_pi/
ImageJ software	U.S. National Institutes of Health, Bethesda, Maryland, USA
MASCOT search algorithm version 2.2.06	Matrix Science Ltd., London, UK
Microsoft® Excel software	Microsoft Inc., Redmond, WA, USA
Origin version 8.0	Microcal Software, Northampton, MA, USA
Protein Analysis Through Evolutionary Relationships (Panther)	http://www.pantherdb.org

Proteome Discoverer version 1.0	Thermo Fisher Scientific Inc., San Jose, CA, USA
PubMed	http://www.ncbi.nlm.nih.gov/
SPSS version 17.0	SPSS, Chicago, IL, USA
the International Protein Index (IPI)	http://www.ebi.ac.uk/IPI/IPIhelp.html

3.3 Buffers and solutions

1) ELISA

1.2 M NaOH/0.5 M HEPES	2.4 g NaOH 5.95 g HEPES fill distilled water to 50 mL

2) HPLC/MS

0.1% Formic acid	100 µL formic acid (100%) fill distilled water to 100 mL
50% Acetonitrile	10 mL acetonitrile fill distilled water to 20 mL
5 mM Ammonium bicarbonate	8 mg ammonium bicarbonate fill distilled water to 20 mL
10 mM Dithiothreitol	31 mg dithiothreitol fill 5 mM ammonium bicarbonate to 20 mL
100 mM Iodoacetamide	360 mg iodoacetamide fill 5 mM ammonium bicarbonate to 20 mL
Wash solution	10 mL 50% methanol 1 mL 5% acetic acid fill distilled water to 20 mL

3) Microdialysis

5% BSA	50 mg BSA 1 mL 0.9% NaCl
100 mM EDTA	0.37 g fill distilled water to 10 mL
PBS	0.19 g KCl 0.20 g KH_2PO_4 7.94 g NaCl 1.42 g Na_2HPO_4 fill distilled water to 1 L and sterilized by 0.22 µm filter

	pH 7.4
Perfusion fluid (PER)	8.58 g NaCl 0.30 g KCl 0.34 g $CaCl_2 \cdot 2H_2O$ fill distilled water to 1 L and sterilized by 0.22 µm filter pH 6.0
Protein solution	400 pg/mL IL-6 400 pg/mL VEGF 400 pg/mL TGF-ß1 5% BSA/0.9% NaCl Filled 0.9% NaCl to 1 mL

4 Methods

4.1 Background

By searching the literature in PubMed (http://www.ncbi.nlm.nih.gov/), several cytokines and growth factors, which potentially function during the early stage of bone defect healing, were selected to be monitored in the microdialysates or blood plasma for 24 h after bone defects. The eligibility criteria for the selection of those cytokines and growth factors included:

1) The gene expressions or the production of those cytokines and growth factors have been reported within 24 h after bone fracture,
2) The molecular weights of those cytokines and growth factors are less than 100 kDa.

Their nature molecular weight (MW) and isoelectric point (pI) were described by previous researches via searching on PubMed. If not previously described, the MW and pI of the resepective molecule was caluculated by the Compute pI/Mw tool at the ExPASy Molecular Biology Server (http://web.expasy.org/compute_pi/) in Swiss-Prot database to obtain a theoretical value (Gasteiger et al., 2005). By entering the UniProtKB/Swiss-Prot protein identifiers (ID) (e.g. IL6_RAT), theoretical pI/Mw could be calculated according to the amino sequence of the specific protein or the domain of interest of the protein according to the Swiss-Prot database.

4.2 *In vitro* microdialysis

4.2.1 Preparation of the protein solution

The recombinant rat cytokine and growth factors (TGF-β1, IL-6 and VEGF) as lyophilized powders were reconstituted in 2 mL 0.9% NaCl/5% BSA to produce a concentration of 2000 pg/mL for IL-6 and VEGF, and 4000 pg/mL for TGF-β1. Finally, a standard solution yielding 400 pg/mL for each protein was prepared.

4.2.2 Microdialysis sampling procedure

The probes were flushed with perfusates for 15 min at flow rate of 5 µL/min. Afterwards the probes were inserted into the protein mixtures and flushed for 15 min at appropriate conditions. Before starting sample collection, 25 µL protein solution was taken to determine the concentration of the single cytokine or growth factor. Then the probe was immersed into the protein solution placed in Thermomixer® at 37°C. The microdialysates were collected for 4 h at 0.5 µL/min, 2 h at 1.0 µL/min and 1 h at 2.0 µL/min. Once the condition changed, the probe was flushed by perfusate for 15 min for equilibration. Each microdialysate was divided into 3 aliquots and stored at -20°C. PBS, PER and 0.9% NaCl were used as crystalloid

perfusate. The colloids BSA (1%) and Dextran-70 (0.01%–0.4%) were added in certain experiments. To avoid protein degradation 100 mM EDTA was added into the microdialysate to get a final concentration of 10 mM and microdialysates were stored on ice during the whole sampling procedure.

4.3 *In vivo* microdialysis

4.3.1 Surgical procedure

Approval for the animal experiments was obtained from the local animal care committee (AZ 24-9168.11-1/2010-22). Male adult Wistar rats weighting 400-650 g were used and an established femoral critical-size defect (hereinafter referred to bone defect) rat model was employed (Drosse et al., 2008). The animals were anesthetized by an intraperitoneal injection of a mixture of 9 mg ketamine and 1 mg xylazine per 100 g body weight. The right hind limb was shaved and disinfected. A 5-cm skin incision was made along the anterior surface of the right femoral diaphysis. The muscle was carefully dissected from the femur. A titanium-coated polyether ether ketone (PEEK) RatFix^{TM} plate was placed and fixed with 4 screws for mechanical support. A 6-mm mid-diaphysis segmental defect was created with a gigli saw. Then the microdialysis probe was insert and fixed in the defect to avoid dislocation. The wound was closed with suture and wetted with sterile PBS to prevent tissue dehydration. The rat was kept under anaesthesized condition by administration of a mixture of 4.5 mg ketamine and 0.5 mg xylazine per 100 g body weight. Additionally, 1 mL mixture of 0.5 mL 10% glucose and 0.5 mL 0.9% NaCl was administered intraperitoneally. The rats with soft tissue defect were subjected to the identical surgical procedures without creating the bone defect. The microdialysis probe was put between muscle and diaphysis. All rats were sacrificed after the end of the microdialysis. Fig. 4 illustrates the surgical procedure of creating the critical-size bone defect and the experimental setting.

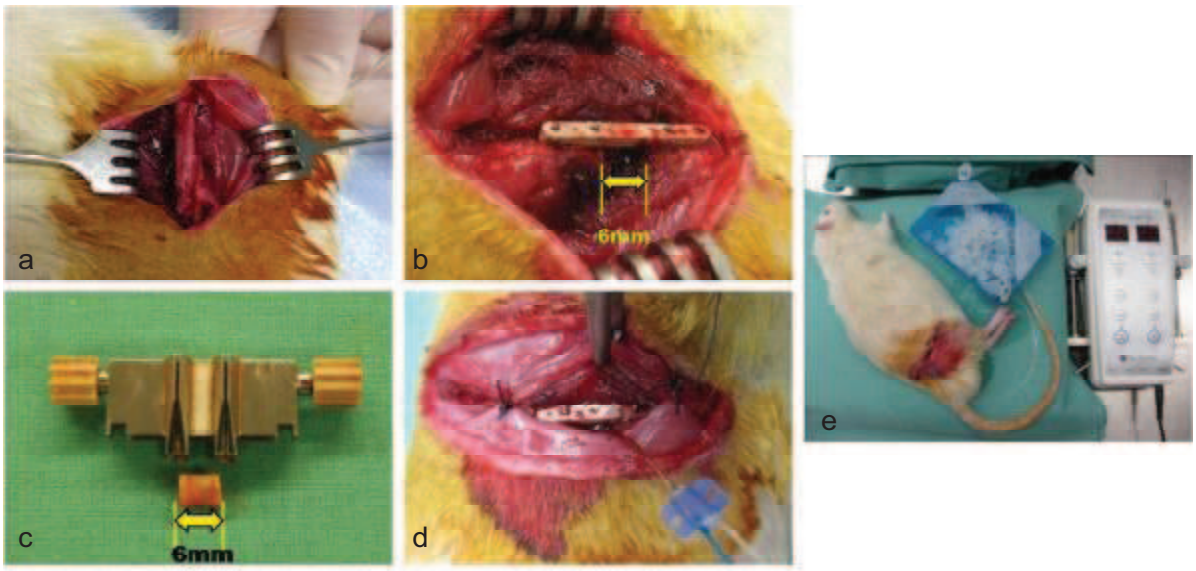

Fig. 4: Surgical procedure to create a critical size bone defect in a rat for microdialysis. **a)** Exposure of the right femur. **b)** Stabilization of the bone defect in the rat femur by a PEEK RatFix^{TM} plate. **c)** Explanted 6-mm mid-diaphysis segment with the drill- & saw guide. **d)** Insertion of the microdialysis probe into the bone defect and fixed to the plate after the bone was stabilized by the plate. **e)** The experimental set-up for *in vivo* microdialysis. The probe was connected to the microdialysis pump. The samples were collected on ice.

4.3.2 Sample collection

To identify the optimal microdialysis conditions, 7 rats were recruited for this study (rats with bone defect, n=4; rats with soft tissue defect, n=3). The probes were perfused at flow rates of 0.5, 1.0 and 2.0 µL/min respectively by perfusing crystalloid perfusate PER or PER adding Dextran-70 (0.01–0.4%) (Table 1, Table 2). The microdialysis probes were flushed with the perfusates at a flow rate of 2.0 µL/min. For each condition, microdialysate was collected hourly throughout the experiment with 15 min equilibration at a flow rate of 2.0 µL/min when condition changed. The microdialysate were stored on ice during sampling procedure. To avoid the protein degradation 100 mM EDTA was added to get the final concentration of 10 mM. After the microdialysis, the probes were stored in -20°C.

Table 1: Microdialysis recovery arrangement for rats with soft tissue defect (n=3). x: start point of microdialysis recovery; →: recovery order for each rat

Flow rate (µl/min)	PER			PER/ 0.04% Dextran-70			PER/ 0.02% Dextran-70			PER/ 0.01% Dextran-70		
	0.5	1.0	2.0	0.5	1.0	2.0	0.5	1.0	2.0	0.5	1.0	2.0
Duration (h)	1	1	1	1	1	1	1	1	1	1	1	1
Right femur	x	→	→	→	→	END						
Left femur							x	→	→	→	→	END

Table 2: Microdialysis recovery time point arrangement for rats with bone defect (n=4).

Flow rate (µl/min)	PER			PER/ 0.4% Dextran-70			PER/ 0.2% Dextran-70			PER/ 0.1% Dextran-70		
	0.5	1.0	2.0	0.5	1.0	2.0	0.5	1.0	2.0	0.5	1.0	2.0
Duration (h)	1	1	1	1	1	1	1	1	1	1	1	1
Rat 1	x	→	→	→	→	→	→	→	END			
Rat 2				x	→	→	→	→	→	→	→	END
Rat 3	→	→	END				x	→	→	→	→	→
Rat 4	→	→	→	→	→	END				x	→	→

Flow rate (µl/min)	PER			PER/ 0.04% Dextran-70			PER/ 0.02% Dextran-70			PER/ 0.01% Dextran-70		
	0.5	1.0	2.0	0.5	1.0	2.0	0.5	1.0	2.0	0.5	1.0	2.0
Duration (h)	1	1	1	1	1	1	1	1	1	1	1	1
Rat 1	x	→	→	→	→	→	→	→	END			
Rat 2				x	→	→	→	→	→	→	→	END
Rat 3	→	→	END				x	→	→	→	→	→
Rat 4	→	→	→	→	→	END				x	→	→

To determine the concentration of certain cytokines and growth factors, microdialysates were collected for 8 h perfusing with PER or 0.9% NaCl (2 h-interval) and 24 h (3 h-interval) perfusing with PER/0.01% Dextran-70 or PER/1% BSA at a flow rate of 2.0 µL/min (Table 3). Moreover, to identify the proteins absorbed on the probes during microdialysis, the probes were explanted after finishing microdialysis. Additionally a probe, which was implanted from 24–48 h after bone defect, was explanted for analysis. All microdialysates and microdialysis probes were stored in -20°C.

Table 3: Microdialysis recovery arrangement to investigate the proteins in the microdialysates after surgery *in vivo*.

Number of rats	Group	Perfusate	Time	Protease inhibitor
6	Bone defect	PER	8 h	-
6	Bone defect	0.9% NaCl	8 h (2 h-interval)	+
3	Bone defect	PER/0.01% Dextran-70	24 h (3 h-interval)	+
8	Bone defect	PER/1% BSA	24 h (3 h-interval)	+
8	Soft tissue defect	PER/1% BSA	24 h (3 h-interval)	+

4.4 Plasma samples

To obtain plasma samples, 50 µL–100 µL blood was collected from the tail vein of rats

with soft tissue defect (n=4) or critical-size bone defect (n=6) in 1.5 mL tubes which contained 50 µL 100 mM EDTA. The collection was executed pre-surgery and after surgery at certain intervals. For 2 rats with soft tissue defect and 4 rats with bone defect, blood samples were collected hourly for 8 h after the surgery. Further, for 2 rats with soft tissue defect and 2 rats with bone defect, the blood samples were collected in 3 h-interval for 24 h after surgery. After centrifuging the samples for 5 min at 3000 rpm, the resulting plasma were collected and stored at -20°C.

4.5 Determination of the fluid recovery

The microdialysate volume was measured immediately after sample collection. The fluid recovery is defined as the percentage of the volume of collected fluid $V_{microdialysate}$ to the theoretical volume of the fluid V_{theory}. The fluid recovery is calculated based on the Eq. 3

$$\text{Fluid recovery} = \frac{V_{microdialyste}}{V_{theory}} \times 100\% \qquad \text{Eq. 3}$$

4.6 Determination of the relative recovery

To determine the RR in the *In vitro* study, the concentration of a certain cytokine or growth factor in a microdialysate (C_d) and in protein solution before collection (C_e) were measured by enzyme-linked immunosorbent assay (ELISA). The RR of a certain cytokine or growth factor is calculated based on the Eq. 2.

$$RR = \frac{C_d}{C_e} \times 100\% \qquad \text{Eq. 2}$$

4.7 Total protein measurement

A sample volume of 2 µL was used for measuring the total protein concentration at wavelength of 280 nm on a NanoDrop-2000 c Spectrophotometer.

4.8 Cytokine and growth factor analysis

The cytokines and growth factors IL-1β, IL-6, TNF-α, TGF-β1, PDGF-BB, VEGF and BMP-2 were determined by ELISA. The samples from *in vitro* study were only analyzed for IL-6, TGF-β1 and VEGF ELISA. Furthermore, to detect further cytokines and chemokines in the microdialysates, a proteome profiler™ array was performed.

4.8.1 IL-1β, IL-6, TNF-α and PDGF-BB ELISA

The 4 cytokines and growth factors IL-1β, IL-6, TNF-α and PDGF-BB were determined by using 4 corresponding individual ELISA kits through a similar procedure. The standards of IL-1β (0–2000 pg/mL), IL-6 (0–4000 pg/mL), TNF-α (0–2000 pg/mL) and PDGF-BB (0–2000 pg/mL) were reconstituted by using corresponding calibrator diluent RD5Y, RD5-16, RD5-17 and RD6-3 in their individual kit respectively.

For IL-1β concentration measurement, 50 µL assay diluents RD1x was added to each well of the microplate which has been pre-coated with monoclonal IL-1β antibody. Then 50 µL standard of IL-1β and the final volume of sample were placed into each well.

For IL-6 concentration measurement, 50 µL assay diluent RD1-54 was added to each well of the microplate which has been pre-coated with monoclonal IL-6 antibody. Then 50 µL standards of IL-6 and the final volume of samples were placed into each well.

For TNF-α concentration measurement, 50 µL assay diluent RD1-41 was added to each well of the microplate which has been pre-coated with monoclonal TNF-α antibody. Then 50 µL standard of TNF-α and the final volume of sample were placed into each well.

For PDGF-BB concentration measurement, 50 µL assay diluent RD1x was added to each well of the microplate which has been pre-coated with monoclonal PDGF-BB antibody. Then 50 µL standard of PDGF-BB and the final volume of sample were placed into each well.

Afterwards the microplates were incubated at room temperature for 2 h. Following washing the microplates 5 times, 100 µl conjugate which contained enzyme-linked polyclonal antibody specific for the corresponding cytokine or growth factor was added in each well. After incubating for 2 h at room temperature, each well was washed 5 times again to remove unbound antibody-enzyme reagent. Then 100 µl substrate was added to each well and the microplates were incubated in the dark for 30 min. The reaction was stopped by adding 100 µL stop solution in each well.

The optical density was read by a microplate reader at 450 nm and 540 nm. Finally, the concentration of each cytokine or growth factor was calculated using the software Origin version 8.0 based on the standard curve. The detection limits were 5 pg/mL for IL-1β, 21 pg/mL for IL-6, 5 pg/mL for TNF-α and 7.7 pg/mL for PDGF-BB according to the instruction in the manual.

4.8.2 VEGF ELISA

The standards of VEGF (0–2000 pg/mL) were reconstituted by using calibrator diluent RD5-3. Then, 50 µL assay diluent RD1-41 was added to each well of the microplate which has been pre-coated with monoclonal VEGF antibody. Afterwards, 50 µL standard of VEGF and the final volume of sample were placed into each well of the microplate. The microplate

was incubated at room temperature for 2 h on the shaker at 300 rpm. Following washing the microplate 5 times, 100 µl conjugate which contained enzyme-linked polyclonal antibody specific for rat VEGF was added in each well. After incubating for 1 h at room temperature on the shaker at 300 rpm, each well was washed 5 times again to remove unbound antibody-enzyme reagent. Then 100 µl substrate was added to each wells and the microplate was incubated in dark for the 30 min. The reaction was stopped by adding 100 µL stop solution in each well. The optical density was read by a microplate reader at 450 nm and 540 nm. Finally, the concentrations of VEGF were calculated using the software Origin version 8.0 based on the standard curve. The detection limit was 8.4 pg/mL according to the instruction in the manual.

4.8.3 TGF-β1 ELISA

The standards of TGF-β1 (0–2000 pg/mL) were reconstituted by using calibrator diluent RD5-53 (1x). Meanwhile, 40 µL final volume of the samples were activated by adding 10 µL 0.1 mM HCl. After incubating for 10 min at room temperature, the samples were neutralized by adding 8 µL 1.2 M NaOH/0.5 M HEPES. Then, 50 µL assay diluent RD1-73 was added to each well of the microplate which has been pre-coated with monoclonal TGF-β1 antibody. Afterwards, 50 µl prepared sample and standard were placed into each well of the microplate. Then the microplate was incubated at room temperature for 2 h. Following washing the microplate 4 times, 100 µl conjugate which contained enzyme-linked polyclonal antibody specific for rat TGF-β1 was added in each well. After incubating for 2 h at room temperature, the each well was washed 4 times again to remove unbound antibody-enzyme reagent. Then 100 µl substrate was added to the wells and the microplate was incubated in the dark for 30 min. The reaction was stopped by adding 100 µL stop solution in each well. The optical density was read by a microplate reader at 450 nm and 540 nm. Finally, the concentration of TGF-β1 was calculated using the software Origin version 8.0 based on the standard curve. The detection limit was 4.6 pg/mL according to the instruction in the manual.

4.8.4 BMP-2 ELISA

A stock solution of BMP-2 was reconstituted by using distilled water: The standards of BMP-2 (0–4000 pg/mL) was prepared by calibrator diluent RD5P (1x). Then, 50 µL assay diluent RD1-193 were added to each well of the microplate which has been pre-coated with monoclonal BMP-2 antibody. Afterwards, 50 µL final volume of standard and sample were placed into each well of the microplate. The microplate was incubated at room temperature for 2 h on shaker at 300 rpm. Following washing the microplate 4 times, 200 µl conjugate which contained enzyme-linked polyclonal antibody specific for BMP-2 was added in each

well. After incubating for 2 h at room temperature on shaker at 300 rpm, each well was washed 4 times again to remove unbound antibody-enzyme reagent. Then 200 µl substrate was added to the wells and the microplate was incubated in the dark for 30 min. The reaction was stopped by adding 50 µL stop solution in each well. The optical density was read by a microplate reader at 450 nm and 540 nm. Finally, the concentration of BMP-2 was calculated using the software Origin version 8.0 based on the standard curve. The detection limit was 11 pg/mL according to the instruction in the manual.

4.8.5 Proteome profiler™ array

The proteome profiler™ array can detect 29 different cytokines and chemokines simultaneously (Table 4). Briefly, microdialysate was collected with PER/1% BSA in 3 h-interval for 6 h from bone defects (n=2) and soft tissue defects (n=2). Then 2 mL block buffer was added into each well of a 4-well multi-dish. A membrane was placed into the multi-dish and then was incubated for 1 h on shaker. Meanwhile, each pooled sample was added to 0.5 mL block buffer and adjusted to a final volume of 1.5 mL. Furthermore, to each sample, 15 µL detection antibody cocktail was added. Afterwards, it was incubated for 1 h at room temperature. After removing the block buffer from the 4-well multi-dish, the sample/antibody mixture was placed into the 4-well multi-dish. Then the membrane was incubated at 4°C overnight on shaker. After washing the membrane with block buffer 3 times for 10 min, 2 mL diluted labeled streptavidin-horseradish peroxidase was added to each well and the membrane was incubated for 30 min at room temperature on shaker. Then the membrane was washed with block buffer 3 times again. Afterwards, the immunoreactive spots were visualized using chemiluminescent reagents Amersham™ ECL Plus Western Blotting Detection system. The membrane was scanned by MF-ChemiBIS 1.6. Histogram profile of each cytokine or chemokine was quantified by mean spot pixel densities (PD) using ImageJ software. The negative control was subtracted from each spot. To normalize the PD between membranes, PD of each spots on each membrane were corrected according to the formula:

$$\text{corrected PD}_{\text{spot on membrane x}} = \frac{\text{Mean PD}_{\text{positive control of all membranes}}}{\text{Mean PD}_{\text{positive control of membrane x}}} \times \text{PD}_{\text{spot on membrane x}}$$

Table 4: Cytokines and chemokines spotted on the membrane in the proteome profile array.

Cytokines and chemokines							
CXCL-1	CXCL-3α	CXCL-2	CNTF	CX3CL1	GM-CSF	sICAM-1	IFN-γ
IL-1α	IL-1β	IL-1ra	IL-2	IL-3	IL-4	IL-6	IL-10
IL-13	IL-17	CXCL-10	CXCL-5	L-Selectin	CXCL-9	CCL3	CCL-20
CCL5	CXCL-7	TIMP-1	TNF-α	VEGF			

CNTF, ciliary neurotrophic factor; GM-CSF, granulocyte-macrophage colony-stimulating

factor; sICAM, soluble form of intercellular adhesion molecule; IFN-γ, interferons-γ; TIMP, tissue inhibitor of metalloproteinases

4.9 Proteomic analysis

Protein mixtures obtained from microdialysates as well as those absorbed on the surface of the microdialysis probes were analyzed by proteomics. The probes were explanted from rats with bone defect after 12 h (n=1), 17 h (n=1), 24 h (n=2) and 24–48 h (n=1) and from rats with soft tissue defect after 15 h (n=1) or 24 h (n=2). The microdialysates collected for 8 h (n=6) were prepared for analysis by Dr. Stefan Kalkhof (Department of Proteomics, The Helmholtz Centre for Environmental Research, Leipzig). The microdialysates were desalted and analyzed by precipitation. Meanwhile, the proteins on the probe were separated by 5–20% gradient sodium dodecyl sulfate polyacrylamide gel electrophoresis (SDS-PAGE) using a constant current of 15 mA for 2 h and 30 mA for 2 h, which was performed by Dr. Ute Hempel (Institute of Physiological Chemistry, TU Dresden). Each lane was cut into 8 slices of approximately 1 cm^2. Each slice was washed twice with 200 µL wash solution for 1 h on shaker. Then, 200 µL of acetonitrile was added. The samples was kept shaking at room temperature for 5 min. The gel pieces were dehydrated for 5 min at room temperature. Afterwards, the proteins on each gel piece was reduced in 60 µL 10 mM dithiothreitol at room temperature shaking for 30 min. Later, proteins in gels were alkylated with 60 µL 100 mM iodoacetamide shaking for 30 min at room temperature. Next 200 µL of acetonitrile was added to the gel pieces for 5 min shaking and then the gel pieces were dehydrated for 5 min. Thereafter each gel piece was rehydrated in 100 µL of 10 mM ammonium bicarbonate for 10 min shaking at room temperature. Then 200 µL of acetonitrile was added for 5 min shaking and the gel pieces was dehydrated for 5 min again. Following, proteins in gel were digested with 20 µL 10 µg/mL trypsin with overnight incubation at 37°C and the reaction was stopped by adding 5% formic acid (final concentration: 2%). The containing peptides were extracted with 50% acetonitrile and later were dried using vacuum centrifugation. The peptides were reconstituted in 20 µL 0.1% formic acid.

The samples were analyzed by nano-high performance liquid chromatography (HPLC) prior to tandem mass spectrometry (MS/MS) (Dr. Stefan Kalkhof, Department Proteomics, UFZ Leipzig). Nano-HPLC system coupled to an orbitrap mass spectrometer via a nanoelectrospray ion source was used.

Database search of proteins derived from the microdialysates and proteins adsorbed on the probes were performed by using Proteome Discoverer utilizing the MASCOT search algorithm using the International Protein Index (IPI) database.

The identified proteins were clustered by Panther (www.pantherdb.org) based on

annotation of cellular component, function, biological process and overrepresented pathway. Moreover, UniProtKB (http://www.uniprot.org/) was used to complete annotation for the unidentified proteins in Panther database.

4.10 Histological analysis

The fracture hematoma were explanted from critical-size bone defect of 5 rats at different time points (9, 12, 24, 45 and 48 h) and were fixed in 4% formalin for 48 h at 4°C. Samples were dehydrated for 8 hours by tissue processor STP 420 using a graded series of ethanol (40%, 70%, 96% and 100%) following clearing using xylene. Then the samples were embedded in paraffin. Sections of 1 µm were cut from the center of the hematoma on a rotation microtome. The sections were incubated for 15 min in hematoxylin, followed by a differentiation step with water for 5 minutes and finally stained with eosin for 1 min. After washing with water to remove the excess dyes from the tissue the sections were mounted in Canada balsam The glass cover lips were placed on top of the slices and the stained tissue sections were analyzed in a Leica light microscope with a Leica camera at magnification of ×400. The amount of mononucleated and multinucleated cells whose nuclei were stained blue were counted per low power field on 30 histological slices per rat.

4.11 Statistical analysis

Samples were analyzed by Kruskal-Wallis test. Furthermore, once a significance was shown, the pair comparison test was performed to compare the data at the different time points or intervals. Mann-Whitney-Wilcoxon test was used to calculate the difference of data between rats with soft tissue defect and rats with bone defect at the same time point or interval. The binomial test was used to compare then protein list to the reference list in the Panther database for determination of overrepresentation of pathway term in Panther. The values of $p<0.05$ were considered statistically significant.

5 Results

5.1 Protein selection

After reviewing the current literature, IL-6, IL-1β, TNF-α, TGF-β1, VEGF, PDGF-BB and BMP-2 were selected for detailed analysis. The molecular weight of these cytokines and growth factors were below 100 kDa and they have been confirmed to be expressed within 24 h after bone fracture (Table 5). Because none of the natural pI and molecular weight of BMP-2 in rats was reported among the previous researches, the theoretical pI and molecular weight of BMP-2 was calculated and tabulated.

Table 5: Physiological properties of the selected cytokines and growth factors.

Protein	Nature MW (kDa)	Theoretical pI
IL-6	21.6 (Wang et al., 2007)	7.7
IL-1β	17.0 (Hazuda et al., 1991)	8.4
TNF-α	51.0 (Shubayev & Myers, 2001)	4.9
TGF-β1	12.5 (Hill et al., 2000)	8.6
VEGF	40.0 (Ray et al., 2000)	9.3
PDGF-BB	30.0 (Han et al., 1992)	9.4
BMP-2	12.9	8.2

5.2 Determination of fluid recovery *in vitro* and *in vivo*

The fluid recovery is a parameter to identify the level of fluid loss and indexes the potential of the molecule recovery. To optimize the conditions for microdialysis, the fluid recoveries were analyzed at the flow rates of 0.5, 1.0 and 2.0 µL/min when using PER and PER with different concentrations of colloids (0.01, 0.02 and 0.04% Dextran-70 or 1% BSA). Although there was no statistical significant influences of the flow rate and perfusate on the fluid recovery *in vitro*, the colloid perfusate resulted in a higher fluid recovery at the same flow rate (Fig. 5). At flow rate of 2.0 µL/min the fluid recovery was 87.5±2.4% when using PER. The addition of 0.01%, 0.02 or 0.04% Dextran-70 increased the fluid recovery to 99.2±5.3%, 99.6±0.6% and 91.2±1.8% at the same flow rate. PER also induced the lower fluid recovery at flow rate of 0.5 µL/min (67.1±5.3%) and 1.0 µL/min (82.5±1.2%), whereas after adding colloids into PER the fluid recovery increased above 83.6±1.8% and 91.2±1.8% at flow rate of 0.5 and 1.0 µL/min respectively.

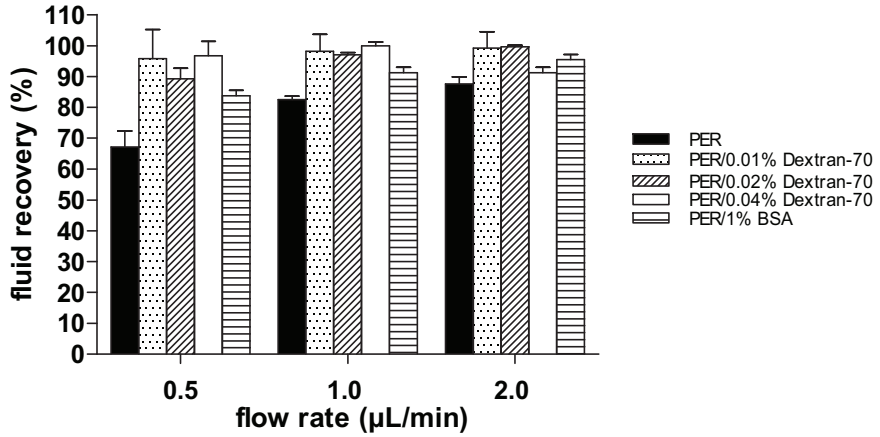

Fig. 5: Fluid recovery from *in vitro* microdialysis perfused under the different conditions. Data represent mean±standard deviation (SD) and n=2 for each condition. The samples were collected for 4 h at 0.5 µL/min, 2 h at 1.0 µL/min or 1 h at 2.0 µL/min and at each flow rate. The probes were perfused with PER, PER/0.01% Dextran-70, PER/0.02% Dextran-70, PER/0.04% Dextran-70 or PER/1% BSA.

In vivo, the fluid recovery was determined when using PER or PER with 0.01–0.4% Dextran-70 at various flow rates of 0.5, 1.0 and 2.0 µL/min from rats with bone defect (n=4) and rats with soft tissue defect (n=3).

The results of the fluid recovery from rats with soft tissue defects were given in Fig. 6. Perfusing PER and PER/0.02% Dextran-70 exhibited lower fluid recovery (86.2±9.3% and 92.2±8.4%) which was used at the initial 1 h after surgery at flow rate 0.5 µL/min compared to using PER/0.01% and 0.04% Dextran-70 (101.0±5.1% and 100.0±5.8%). At higher flow rate of 1.0 and 2.0 µL/min, all fluid recoveries were above 98% for all perfusates.

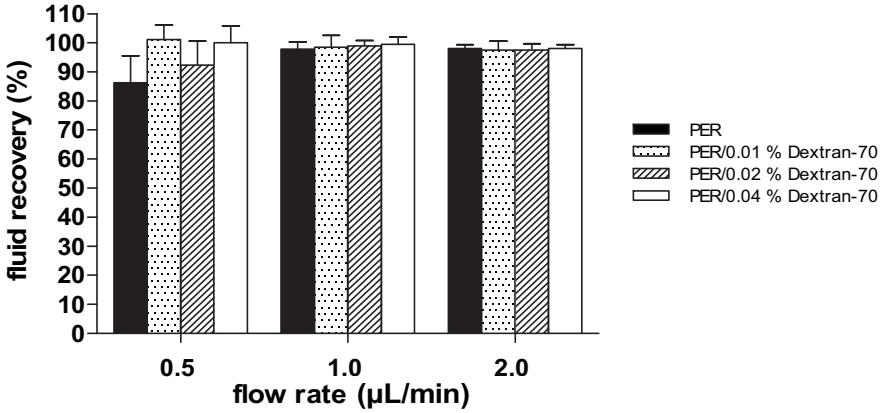

Fig. 6: Fluid recovery from *in vivo* microdialysis in rats with soft tissue defect. Data represent mean±SD and n=3 for each condition. The samples were collected for 1 h at each flow rate (0.5, 1.0 and 2.0 µL/min) using PER, PER/0.01% Dextran-70, PER/0.02% Dextran-70 or PER/0.04% Dextran-70.

In rats with bone defect, sampling procedure started with different perfusates alternatively (Table 2). When the concentration of Dextran-70 in PER were 0.1–0.4%, at a flow rate of 0.5 µL/min, the fluid recovery significantly decreased to 84.4 % after adding 0.2% and 0.4% Dextran-70 in PER ($p<0.05$) (Fig. 7a). When the concentrations of Dextran-70 decreased to 0.01–0.04% in PER, only 2 probe remained to be perfused when using PER/0.01% and 0.02% Dextran-70 due to the death of rats. The flow rates and perfusates did not affect the fluid recovery that was over 95% (Fig. 7b).

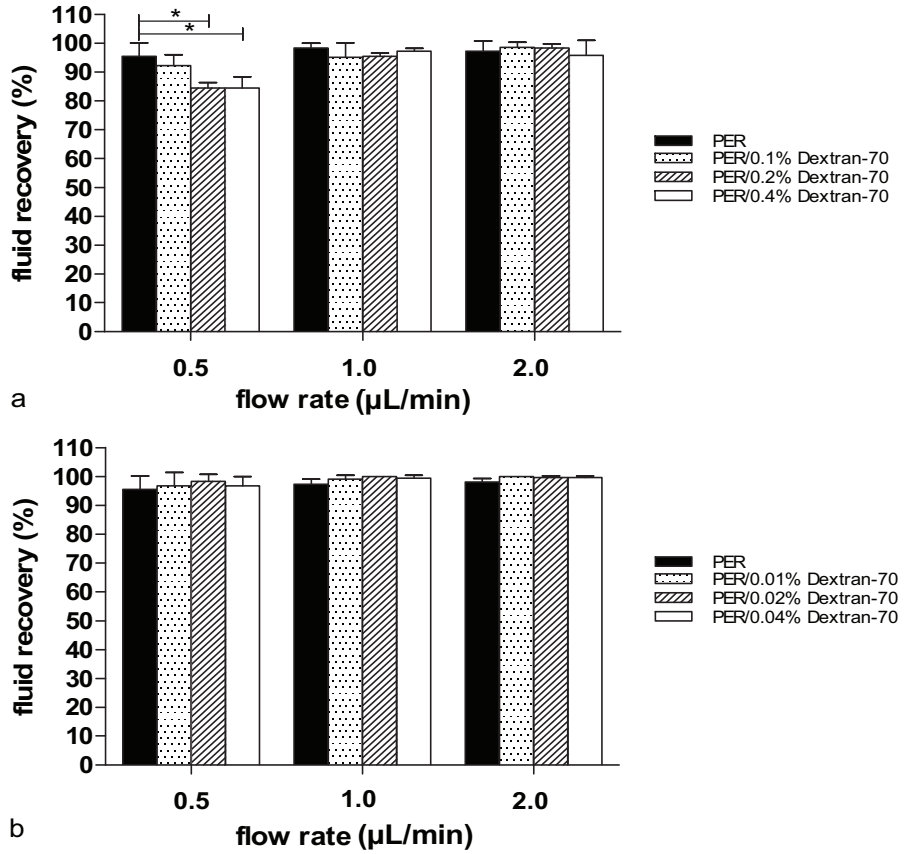

Fig. 7: Fluid recovery from *in vivo* microdialysis in rats with bone defect. Data represent mean±SD. **a)** Samples were collected hourly at flow rates of 0.5, 1.0 and 2.0 µL/min using PER (n=6), PER/0.1% Dextran-70, PER/0.2% Dextran-70 or PER/0.4% Dextran-70 (n=3). **b)** Samples were collected hourly at flow rates of 0.5 (n=2), 1.0 and 2.0 µL/min using PER (n=6), PER/0.01% Dextran-70, PER/0.02% Dextran-70 and PER/0.04% Dextran-70 (n=3). (* $p<0.05$)

To investigate the temporal profiles of the fluid recovery, the microdialysates were collected in 3 h-interval for 24 h when using colloid perfusates at a flow rate of 2.0 µL/min. There were no significant differences of the fluid recovery among the three conditions for 24 h (Fig. 8). Moreover, for all 3 conditions the fluid recovery was over 90% and since

interval of 6–9 h, the fluid recovery was above 95%. Further, the surgery type also did not affect the fluid recovery. For rats with bone defect as well as for rats with soft tissue defect the fluid recoveries were above 95% at 2.0 µL/min (Fig. 8).

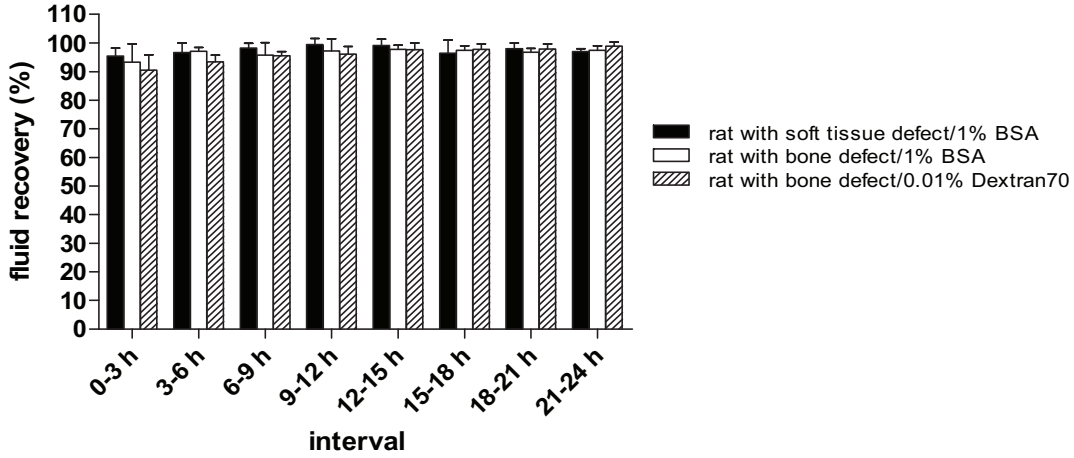

Fig. 8: Temporal profiles of fluid recovery from *in vivo* microdialysates. Data represent mean±SD. Samples were collected at a flow rate of 2.0 µL/min in 3 h-intervals for 24 h. PER/1% BSA was perfused in rats with bone defect and rats with soft tissue defect (n=8), and PER/0.01% Dextran-70 was perfused in rats with bone defect (n=3).

5.3 Determination of relative recovery (RR) *in vitro*

To estimate the RR *in vitro*, mixtures of IL-6, TGF-β1 and VEGF was recovered at different conditions. The crystalloid perfusates (0.9% NaCl, PBS or PER) and the colloid perfusates (0.9% NaCl/1% BSA, PBS/1% BSA, PER/1% BSA, PER/0.01% Dextran-70, PER/0.02% Dextran-70 and PER/0.04% Dextran-70) were perfused at flow rates of 0.5, 1.0 and 2.0 µL/min. EDTA was added in the sampling tubes in attempt to avoid degradation of the proteins. However, EDTA did not influence RR. VEGF concentration was below the detection limit of ELISA among all samples. The detection of IL-6 and TGF-β1 was tabulated in Table 6.

Table 6: The detection of IL-6 and TGF-β1 *in vitro* microdialysate when using different perfusates. *, n=1; **, n=2; ***, n=4 for IL-6 and n=2 for TGF-β1; ****, n=5 for IL-6 and n=3 for TGF-β1; -, not detected; +, detected in single microdialysates (less than half); ++, detected in most microdialysates; +++ detected in all microdialysates.

Perfusate	IL-6	TGF-β1
0.9% NaCl*	-	-
PBS*	-	-
PER****	+	+
0.9% NaCl/1% BSA**	+	+++
PBS/1% BSA*	-	+++
PER/1% BSA****	++	+++
PER/0.01% Dextran-70**	+	+
PER/0.02% Dextran-70***	+	+
PER/0.04% Dextran-70***	+	++

TGF-β1 was undetectable in the microdialysates collected when using crystalloid perfusates. When using colloid perfusates, TGF-β1 was detected. Among the different crystalloid perfusates, the highest RR was 11.2% at flow rate of 0.5 µL/min when using PER/1% BSA (Fig. 9). Further, at the same flow rate adding 1% BSA to PER had a higher RR (6.3–11.2% at a flow rate of 0.5 µL/min, 4.7–8.0% at a flow rate of 1.0 µL/min and 0–10.2% at a flow rate of 2.0 µL/min) than adding 0.01–0.04% Dextran-70 to PER (0–7.1% at a flow rate of 0.5 µL/min, 0–4.6% at a flow rate of 1.0 µL/min and 0% at a flow rate of 2.0 µL/min) (Fig. 9).

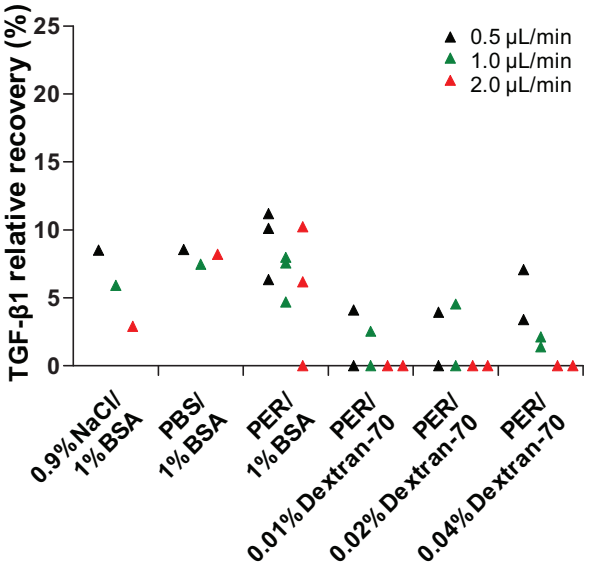

Fig. 9: Relative recovery of TGF-β1 from *in vitro* microdialysis. Data represent individual values. The probes were perfused with 0.9% NaCl/1% BSA (n=1), PBS/1% BSA (n=1),

PER/1% BSA (n=3), PER/0.01% Dextran-70 (n=2), PER/0.02% Dextran-70 (n=2) and PER/0.04% Dextran-70 (n=2) at flow rates of 0.5, 1.0 and 2.0 µL/min. Samples were collected for 4 h at 0.5 µL/min, 2 h at 1 µL/min or for 1 h at 2 µL/min.

Among the crystalloid perfusates, IL-6 was only detected using PER *in vitro*. However, at different flow rates (0.5–2.0 µL/min) IL-6 was detected in 4 out of 15 microdialysates with the highest RR of 15.0%. After adding BSA to perfusates, IL-6 was detected in 9 out of 21 microdialysates with maximal RR of 23.6% when using 0.9% NaCl/1% BSA at flow rate of 0.5 µL/min (Fig. 10). When adding different colloids in PER, IL-6 was detected in 8 out of 15 microdialysates using PER/1% BSA with maximal RR 20.4% at flow rate of 1.0 µL/min. Whereas IL-6 was detectable in 5 out of 30 microdialysates using PER/(0.01–0.04%) Dextran-70 with maximal RR 7.1% at flow rate of 1.0 µL/min (Table 6, Fig. 10).

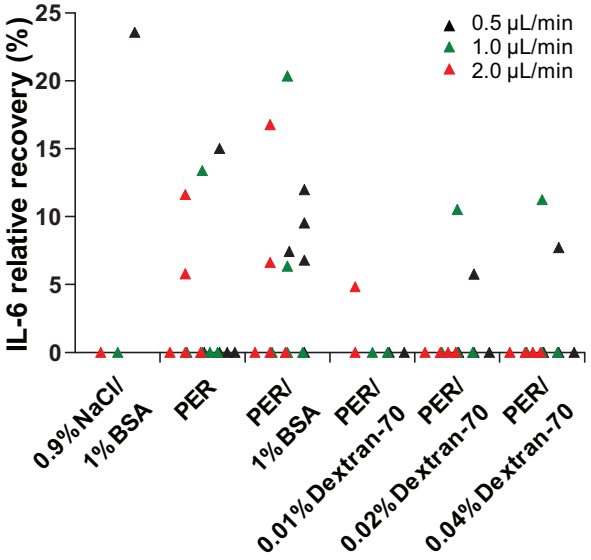

Fig. 10: Relative recovery of IL-6 from *in vitro* microdialysis. Data represent individual values. The probes were perfused with 0.9% NaCl/1% BSA (n=1), PER (n=5), PER/1% BSA (n=5), PER/0.01% Dextran-70 (n=5), PER/0.02% Dextran-70 (n=5) or PER/0.04% Dextran-70 (n=2) at the flow rates of 0.5, 1.0 and 2.0 µL/min. Samples were collected for 4 h at 0.5 µL/min, 2 h at 1 µL/min or for 1 h at 2 µL/min.

5.4 Determination of total protein concentration *in vivo*

The total protein concentration was an index of recovery efficiency for *in vivo* microdialysis to optimize recovery conditions. In rats with soft tissue defect, the total protein concentration decreased with increasing flow rates regardless of perfusates but without statistical significant (n=3) (0.26±0.14–0.80±0.13 mg/mL at a flow rate of 0.5 µL/min, 0.17±0.06–0.22±0.07 mg/mL at a flow rate of 1.0 µL/min, 0.08±0.06–0.11±0.06 mg/mL at a flow rate of 2.0 µL/min) (Fig. 11). Dextran-70 did not increase the concentration of total

protein in microdialysates. The total protein concentrations of microdialysates that were collected when using PER and PER/0.02% Dextran-70 at the flow rate of 0.5 µL/min were higher because microdialysis started without equilibration and these had been the condition immediately after surgery.

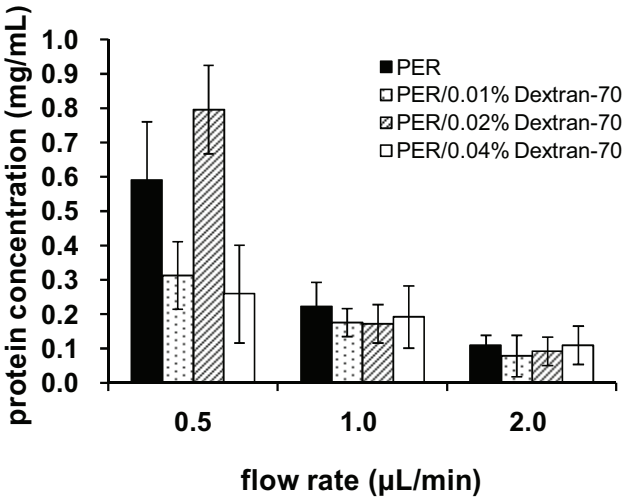

Fig. 11: Total protein concentrations from *in vivo* microdialysates. Data represent mean±SD. PER and PER adding 0.01%, 0.02% and 0.04% Dextran-70 were used as perfusates at the flow rates of 0.5, 1.0 and 2.0 µL/min (n=3) collected hourly from rats with soft tissue defect.

In rats with bone defect addition of Dextran-70 neither significantly increased the concentration nor the amount of total protein in microdialysates (n=4). At a flow rate of 2.0 µL/min the concentration of total protein was 0.12±0.07 mg/mL when using PER, whereas the concentrations were 0.11±0.02–0.21±0.08 mg/mL when adding 0.01–0.4% Dextran-70. The concentration of total protein decreased with increasing flow rates from 0.60±0.14 mg/mL to 0.10±0.06 mg/mL (Fig. 12). Therefore, all perfusates can be used for microdialysis. Nevertheless, using PER/0.01% and 0.2% Dextran-70 at a flow rate of 2.0 µL/min recovered more amounts of total protein than using other perfusates. Concerning to the little effects of the flow rates on RR and higher amount of protein obtained, a flow rate of 2.0 µL/min was used during microdialysis study to increase the sample volumes.

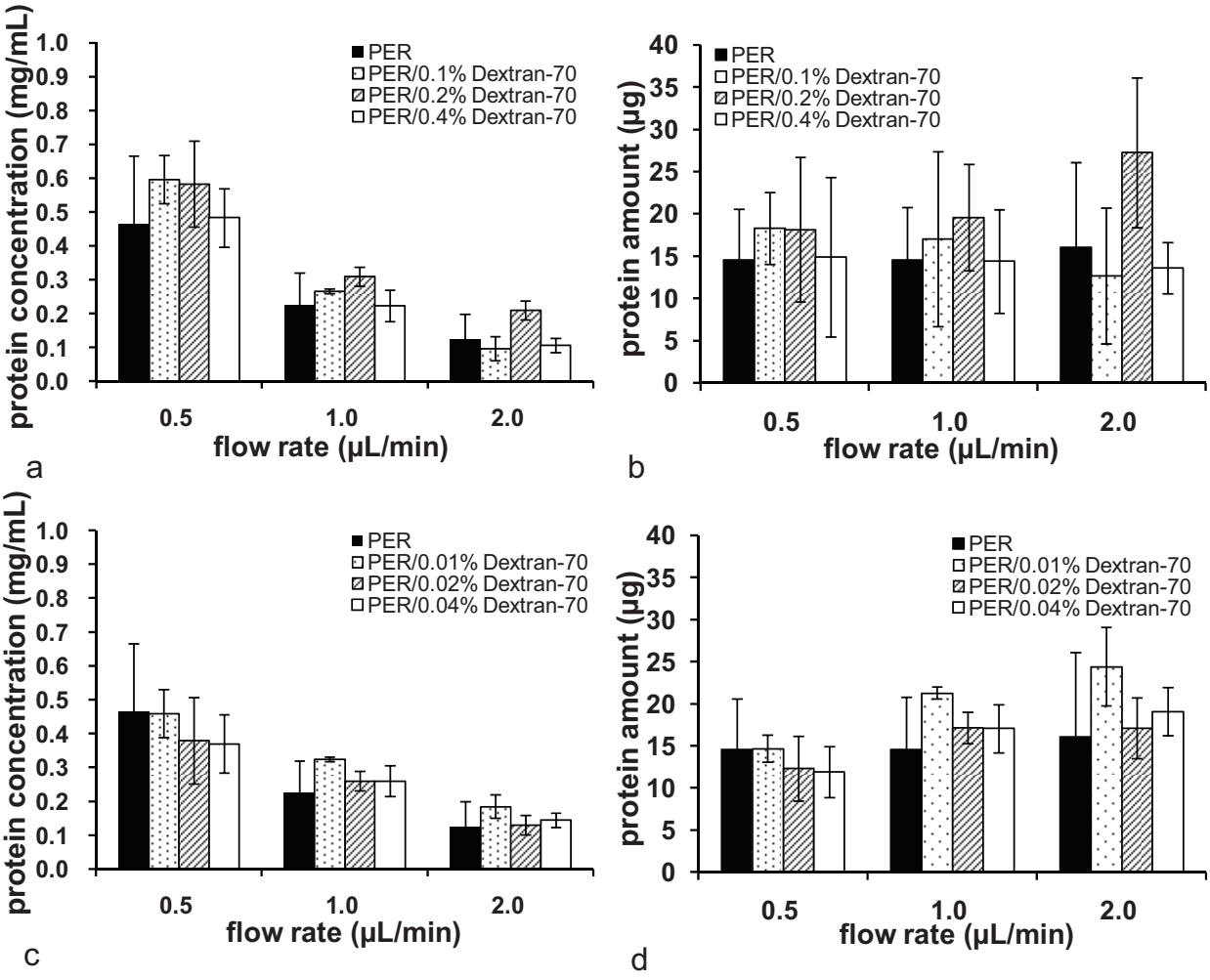

Fig. 12: Concentration and amount of total protein from *in vivo* microdialysates in rats with bone defect. Data represent mean±SD. **a, b)** Samples were collected using PER (n=6), PER/0.1% Dextran-70, PER/0.2% Dextran-70 and PER/0.4% Dextran-70 (n=3) at flow rates of 0.5, 1.0 and 2.0 µL/min. **c, d)** Samples were collected using PER (n=6), PER/0.01% Dextran-70 (n=3), PER/0.02% Dextran-70 (n=2) and PER/0.04% Dextran-70 (n=2) at the flow rates of 0.5, 1.0 and 2.0 µL/min. **a, c)** showed the concentration of total protein and **b, d)** showed the amount of total protein.

The total protein concentration was determined in microdialysates collected from rats with bone defect at a flow rate of 2.0 µL/min. The microdialysates were collected for 8 h when using PER (n=6), for 8 h in 2 h-intervals when using 0.9% NaCl (n=6) and in 3 h-intervals for 24 h when using PER/0.01% Dextran-70 (n=3) (Fig. 13). After collecting 8 h the concentration of total protein was 0.36±0.24 mg/mL. For both interval series, total protein concentration peaked in the first 2 h- and 3 h-interval sample with 0.20±0.12 mg/mL and 0.44±0.18 mg/mL (Fig. 13). After the first interval, the concentrations of total protein decreased to 0.14–0.17 mg/mL when using 0.9% NaCl for 8 h, and decreased to 0.15–0.23 mg/mL when perfusing PER/0.01% Dextran-70 for 24 h. For both series, after the

first interval the concentration of total protein was constant over time.

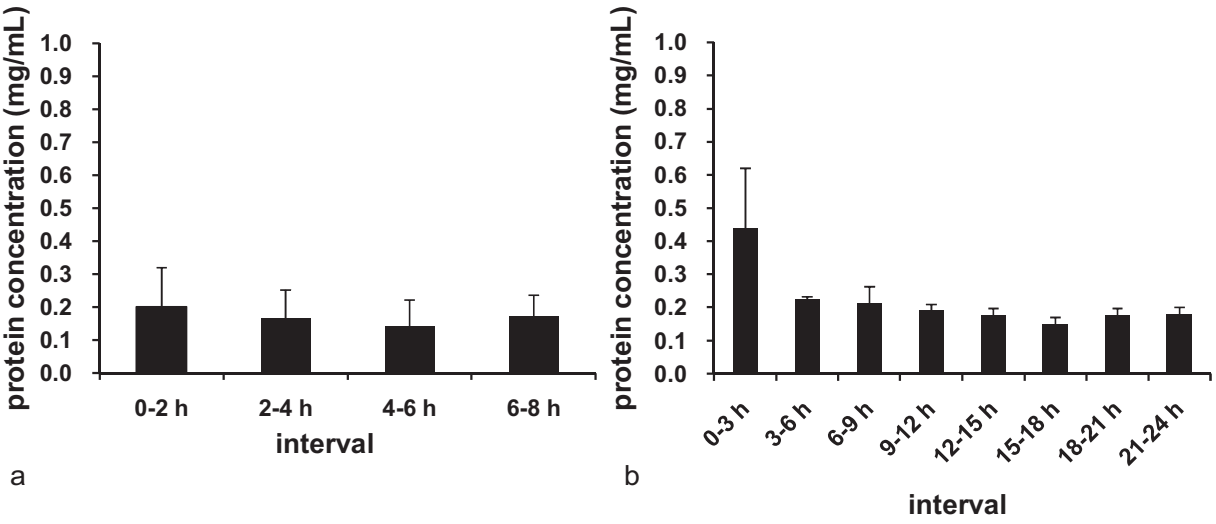

Fig. 13: Total protein concentrations from *in vivo* microdialysates. Samples were collected in rats with bone defect at a flow rate of 2.0 µL/min. Data represent mean±SD. **a)** Samples were collected for 8 h in 2 h-intervals by perfusing 0.9% NaCl (n=6). **b)** Samples were collected in 3 h-intervals for 24 h by perfusing PER/0.01% Dextran-70 (n=3).

5.5 Determination of cytokine and growth factor concentration in the microdialysate *in vivo*

The concentrations of IL-6, IL-1β, TNF-α, TGF-β1, VEGF, PDGF-BB and BMP-2 were determined by ELISA in microdialysates collected from rats with bone defect using PER for 8 h (n=6 rats), using 0.9% NaCl for 8 h in 2 h-interval (n=6), PER/0.01% Dextran-70 (n=3) or PER/1% BSA (n=8) in 3 h-interval for 24 h. The concentrations of these cytokines and growth factors were also determined in microdialysates collected from 6 rats with soft tissue defect for 24 h in 3 h-interval with PER/1% BSA (n=8). The flow rate was 2.0 µL/min for all experiments.

5.5.1 IL-6 concentration

During 8 h perfusion of PER, IL-6 was detectable among 5 of 6 microdialysates with a mean of measurable IL-6 of 124.7±17.5 pg/mL. By perfusing 0.9% NaCl for 8 h in 2 h-intervals, IL-6 was detectable in 2 of 6 rats with a slight increasing concentration from 105.4±28.4 pg/mL in 0–2 h interval after surgery to 172.2±17.5 pg/mL in 6–8 h interval after surgery (Fig. 14a). When using PER/0.1% Dextran-70 as perfusate, IL-6 was detectable in only 6 of 24 microdialysates (n=3). The highest IL-6 concentration was detected in the interval of 6–9 h (241.3 pg/mL) (Fig. 14b).

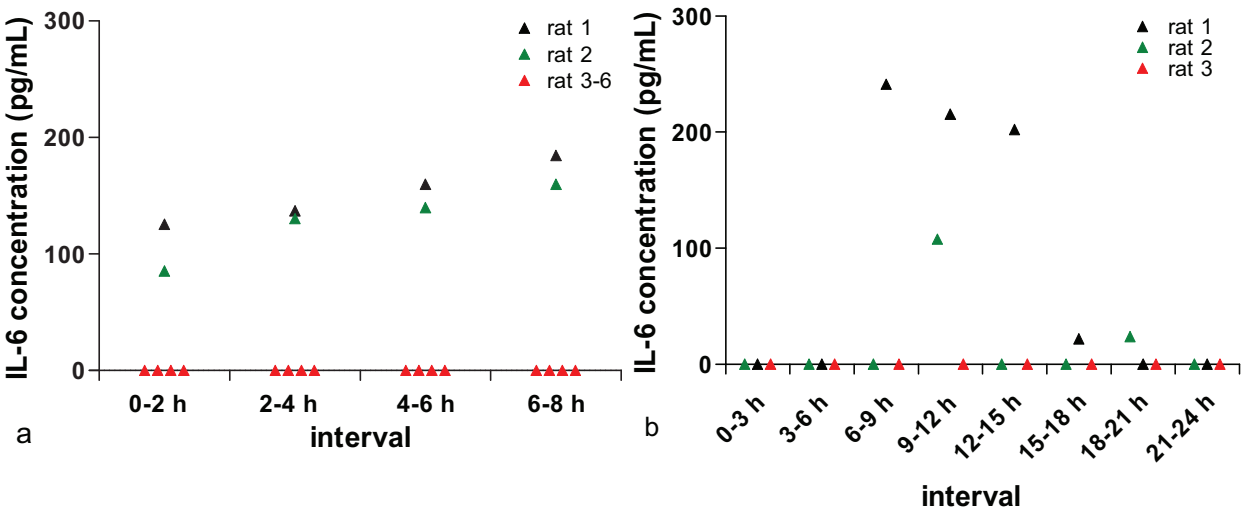

Fig. 14: IL-6 concentration from *in vivo* microdialysates. Data represent individual values. **a)** Samples were collected for 8 h in 2 h-intervals when perfusing 0.9% NaCl in rats with bone defect at 2.0 µL/min (n=6). **b)** Samples were collected in 3 h-intervals for 24 h when perfusing PER/0.01% Dextran-70 in rats with bone defect at 2.0 µL/min (n=3).

With PER/0.01% Dextran-70 or 0.9% NaCl no continuous collection of IL-6 was possible. When perfusing PER/1% BSA, IL-6 was continuously detectable in 3 h-intervals for 24 h from the rats with bone defect (n=8) and with soft tissue defect (n=8). For rats with bone defect, the highest IL-6 concentration (309.1±306.3 pg/mL) was determined in the interval of 12–15 h after surgery but insignificant differences were across all intervals (Fig. 15). After 21–24 h collection the IL-6 concentrations declined to 118.1±121.9 pg/mL. Among the microdialysates from the rats with soft tissue defect, the IL-6 concentration peaked in 6–9 h interval with 579.5±277.3 pg/mL, and then decreased to 117.8±145.9 pg/mL at final 21–24 h. Moreover, a significant increase in IL-6 concentrations were detected between 0–3 h and 9–12 h and 12–15 h after surgery ($p<0.05$) (Fig. 15). In the interval of 6–9 h the IL-6 concentration was significantly higher in the microdialysates from rats with soft tissue defect (579.5±277.8 pg/mL) than from rats with bone defect (224.1±180.0 pg/mL).

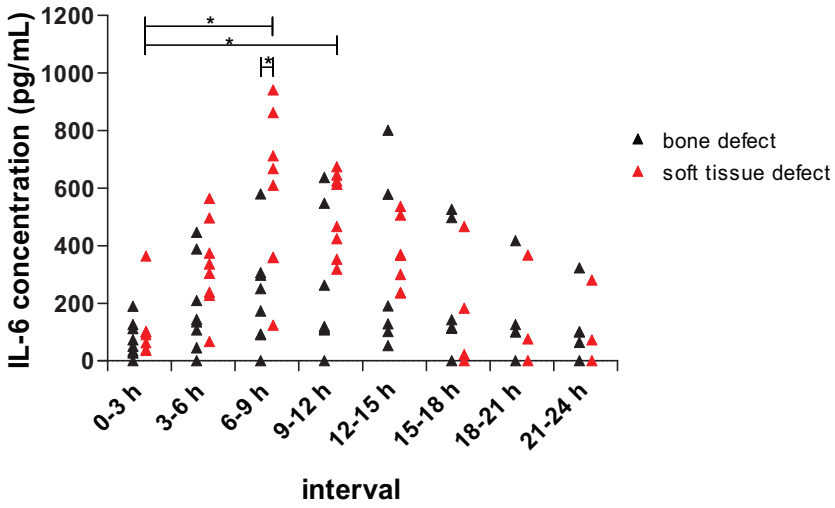

Fig. 15: IL-6 concentration from *in vivo* microdialysates. Data represent the individual values. Samples were collected in 3 h-intervals for 24 h in rats with bone defect and with soft tissue defect (n=8) and determined by ELISA. PER/1% BSA was used as perfusate at a flow rate of 2.0 µL/min. (* $p < 0.05$)

5.5.2 TGF-β1 concentration

TGF-β1 was undetectable in microdialysates when PER/0.01% Dextran-70 or 0.9% NaCl were used as perfusate. During 8 h perfusing by PER, TGF-β1 was only detected in 1 of 6 microdialysates with a concentration of 12.7 pg/mL. Addition of 1% BSA to PER resulted in a continuous detection of TGF-β1. The concentration of TGF-β1 did not show a significant changes for 24 h neither in bone defect nor in soft tissue defect. During 24 h after surgery, the mean concentration of TGF-β1 ranged between 3.6±7.1 pg/mL and 44.7±56.4 pg/mL for rats with bone defect and between 4.1±8.2 pg/mL and 13.5±17.1 pg/mL for rats with soft tissue defect. Moreover, there were no significant differences between the TGF-β1 concentrations from rats with bone defect and rats with soft tissue defect at each 3 h-interval (Fig. 16).

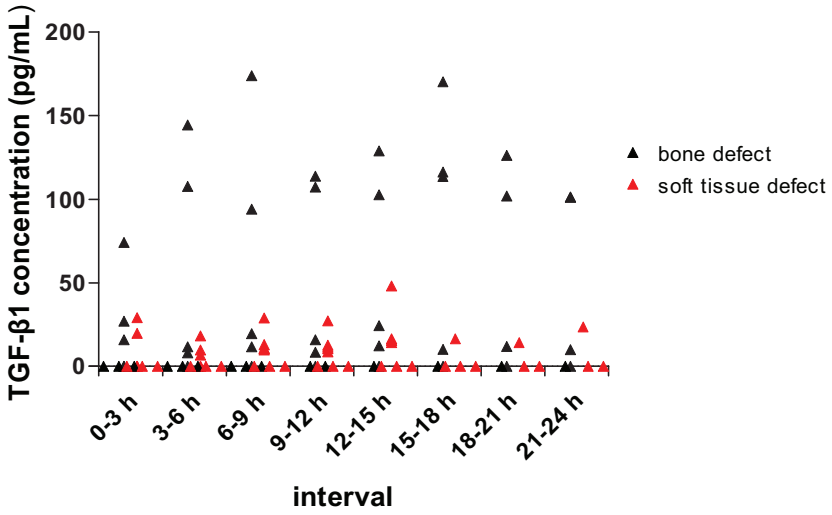

Fig. 16: TGF-β1 concentration from in vivo microdialysates. Data represent the individual values. Samples were collected in 3 h-intervals for 24 h in rats with bone defect and with soft tissue defect (n=8) and determined by ELISA. PER/1% BSA was used as perfusate at a flow rate of 2.0 µL/min.

5.5.3 IL-1β concentration

IL-1β concentration in the microdialysates was below the detection limit of the ELISA when using PER (8 h) or 0.9% NaCl (2 h-intervals) at 2.0 µL/min. Furthermore, IL-1β was undetectable in microdialysates collected from soft tissue defect. Once the colloid 0.01% Dextran-70 (n=3) or 1% BSA (n=3) was added in PER, IL-1β was detectable in 4 of 24 microdialysates when using PER/0.01% Dextran-70 and in 2 of 22 microdialysates when using PER/1% BSA from rats with bone defect. The IL-1β concentrations in microdialysates were collected within 9 h after bone defect between 5.4–7.2 pg/mL when perfusing PER/0.01% Dextran-70, whereas the IL-1β concentrations were 9.56 pg/mL and 30.4 pg/mL from interval of 3–6 h and 6–9 h respectively when perfusing PER/1% BSA.

5.5.4 TNF-α concentration

TNF-α was detectable in 3 microdialysates collected by perfusing PER within 8 h after bone defect with concentrations between 13.4 pg/mL and 26.0 pg/mL. In other series TNF-α was undetectable in microdialysates collected neither from bone defects nor soft tissue defects regardless of the perfusates.

5.5.5 PDGF-BB, BMP-2 and VEGF concentration

The concentrations of VEGF, PDGF-BB, BMP-2 were below the detection limits of ELISA in all microdialysates. iii

5.6 Determination of further cytokines and chemokines in the microdialysate *in vivo*

To identify further proteins which potentially were involved in bone healing, the microdialysates, which were collected by perfusing PER/1% BSA at a flow rate of 2.0 µL/min for 6 h in 3 h-intervals, were analyzed by a proteome profiler™ array. The microdialysates from rats with bone defect (n=2) or with soft tissue defect (n=2) were pooled based on interval of 0–3 h and 3–6 h. Among the 29 designed cytokines and chemokines CXCL-1, CXCL-5 and CXCL-7 were detected in the tested pooled microdialysates (Fig. 17).

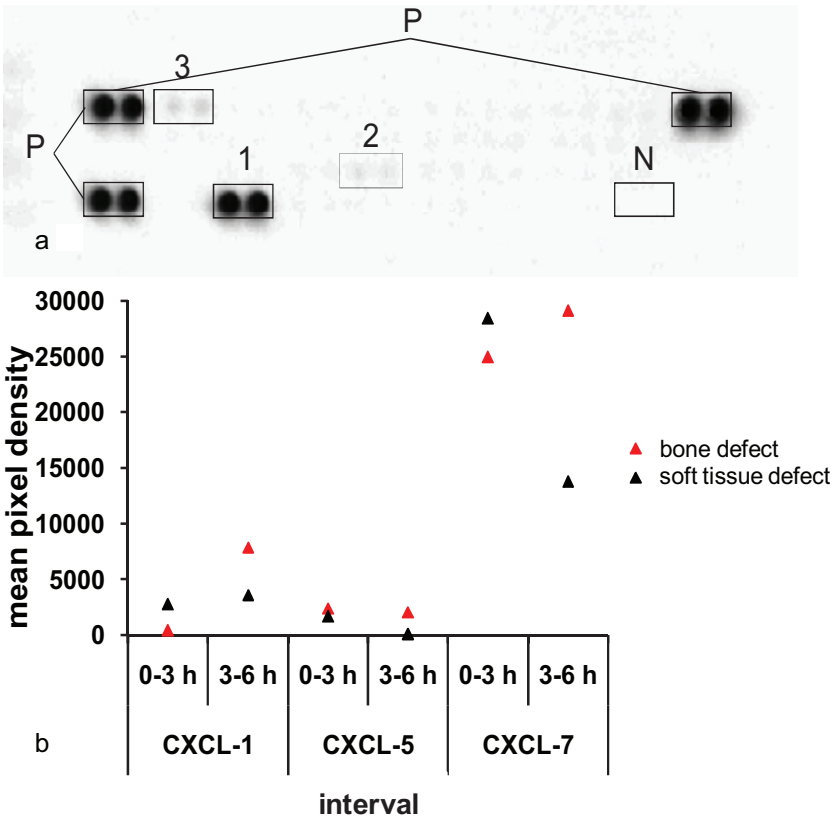

Fig. 17: Rat proteome profiler™ array. Samples were pooled by microdialysates collected for 6 h in 3 h-intervals at a flow rate of 2.0 µL/min from 2 rats with bone defect and with soft tissue defect respectively. **a)** Array analysis revealed the detected cytokines and chemokines in microdialysates. Spot 1, CXCL-7; spot 2, CXCL-5; spot 3, CXCL-1; spot P, positive control; spot N, negative control. **b)** Quantification of pixel density via software ImageJ.

The quantification of the mean PD showed an elevation of the secretion of CXCL-1 in the pooled microdialysates from 0–3 h to 3–6 h after bone defect and soft tissue defect. CXCL-1 was secreted stronger in rats with soft tissue defect than in rats with bone defect during first 3 h-interval. During the interval of 3–6 h after surgery, the secretion of CXCL-1 elevated in rats with bone defect, whereas in rats with soft tissue defect it elevated slightly. CXCL-5 secretion slightly decreased from 0–3 h to 3–6 h after bone defect and soft tissue defect.

Furthermore, in the interval of 3–6 h the level of CXCL-5 decreased in rats with soft tissue defect. Compared to CXCL-1 and CXCdL-5, CXCL-7 was intensively secreted within interval of 0–3 h after bone defect or soft tissue defect. In the interval of 3–6 h the secretion of CXCL-7 slightly increased in the rats with bone defect, while it was reduced 55% in rats with soft tissue defect.

5.7 Protein determination using HPLC-MS/MS analysis

To comprehensively investigate and annotate the proteins recovered in the microdialysates and the proteins absorbed on the probes, the proteins in the microdialysate and on the probe were identified by HPLC-MS/MS. The microdialysates were collected by perfusing PER for 8 h at a flow rate of 2.0 µL/min and the probes had been explanted within 24 h after bone defect or soft tissue defect.

5.7.1 Proteins in the microdialysate

In total, 36 proteins were identified in the 8 h microdialysates collected from 6 rats with bone defect with concentration of 0.37±0.24 mg/mL (Table 7). The molecular weight varied between 9.0 to 3701.5 kDa (median: 32.8 kDa) with 44.4% below 30 kDa and with 78.4% below 100 kDa. A comparison of proteins with the proteins detected on the probe revealed, that 6 proteins were exclusively detected in the microdialysate (Prothymosin alpha; Actin, cytoplasmic 1; Musculoskeletal embryonic nuclear protein 1; Signal recognition particle receptor subunit beta 77 kDa protein; Myotilin; Hbe1 Epsilon 1 globin). But these proteins were ubiquitously produced in cells.

Table 7: Proteins identified from *in vivo* microdialysates collected for 8 h from rats with bone defect by the IPI database via HPLC-MS/MS signal data analysis (n=6).

IPI ID	Protein name	Molecular weight (kDa)
IPI00327075	Musculoskeletal embryonic nuclear protein 1	9.0
IPI00421832	Dermcidin	11.3
IPI00231350	Parvalbumin alpha	11.9
IPI00393595	Prothymosin alpha	12.4
IPI00205036	Hemoglobin alpha 2 chain	15.3
IPI00287835	Hemoglobin subunit alpha-1/2	15.3
IPI00230897	Hemoglobin subunit beta-1	16.0
IPI00231192	Hemoglobin subunit beta-2	16.0
IPI00207146	Zero beta-1 globin	16.0
IPI00212478	Hbe1 Epsilon 1 globin	16.1
IPI00211927	Lysozyme C-1	16.7
IPI00231699	Troponin I, slow skeletal muscle	21.7
IPI00231650	Histone H1.2	22.0
IPI00766273	Similar to Histone H1.2	22.2
IPI00766956	Histone cluster 1, h1b	22.6
IPI00210941	Isoform 2 of Tropomyosin alpha-3 chain	28.7
IPI00197888	Isoform 1 of Tropomyosin alpha-1 chain	32.7
IPI00230775	Isoform 1 of Tropomyosin beta chain	32.8
IPI00393158	33 kda protein	32.9
IPI00767644	Ankyrin repeat domain 2	37.1
IPI00189819	Actin, cytoplasmic 1	41.7
IPI00189813	Actin, alpha skeletal muscle	42.0
IPI00200591	Serine protease inhibitor A3L	46.3
IPI00200593	Serine protease inhibitor A3K	46.5
IPI00195516	Hemopexin	51.3
IPI00190185	Myotilin	55.1
IPI00191737	Serum albumin	68.7
IPI00476177	Signal recognition particle receptor subunit beta 77 kDa protein	76.4
IPI00201262	Alpha-1-inhibitor 3	163.7
IPI00480639	Complement component 3 (fragment)	186.3
IPI00189811	Myosin-7	222.9
IPI00780102	Myosin, heavy polypeptide 1, skeletal muscle, adult	223.1
IPI00476111	Myosin-4	223.4
IPI00554308	Myosin, heavy polypeptide 2, skeletal muscle, adult	223.5
IPI00870537	Nebulin	850.2
IPI00210193	Similar to titin isoform N2-B	3701.5

5.7.2 Proteins on the surface of the probe

To identify the proteins absorbed on probes the proteins were separated by a gradient SDS-PAGE (Fig. 18). Those probes were implanted in rats with bone defect for 12 h (n=1), 17 h (n=1), 24 h (n=2) or 24–48 h (n=1) and rats with soft tissue defect for 15 h (n=1) or 24 h (n=2). Several strong staining bands were visible including a large intensive band at 66 kDa referring to the serum albumin from blood plasma or BSA from perfusate.

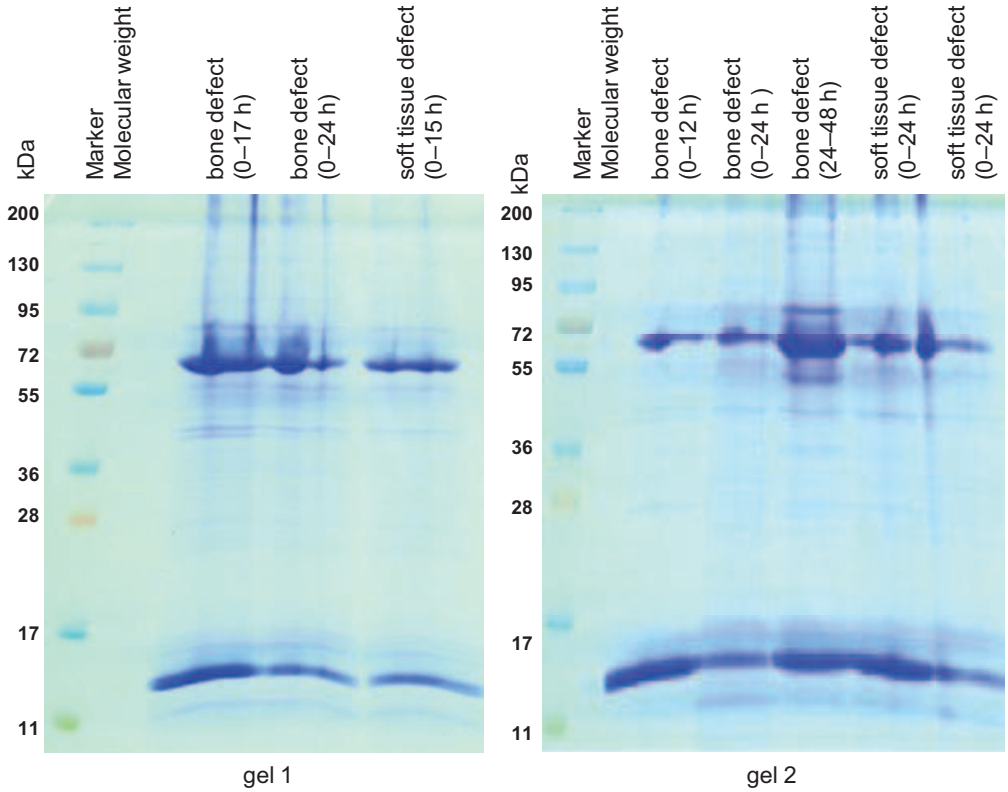

Fig. 18: Gradient SDS-PAGE of the proteins on the probes. The probes implanted in rats with bone defect for 12 h (n=1), 17 h (n=1), 24 h (n=2) or 24–48 h (n=1) and rats with soft tissue defect for 15 h (n=1) or 24 h (n=2).

After HPLC-MS/MS analysis, 1322 different proteins were identified on the probes independent of the probe. Among them 884 proteins were detected on probes implanted in rats with bone defect, 1063 proteins on the probes implanted in rats with soft tissue defect. Out of 259 proteins were exclusively identified in bone defect, 438 exclusively in soft tissue defect and 625 proteins in bone defect as well as in soft tissue defect (Fig. 19).

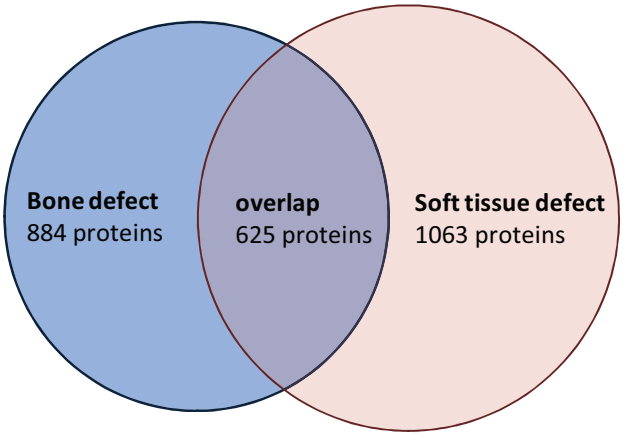

Fig. 19: Distribution of all proteins identified on probe from rats with bone defect and with soft tissue defect. Proteins were represented for each proteome with two circles; subsets in common (in purple) are indicated within the diagram.

The molecular weight of the proteins ranged from 0 to 3701 kDa with a median of 37.7 kDa (Fig. 20). Moreover, 87.9% of the proteins were below the MWCO of the probe. The distribution of the molecular weight was illustrated in Fig. 20.

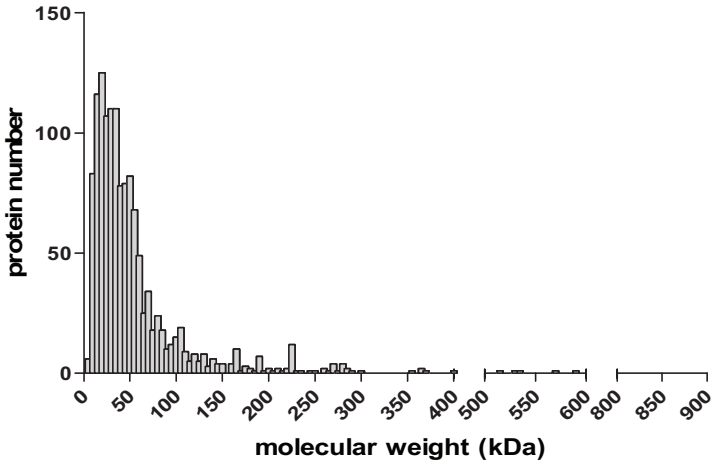

Fig. 20: Distribution of molecular weight of the proteins on the surface of probes. Samples were collected from bone defect and soft tissue defect after explantation (n=8).

5.8 Protein annotation

To allocate the identified proteins from microdialysates and probes to cellular components and biological processes the Panther classification system was used. For the Panther annotation, 19 of 36 (52.8%) proteins in the microdialysates were identified in Panther database. Whereas among the proteins on the probes, 518 of 884 (58.6%) proteins from bone defects and 652 of 1063 (61.3%) proteins from soft tissue defects were identified in Panther database (Table 8). Moreover, the identified protein can be assigned in different

cellular component, biological processes or pathways.

Table 8: Proportion of proteins identified by Panther database for protein annotation.

Sample	Surgery type	Total protein	Identified protein	Percentage
Microdialysate	Bone defect	36	19	52.8%
Probe	Bone defect	884	518	58.6%
	Soft tissue defect	1063	652	61.3%

1) Clustering according to the cellular component

The cellular localization of the proteins is shown in Fig. 21. The proteins in the microdialysates and on the probes had a similar distribution between intracellular and extracellular region. The results show a majority (86.4%-88.9%) of proteins which collected either from microdialysate or probes derived from the cellular origin including protein complex, ribonucleoprotein complex, plasma membrane or intracellular origin. Whereas only a small amount (11.1%–13.6%) were from the extracellular origin.

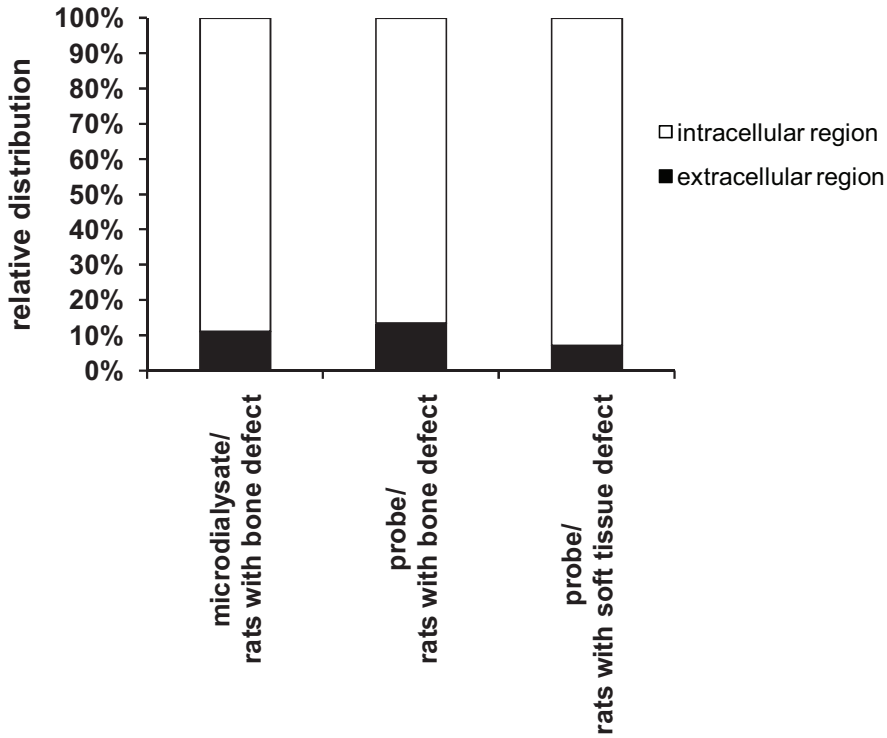

Fig. 21: Distribution of the protein hits in the functional classification of the cellular component against the total number of proteins identified by Panther. Proteins from *in vivo* microdialysates recovered for 8 h in rats with bone defect (n=6). The proteins on the probes implanted in the bone defect for 12–24 h (n=4) and during 24–48 h (n=1), and in the soft tissue defect for 15–24 h (n=3).

2) Clustering according to biological process

In total, 9, 17 and 16 biological processes were identified by analyzing the proteins in the

microdialysates and the probes explanted from rats with bone defect and soft tissue defect (Fig. 22). The distribution of the proteins in the biological process was similar between the probes explanted from rats with bone defect and soft tissue defect (Fig. 22b). For both of them, metabolic processes formed the biggest cluster according to the proteins on the probes. Following the metabolic processes, either in bone defect or in soft tissue defect, the proteins enriched in the clusters of “cellular process”, “cell communication” and “immune system process”. Among the identified processes “immune system process” and “response to stimulus” were important biological processes. Although on the probes from bone defect less kinds of protein were detected, higher percentage of proteins were classified to the category of “immune system process” (21.0% for bone defect *vs.* 16.4% for soft tissue defect) and “response to stimulus” (15.6% for bone defect *vs.* 11.0% for soft tissue defect) (Fig. 22b). Many important humoral proteins were found to be involved in these two processes during bone defect and soft tissue defect healing: They included complement components, chemokines, insulin-like growth factor-binding protein complex acid labile chain, IL-1 receptor antagonist protein (IL-1ra), IL-1 receptor type II (IL-1R2), macrophage migration inhibitory factor (MIF) and similar to coagulation factor IX. Furthermore, with a comparison of selected proteins between bone defect and soft tissue defect, CXCL-2, CXCL-3 and CXCL-7 were only found in rats with bone defect in both processes, while CXCL-4 were only found in rats with bone defect and involved in “immune system process” (Table 9). Moreover, as the children term of “response to stimulus”, in the biological process of “blood coagulation” 17 proteins deriving on probes in bone defect and 9 proteins in soft tissue defect was involved including chemokines, complement components, integrins (Table 10).

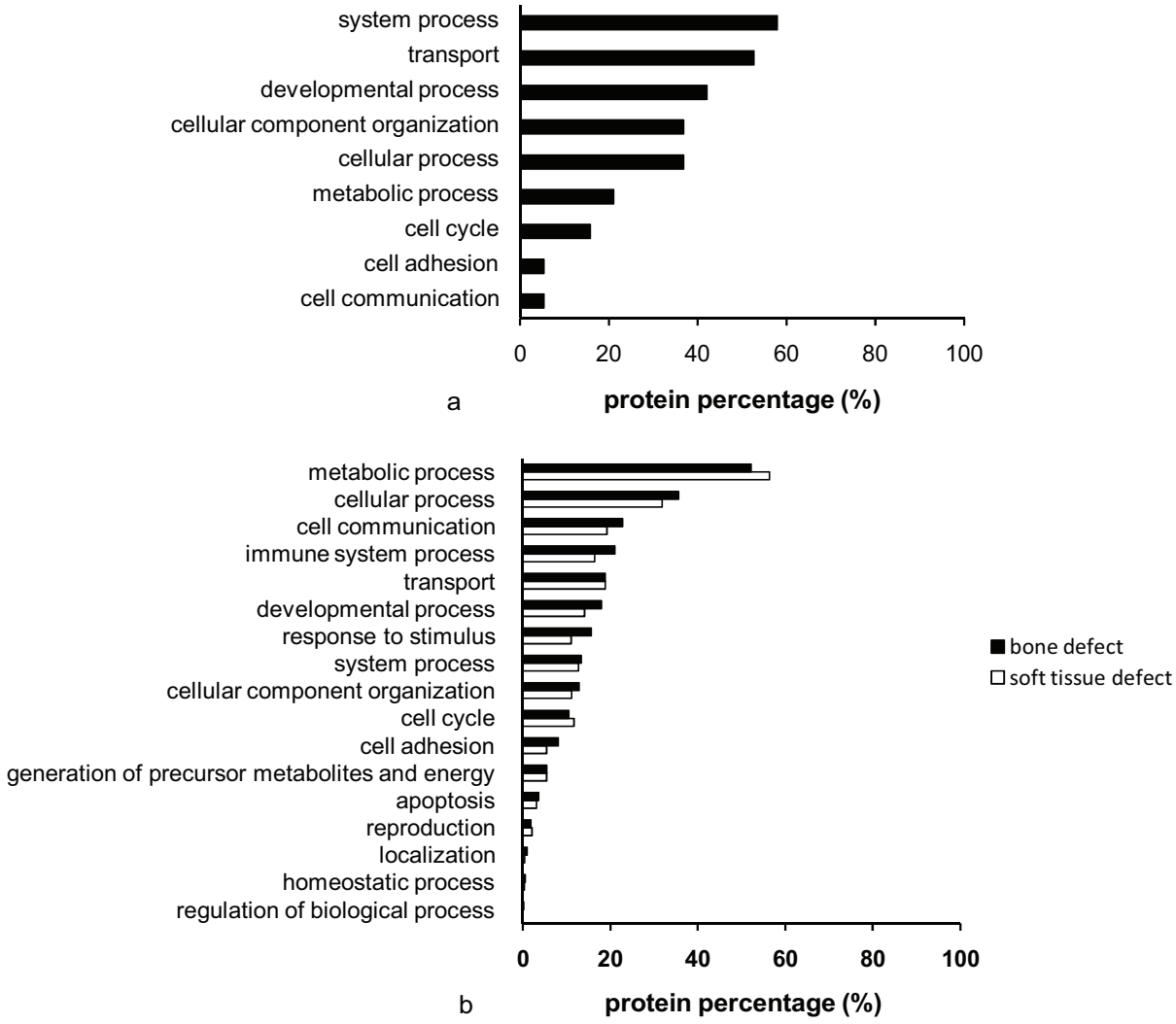

Fig. 22: Biological process classification of identified proteins using Panther classification system. a) Proteins collected from microdialysates for 8 h (n=6). **b)** Proteins from the probes which were implanted in bone defect for 12 h (n=1), 17 h (n=1), 24 h (n=2) or during 24–48 h (n=1) and in soft tissue defect for 15 h (n=1) or 24 h (n=2).

Table 9: Selected important proteins. The tabulated proteins were selected from 107 and 81 proteins involved in “immune system process” and “response to stimulus” on the probes explanted from bone defect, whereas 109 and 72 proteins involved in “immune system process” and “response to stimulus” on probes explanted from soft tissue defect were used for selection. Probes were implanted for 12 h (n=1), 17 h (n=1), 24 h (n=2) or during 24–48 h (n=1) in rats with bone defect and for 15 h (n=1) or 24 h (n=2) in soft tissue defect.

ID	Protein	Immune system process		Response to stimulus	
		Bone defect	Soft tissue defect	Bone defect	Soft tissue defect
IPI00365896	Complement factor properdin	+		+	
IPI00204451	Complement factor I	+		+	
IPI00382185	Da1-24 (protein cfb)	+			
IPI00215296	C1q subcomponent subunit A	+		+	
IPI00215299	C1q subcomponent subunit C	+		+	
Ipi00209973	C4 binding protein, alpha	+	+	+	+
IPI00422037	C4, gene 2	+		+	
IPI00764698	Similar to C5 precursor	+	+	+	+
IPI00331776	C6	+		+	
IPI00780574	C8, gamma polypeptide	+	+	+	+
IPI00231423	C9 protein	+	+	+	+
IPI00188225	C-reactive protein (CRP)	+	+	+	+
IPI00231328	CXCL-2	+		+	
IPI00778837	CXCL-3	+		+	
IPI00206634	CXCL-4	+			
IPI00197780	CXCL-7	+		+	
IPI00194341	Galectin-3	+	+	+	
IPI00202416	Insulin-like growth factor-binding protein complex acid labile chain		+	+	
IPI00214461	IL-1 receptor antagonist protein (IL-1ra)	+	+	+	+
IPI00199341	IL-1 receptor type II (IL-1R2)	+		+	
IPI00230907	MIF	+	+	+	
IPI00765267	Similar to coagulation factor IX	+	+	+	+

Table 10: Proteins on the probes involved in biological process of “blood coagulation” using Panther classification system. The probes were implanted in bone defect for 12 h (n=1), 17 h (n=1), 24 h (n=2) or during 24–48 h (n=1) and in soft tissue defect for 15 h (n=1) or 24 h (n=2).

ID	Protein	Bone defect	Soft tissue defect
IPI00204451	Complement factor I	+	
IPI00382185	Da1-24 (protein cfb)	+	
IPI00554226	Complement component factor h-like 1	+	
IPI00209973	C 4 binding protein, alpha	+	+
IPI00331776	C6	+	
IPI00780574	C8, gamma polypeptide	+	+
IPI00231423	C9 protein	+	+
IPI00231328	CXCL-2	+	
IPI00778837	CXCL-3	+	
IPI00206634	CXCL-4	+	
IPI00197780	CXCL -7	+	
IPI00210900	Protein AMBP	+	+
IPI00565708	Isoform 1 of Haptoglobin	+	+
IPI00765267	Similar to coagulation factor IX	+	+
IPI00778633	Apolipoprotein H	+	+
IPI00198695	Integrin beta	+	
IPI00360541	Integrin beta 2	+	+
IPI00208961	Similar to collagen alpha-1(X) chain precursor	+	

3) Clustering according to pathway analysis

The overrepresented pathway indicated that more involved proteins were presented among the analyzed protein than expected by comparing with the reference proteome data set. In this study, the statistically overrepresented pathways which were clustered from the proteins on the probes were tabulated in Table 11 ($p<0.05$). In total, 518 proteins and 628 proteins on probes explanted from rats with bone defect (n=5) and soft tissue defect (n=3) were identified by panther for statistical overrepresentation test. Although 9 and 11 pathways were significantly over/down-represented in bone defect and soft tissue defect, only 4 and 3 were particularly related with injury healing. The pathways of “blood coagulation”, “integrin signaling” and “inflammation mediated by chemokine and cytokine signaling” were found to be statistically overrepresent both after bone defect and soft tissue defect. Additionally, “FGF signaling” was only significantly overrepresented after bone defect (Fig. 23). Many proteins were involved in the blood coagulation and more proteins were identified in this pathway from bone defect than soft tissue defect (Fig. 24). Particularly, integrin beta, glycoprotein 9 and similar to murinoglobulin 1 homolog were only detected from bone defect. In the pathway of inflammation mediated by chemokine and cytokine signaling, CXCL-4 were only found in bone defect.

On the other hand, among the 19 proteins identified by Panther in the microdialysates, 2

pathways were statistically overrepresented. Nevertheless, only “nicotinic acetylcholine receptor signaling” was specifically related with healing process. There were 3 proteins (actin, alpha skeletal muscle; myosin, heavy polypeptide 1, skeletal muscle, adult; actin, cytoplasmic 1) involved in this pathway.

Table 11: List of the 4 important statistically overrepresented pathways based on the proteins on the probes using Panther statistical overrepresentation test. In total 518 proteins and 628 proteins on probes explanted from rats with bone defect for 12 h (n=1), 17 h (n=1), 24 h (n=2) or during 24–48 h (n=1) and from soft tissue defect for 15 h (n=1) or 24 h (n=2) were involved the analysis. ($p<0.05$)

ID	Protein name	Bone defect		Soft tissue defect	
		No. of protein	p value	No. of protein	p value
Blood coagulation		15	$9.1x10^{-10}$	12	$1.2 x10^{-5}$
IPI00199695	Serine (or cysteine) peptidase inhibitor, clade F, member 2		+		+
IPI00205389	Isoform 1 of fibrinogen beta chain		+		+
IPI00206780	Plasminogen		+		+
IPI00210947	Heparin cofactor 2		+		+
IPI00212666	Isoform 1 of murinoglobulin-1		+		+
IPI00326140	Alpha-1-macroglobulin		+		+
IPI00392886	Alpha-2-macroglobulin		+		+
IPI00515829	Kininogen 1		+		+
IPI00564327	Murinoglobulin-2		+		+
IPI00679245	T-kininogen 2		+		+
IPI00763879	Glycoprotein Ib (platelet), alpha polypeptide		+		+
IPI00765267	Similar to coagulation factor IX		+		+
IPI00198695	Integrin beta		+		
IPI00204686	Glycoprotein 9		+		
IPI00368704	Similar to murinoglobulin 1 homolog		+		
Integrin signalling pathway		26	$1.2x10^{-9}$	22	$3.0x10^{-5}$
IPI00187747	Ras-related protein Rap-1A		+		+
IPI00200773	Skeletal muscle-specific alpha-actinin 3		+		+
IPI0020902	Alpha-actinin-1		+		+
IPI00210097	Isoform 2B of gtpase kras		+		+
IPI00211512	Actin-related protein 2/3 complex subunit 1B		+		+
IPI00213463	Alpha-actinin-4		+		+
IPI00231966	ADP-ribosylation factor 4		+		+
IPI00285606	Isoform 1 of cell division control protein 42 homolog		+		+
IPI00331953	ADP-ribosylation factor 1		+		+
IPI00360356	Actin, beta-like 2		+		+
IPI00360541	Integrin beta 2		+		+
IPI00363022	Similar to actinin alpha 2		+		+
IPI00363395	Ras-related protein Rap-1b		+		+
IPI00363847	Actin-related protein 2/3 complex subunit 5		+		+
IPI00365286	Vinculin		+		+
IPI00365657	Vasp protein		+		+

Table 11: List of the 4 important statistically overrepresented pathways based on the proteins on the probes using Panther statistical overrepresentation test (continued).

IPI00370158	Ras-related C3 botulinum substrate 2		+		+
IPI00422092	Ras-related C3 botulinum toxin substrate 1		+		+
IPI00764535	Actin-related protein 2/3 complex subunit 2		+		+
IPI00768299	Actin related protein 2/3 complex, subunit 3		+		+
IPI00188921	Collagen alpha-2(I) chain		+		
IPI00191114	Ras homolog gene family, member C		+		
IPI00198695	Integrin beta		+		
IPI00208961	Similar to collagen alpha-1(X) chain precursor		+		
IPI00231965	ADP-ribosylation factor 5		+		
IPI00776522	31 kDa protein		+		
IPI00373752	Filamin, beta				+
IPI00565677	289 kDa protein				+
Inflammation mediated by chemokine and cytokine signaling pathway		19	$6.4x10^{-3}$	21	$9.7x10^{-3}$
IPI00189813	Actin, alpha skeletal muscle		+		+
IPI00204077	Ras homolog gene family, member G		+		+
IPI00210097	Isoform 2B of gtpase kras		+		+
IPI00211512	Actin-related protein 2/3 complex subunit 1B		+		+
IPI00285606	Isoform 1 of cell division control protein 42 homolog		+		+
IPI00360356	Actin, beta-like 2		+		+
IPI00360541	Integrin beta 2		+		+
IPI00363847	Actin-related protein 2/3 complex subunit 5		+		+
IPI00366039	Formyl peptide receptor 1		+		+
IPI00370158	RAS-related C3 botulinum substrate 2		+		+
IPI00372040	Arpc4 protein		+		+
IPI00422092	Ras-related C3 botulinum toxin substrate 1		+		+
IPI00764535	Actin-related protein 2/3 complex subunit 2		+		+
IPI00768299	Actin related protein 2/3 complex, subunit 3		+		+
IPI00780102	Myosin, heavy polypeptide 1, skeletal muscle, adult		+		+
IPI00191114	Ras homolog gene family, member C		+		
IPI00776522	31 kda protein		+		
IPI00206634	CXCL-4		+		
IPI00324979	Arachidonate 5-lipoxygenase-activating protein		+		
IPI00208224	Signal transducer and activator of transcription 3				+
IPI00211615	Serine/threonine-protein kinase PAK 2				+
IPI00212655	Guanine nucleotide-binding protein G(I)/G(S)/G(T) subunit beta-1				+
IPI00212658	Guanine nucleotide-binding protein G(I)/G(S)/G(T) subunit beta-2				+
IPI00366042	Similar to formyl peptide receptor, related sequence 2				+
IPI00565677	289 kda protein				+
FGF signaling pathway		11	$3.8x10^{-2}$		
IPI00196661	14-3-3 protein theta		+		
IPI00210097	Isoform 2B of GTPase KRas		+		
IPI00230835	14-3-3 protein gamma		+		
IPI00230937	Phosphatidylethanolamine-binding protein 1		+		

Table 11: List of the 4 important statistically overrepresented pathways based on the proteins on the probes using Panther statistical overrepresentation test (continued).

IPI00231677	14-3-3 protein eta	+
IPI00285606	Isoform 1 of Cell division control protein 42 homolog	+
IPI00324893	14-3-3 protein zeta/delta	+
IPI00325135	14-3-3 protein epsilon	+
IPI00370158	Ras-related C3 botulinum substrate 2	+
IPI00422092	Ras-related C3 botulinum toxin substrate 1	+
IPI00760126	Isoform Short of 14-3-3 protein beta/alpha	+
IPI00196661	14-3-3 protein theta	+
IPI00210097	Isoform 2B of GTPase KRas	+
IPI00230835	14-3-3 protein gamma	+
IPI00230937	Phosphatidylethanolamine-binding protein 1	+
IPI00231677	14-3-3 protein eta	+
IPI00285606	Isoform 1 of Cell division control protein 42 homolog	+

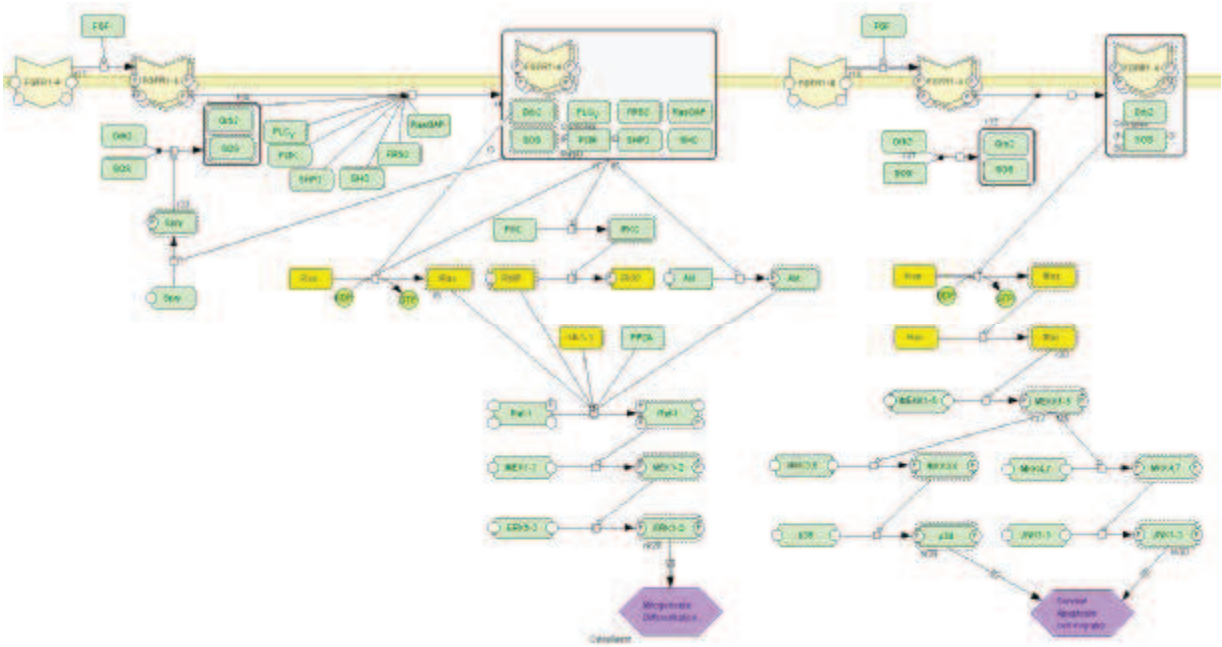

Fig. 23: FGF/FGFR signaling pathway in cells with identified proteins by Panther statistical overrepresentation test. The identified proteins were on probe from rats with bone defect (n=5). FGF signaling is mediated through its binding to FGF receptor which activates ERK1/2, p38 MAPK, SAPK/JNK, PKC and PI3K pathways to induce mitogenisis and differentiation of cells, or survival, apoptosis and migration of cells in various tissue types. Proteins identified on the probes are highlighted in yellow: 14-3-3; Ras (isoform 2B of GTPase KRas); RKIP (Phosphatidylethanolamine-binding protein 1); Rac (RAS-related C3 botulinum substrate 1; Ras-related C3 botulinum toxin substrate 2; isoform 1 of Cell division control protein 42 homolog).

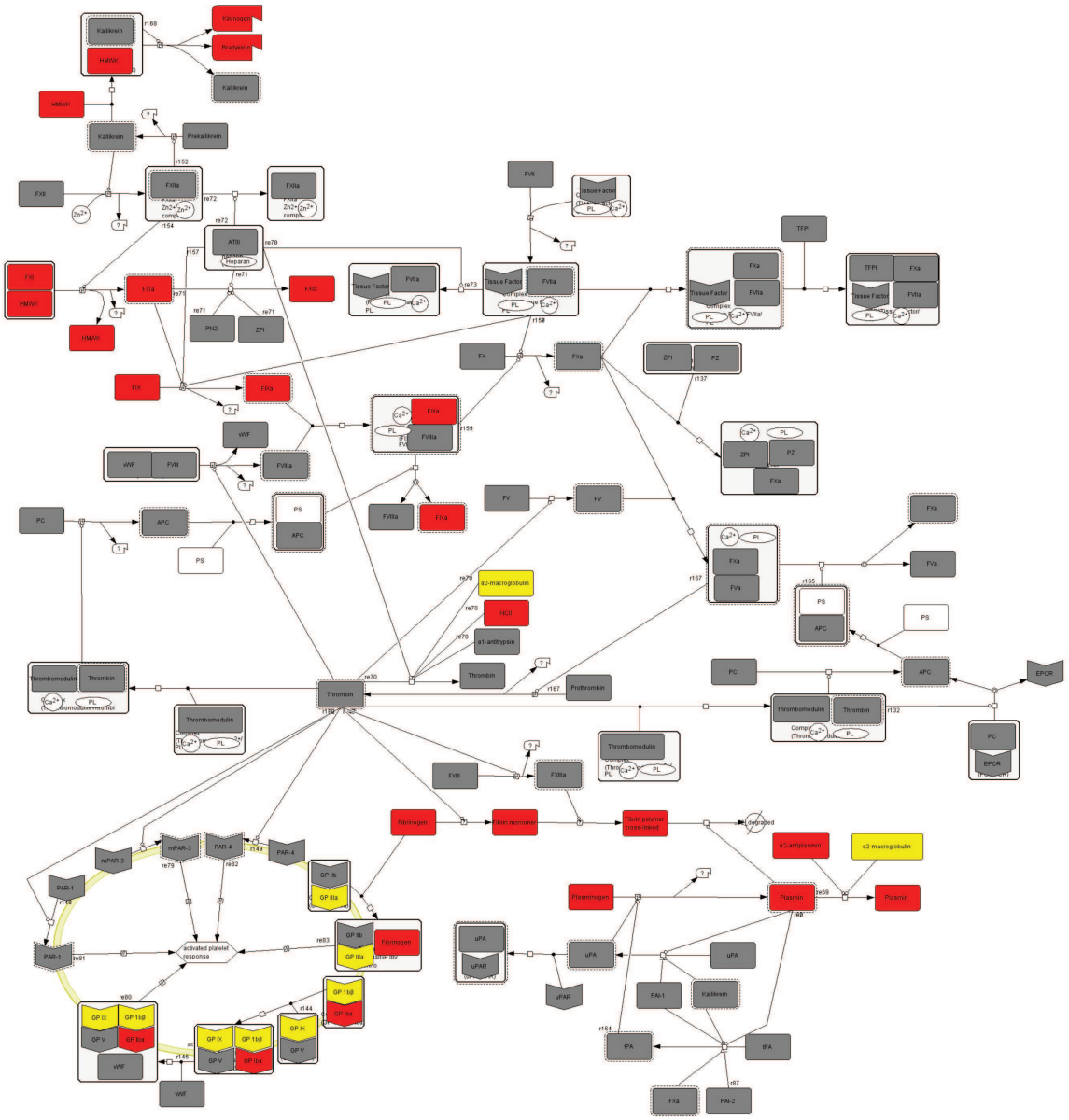

Fig. 24: Blood coagulation pathways with identified proteins by Panther statistical overrepresentation test. Proteins were on probe from rats with bone defect (n=5) and soft tissue defect (n=3). Proteins identified on the probes both from bone defect and soft tissue defect are highlighted in red, while the proteins or the proteins contained the proteins that were only from bone defect are highlighted in yellow: Bradykinin/HMWK/Kinogen (Kininogen 1, T-kininogen 2); FXI/FXIa (similar to coagulation factor IX); Fibrinogen/Fibrin monomer/Fibrin polymer crossed-linked (isoform 1 of fibrinogen beta chain); GPIIIa (integrin beta); GP IX/GP 1bβ (glycoprotein 9); GP 1bα (glycoprotein Ib (platelet), alpha polypeptide); α2-macroglobulin (alpha-1-macroglobulin, alpha-2-macroglobulin, similar to murinoglobulin 1 homolog, isoform 1 of murinoglobulin-1, murinoglobulin-2); HC II (heparin cofactor 2); Plasminogen/Plasmin (plasminogen); α2-antiplasmin (Serine (or cysteine) peptidase inhibitor, clade F, member 2).

4) Functionally relevant proteins

By searching database of Panther, Uniprot or PubMed, a list of important extracellular proteins which were potentially associated with the process of bone healing was selected based on the the total 1322 proteins on probes from rats with bone defect and soft tissue defect and the biological process/pathway analysis using Panther. These 52 selected proteins were extracellular proteins. Moreover, they were involved in the statistical overrepresented pathways and biological processes of “blood coagulation” and others were related to the process of injury healing. These proteins include chemokines (CXCL-2, CXCL-3, CXCL-4 and CXCL-7), complement components (Complement factor I, Da1-24 (protein cfb), Complement component factor h-like 1, C 4 binding protein, alpha, C6, C8, gamma polypeptide, C9 protein and CRP), blood coagulation factor (Similar to coagulation factor IX), MMPs (MMP-8 and MMP-9), ECM proteins (eg. rodent bone protein (RoBo-1), osteonectin and integrins) and other proteins located in the extracellular space. Those selected proteins with the processes and statistical overrepresented pathways were tabulated in (Table 12).

Table 12: The 52 selected proteins which were involved in the bone healing process among all 1322 identified proteins on probe from rats with bone defect and soft tissue defect by HPLC-MS/MS. The probes were implanted in bone defects for 12 h (n=1), 17 h (n=1), 24 h (n=2) or during 24–48 h (n=1) and in soft tissue defects for 15 h (n=1) or 24 h (n=2). The biological processes and statistical overrepresented pathway were analyzed by using Panther. +, detected; n.r, not reported,

ID	Protein name	Bone defect			Soft tissue defect		
			Biologcial process	Statistical overrepresented pathway		Biologcial process	Statistical overrepresented pathway
IPI00187799	Isoform HMW of Kininogen-1	+	n.r	n.r	+	n.r	n.r
IPI00188225	CRP	+	immune system process response to stimulus	n.r	+	immune system process response to stimulus	n.r
IPI00188622	Similar to TGF, beta induced				+	cellular process cell communication developmental process system process cell adhesion	n.r
IPI00189424	Osteonectin				+	cellular process cell communication	n.r
IPI00191715	α1-acid glycoprotein	+	immune system process	n.r	+	immune system process	n.r
IPI00194341	Galectin-3	+	cellular process immune system process cell adhesion apotosis	n.r	+	cellular process immune system process cell adhesion apotosis	n.r
IPI00194927	RoBo-1	+	metabolic process	n.r	+	metabolic process	n.r
IPI00196591	MMP-9	+	n.r	n.r			
IPI00197780	CXCL-7	+	cellular process cell communication immune system process developmental process response to stimulus blood coagulation	n.r			
IPI00198695	Integrin beta	+	developmental process	n.r			
IPI00198970	Ficolin-2	+	cell communication cell adhesion	n.r		cell communication cell adhesion	n.r

Table 12: The 52 selected proteins which were involved in the bone healing process among all 1322 identified proteins on probe from rats with bone defect and soft tissue defect by HPLC-MS/MS (continued).

IPI00199341	IL-1R2	+	cellular process cell communication immune system process	n.r			n.r
IPI00199695	Serine (or cysteine) peptidase inhibitor, clade F, member 2	+	metabolic process developmental process	blood coagulation	+	metabolic process	blood coagulation
IPI00204451	Complement factor I	+	metabolic process cellular process immune system process developmental process response to stimulus reproduction	n.r			
IPI00204686	Glycoprotein 9	+	developmental process	blood coagulation			
IPI00205389	Isoform 1 of fibrinogen beta chain	+	cell communication developmental process cell adhesion	blood coagulation	+	cell communication cell adhesion	blood coagulation
IPI00206634	CXCL-4	+	cellular process cell communication immune system process developmental process response to stimulus blood coagulation	Inflammation mediated by chemokine and cytokine signaling			
IPI00206780	Plasminogen	+	metabolic process developmental process	blood coagulation	+	metabolic process	blood coagulation
IPI00208961	Similar to collagen alpha-1(X) chain precursor	+	metabolic process cellular process cell communication immune system process transport response to stimulus system process cellular component organization cell adhesion localization homeostatic process	integrin signalling			

Table 12: The 52 selected proteins which were involved in the bone healing process among all 1322 identified proteins on probe from rats with bone defect and soft tissue defect by HPLC-MS/MS (continued).

IPI00209973	C4 binding protein, alpha	+	metabolic process cellular process cell communication immune system process developmental process response to stimulus cell adhesion	n.r	+	cellular process cell communication immune system process response to stimulus cell adhesion	n.r
IPI00210900	Alpha-1-microglobulin/bikunin precursor	+	metabolic process immune system process developmental process response to stimulus	n.r	+	metabolic process immune system process response to stimulus	n.r
IPI00210947	Heparin cofactor 2	+	metabolic process developmental process	blood coagulation	+	metabolic process	blood coagulation
IPI00211401	Matrix Gla protein (MGP)				+	cellular process cell communication developmental process	n.r
IPI00212520	MMP-8				+		n.r
IPI00212666	Isoform 1 of murinoglobulin-1	+	metabolic process cellular process cell communication immune system process developmental process response to stimulus	blood coagulation	+	metabolic process cellular process cell communication immune system process response to stimulus	blood coagulation
IPI00214461	IL-1ra	+	cellular process cell communication immune system process response to stimulus	n.r	+	cellular process cell communication immune system process response to stimulus	n.r
IPI00230907	MIF	+	immune system process	n.r	+	n.r	n.r
IPI00231328	CXCL-2	+	cellular process cell communication immune system process developmental process response to stimulus blood coagulation	n.r			

Table 12: The 52 selected proteins which were involved in the bone healing process among all 1322 identified proteins on probe from rats with bone defect and soft tissue defect by HPLC-MS/MS (continued).

IPI00231423	C9 protein	+	metabolic process cellular process cell communication immune system process developmental process response to stimulus cell adhesion	n.r	+	cellular process cell communication immune system process response to stimulus cell adhesion	n.r
IPI00326140	Alpha-1-macroglobulin	+	metabolic process cellular process cell communication immune system process response to stimulus	blood coagulation	+	metabolic process cellular process cell communication immune system process response to stimulus	blood coagulation
IPI00327745	Serum amyloid P-component	+	immune system process response to stimulus	n.r	+	immune system process response to stimulus	n.r
IPI00331776	C6	+	metabolic process cellular process cell communication immune system process developmental process response to stimulus cell adhesion	n.r			
IPI00360541	Integrin beta 2	+	metabolic process cellular process cell communication immune system process developmental process response to stimulus cell adhesion	n.r	+	cellular process cell communication immune system process response to stimulus cell adhesion	Integrin signalling pathway Inflammation mediated by chemokine and cytokine signaling pathway
IPI00363839	Chitinase-3-like protein 1	+	metabolic process	n.r			
IPI00368704	Similar to murinoglobulin 1 homolog	+	developmental process	blood coagulation	+	n.r	n.r
IPI00382185	Da1-24 (protein cfb)	+	developmental process	n.r			
IPI00389471	IGF-1 isoform A preproprotein	+	n.r	n.r			

Table 12: The 52 selected proteins which were involved in the bone healing process among all 1322 identified proteins on probe from rats with bone defect and soft tissue defect by HPLC-MS/MS (continued).

IPI00392886	Alpha-2-macroglobulin	+	metabolic process cellular process cell communication immune system process developmental process response to stimulus	blood coagulation	+	metabolic process cellular process cell communication immune system process response to stimulus	blood coagulation
IPI00515829	Kininogen 1	+	developmental process	blood coagulation	+	n.r	blood coagulation
IPI00554226	Complement component factor h-like 1	+	metabolic process cellular process cell communication immune system process developmental process response to stimulus cell adhesion	n.r			
IPI00555168	Ferritin, Ferritin heavy chain (Ferritin H subunit)	+	n.r	n.r			
IPI00565381	Similar to Ferritin light chain 1	+	transport	n.r	+	transport	n.r
IPI00679203	Ferritin, Ferritin light chain 1 (Ferritin L subunit 1)	+	transport	n.r			
IPI00564327	Murinoglobulin-2	+	metabolic process cellular process cell communication immune system process developmental process response to stimulus	blood coagulation	+	metabolic process cellular process cell communication immune system process response to stimulus	blood coagulation
IPI00565708	Isoform 1 of Haptoglobin	+	metabolic process cellular process immune system process developmental process response to stimulus system process reproduction	n.r	+	metabolic process cellular process immune system process response to stimulus system process reproduction	n.r
IPI00679245	T-kininogen 2	+	developmental process	blood coagulation	+	n.r	blood coagulation

Table 12: The 52 selected proteins which were involved in the bone healing process among all 1322 identified proteins on probe from rats with bone defect and soft tissue defect by HPLC-MS/MS (continued).

IPI00763879	Glycoprotein Ib (platelet), alpha polypeptide	+	metabolic process cellular process cell communication immune system process cell adhesion	blood coagulation	+	cellular process cell communication immune system process developmental process cell adhesion	blood coagulation
IPI00765267	Similar to coagulation factor IX	+	metabolic process cellular process immune system process response to stimulus reproduction	n.r	+	metabolic process cellular process immune system process response to stimulus reproduction	n.r
IPI00777464	Amyloid protein A	+	n.r	n.r			
IPI00778633	Apolipoprotein H	+	metabolic process cellular process cell communication immune system process developmental process response to stimulus cell adhesion	n.r	+	metabolic process cellular process cell communication immune system process response to stimulus cell adhesion	n.r
IPI00778837	CXCL-3	+	cellular process cell communication immune system process developmental process response to stimulus blood coagulation	n.r			
IPI00780574	C8, gamma polypeptide	+	metabolic process immune system process developmental process response to stimulus	n.r	+	immune system process response to stimulus	n.r

5.9 Determination of cytokines and growth factors in the blood plasma

To study the systemic inflammation reaction after bone defect, plasma samples from rats with bone defect or soft tissue defect were analyzed for IL-6, IL-1β, TNF-α, TGF-β1, VEGF, PDGF-BB and BMP-2 ELISA. IL-1β, TNF-α, VEGF and BMP-2 were undetectable in plasma sample. Blood samples were taken hourly for 8 h (n=4 for bone defect, n=2 for soft tissue defect) or in 3 h-intervals for 24 h (n=2 for bone defect, n=2 for soft tissue defect).

5.9.1 Determination of IL-6 in the blood plasma

Before surgery, IL-6 concentration in plasma was below the detection limit of the ELISA. After surgery, IL-6 was only detectable in individual samples. At 1 h after bone defect, the concentration of IL-6 increased to 156.5 pg/mL and the maximal concentration was 450.8 pg/mL at 8 h after bone defect. In the soft tissue defect concentration of IL-6 was 223.4 pg/mL at 8 h. For 24 h in 3 h-intervals, IL-6 was undetected in plamsa after bone defect, and it was only detected in one sample collected at 24 h with concentration of 21.2 pg/mL after soft tissue defect.

5.9.2 Determination of TGF-β1 in the blood plasma

Before surgery, concentration of TGF-β1 was 3239.7±2856.0 pg/mL in plasma. Right after creating the bone defect the concentration of TGF-β1 increased to the highest level of 8398.2±5364.8 pg/mL at 2 h. Afterwards, the concentrations of TGF-β1 were constant with a slightly higher level than pre-surgery within the first 8 h. After soft tissue defect, the concentration of TGF-β1 did not significantly change with an half-fold of those in bone defect within 8 h (Fig. 25 a). Within 24 h after bone defect and soft tissue defect, the concentrations of TGF-β1 decreased over time. Moreover, at 24 h the concentrations of TGF-β1 were similar in both groups with a lower level than pre-surgery (Fig. 25 b).

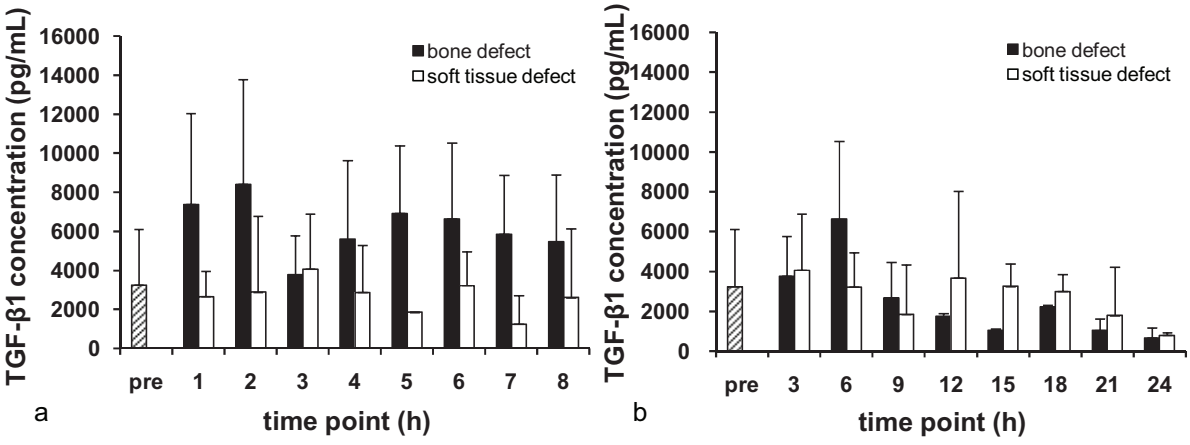

Fig. 25: TGF-β1 concentration in blood plasma. Samples from rats with bone defect (n=4

for 8 h and n=2 for 24 h) and with soft tissue defect (n=2) pre- and after surgery. Data represent mean±SD. **a)** Samples were obtained hourly for 8 h. **b)** Samples were obtained every 3 h for 24 h. pre: pre-surgery.

5.9.3 Determination of PDGF-BB in the blood plasma

The concentrations of PDGF-BB was analyzed in samples taken hourly for 8 h. They increased after surgery in both groups. After soft tissue defect, the concentration of PDGF-BB peaked at 2 h (1365.1±132.9 pg/mL) with 4-fold increase compared to pre-surgery concentration (315.1±233.9 pg/mL). However, after bone defect the concentration did not significant change. After bone defect the concentrations of PDGF-BB increased within 2 h and then fluctuated between 222.1±99.3 pg/mL and 589.4±489.9 pg/mL (Fig. 26).

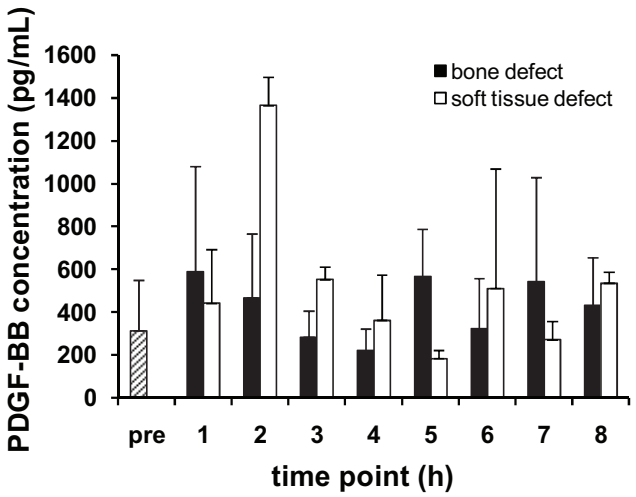

Fig. 26: PDGF-BB concentration in blood plasma. Samples were obtained hourly for 8 h from rats with bone defect (n=4) and rats with soft tissue defect (n=2) pre- and after surgery. Data represent mean±SD. pre: pre-surgery.

5.10 Histological analysis of the hematoma

To examine the cellular changes at the site of bone defect at the early stage of bone healing, the hematoma were explanted from 5 rats with bone defect at 9, 12, 24, 45 and 48 h and histological analysis was performed. Hematoxylin & eosin (H&E) stained hematoma slides revealed that during the whole time course, an infiltration of lymphocytes and PMNs could be observed. At 9 h after explanation, an inflammatory reaction was seen within the hematoma with low numbers of inflammatory cells like neutrophils (bold black arrows) and lymphocytes (narrow black arrow) (Fig. 27 a). At 12 h, there were no significant histological changes (Fig. 27 b). After 24 h a primitive fibrin network (bold white arrow) had formed with abundant infiltration of PMNs (black arrows) and macrophages (Φ) were seen (Fig. 27 c, d).

At 45 and 48 h (Fig. 27 d, e), the fibrin network was enlarged and the number of inflammatory cells was decreased. By counting the inflammatory cells in hematoma, it was shown that the amount of the inflammatory cells peaked at 24 h after bone defect (Fig. 28).

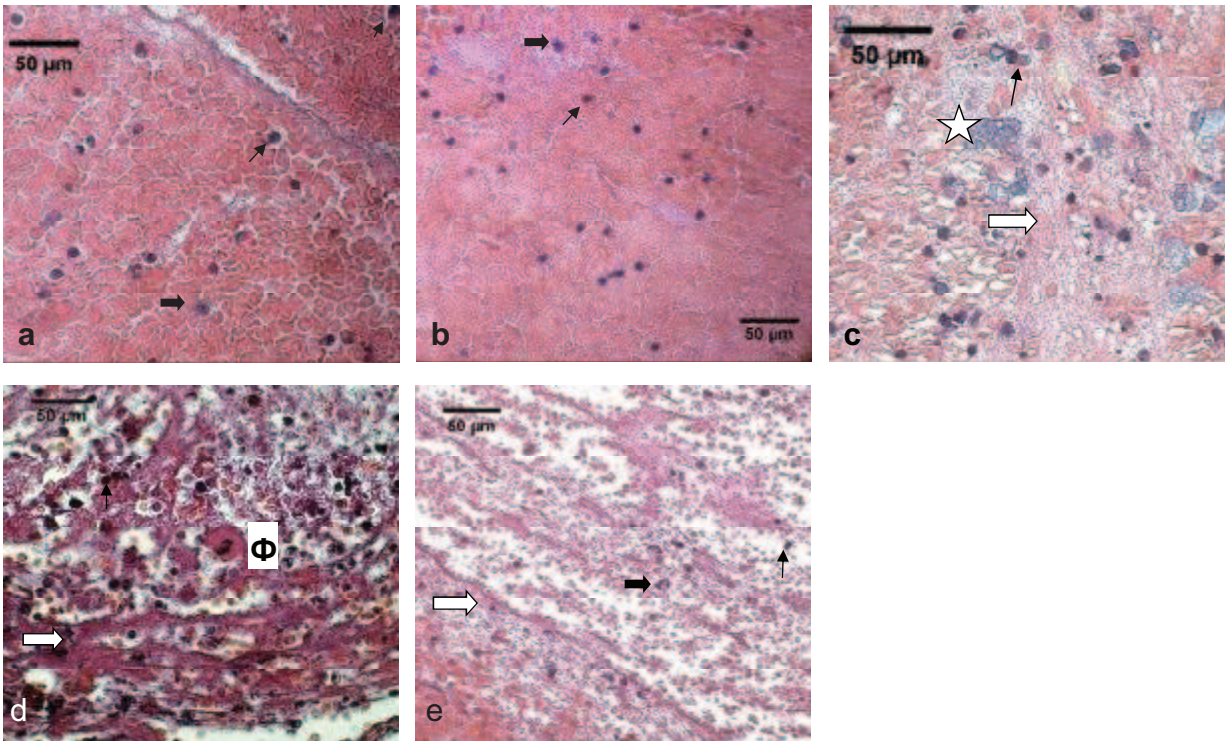

Fig. 27: Histology of the hematoma after surgery from rats with a bone defect. a) Hematoma was explanted 9 h after surgery. **b)** Hematoma was explanted 12 h after surgery. **c)** Hematoma was explanted 24 h after surgery. **d)** Hematoma was explanted 45 h after surgery. **e)** Hematoma was explanted 48 h after surgery**.** Original magnification: ×400, scale bar=50 µm, H&E stain. Lymphocytes (narrow black arrow), PMNs (bold black arrow), primitive fibrin network (bold white arrow), monocyte (white star), macrophage (Φ).

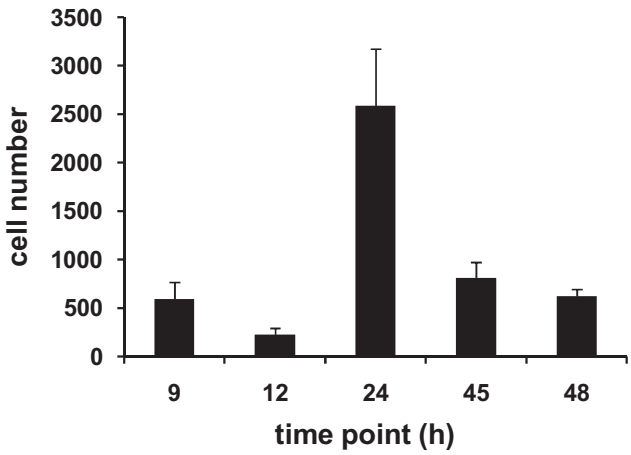

Fig. 28: Cell count of the inflammatory cells per low power field at five different time points in hematoma. Thirty slices were analyzed at each time point. Data represent mean±SD. From H&E stain slices with magnification: ×100.

6 Discussion

Although expression of several mediators in fracture healing has been revealed in previous studies, the profile of the dynamic changes in the specific local mediator release during the early inflammatory stage of bone defect healing so far have remained elusive. In this study, some interstitial markers of inflammation and some important healing proteins were characterized through microdialysis. Among the mediators, cytokines and growth factors are important for the cellular response.

Seven cytokines and growth factors (IL-6, IL-1β, TNF-α, TGF-β1, VEGF, PDGF and BMP-2) were monitored due to their early expression and detection in bone fracture models as demonstrated in gene expression and protein production levels previously (Bourque et al., 1993; Kon et al., 2001; Cho et al., 2002; Schmid et al., 2009). Among them PDGF has 3 isoforms (PDGF-AA, PDGF-AB and PDGF-BB), and PDGF-BB was selected for this study due to its universality and the potent effects on chemotaxis and modulation for osteoprogenitors cells during bone repair (Caplan & Correa, 2011). The molecular weight of these cytokines and growth factors ranges between 12.5–51.0 kDa which potentially were able to pass through the CMA 20 microdialysis probe with a MWCO of 100 kDa. So far, sampling of these cytokines and growth factors from a bone defect site in rats has not been reported. Hence, the essential strategy was to first establish optimal conditions for microdalysis in rats with a long bone critical-size defect.

6.1 Fluid recovery

The recovery of large molecules is accompanied by fluid loss due to the application of high MWCO probes (100–3000 kDa). The disequilibrium of the osmotic pressures/hydrostatic pressure across the membrane causes the influx of water molecules from the perfusate to the interstitial space, which potentially dilutes the protein concentrations in the interstitial compounds and directly alters the chemistry of the interstitial space (Helmy et al., 2009). Under physiological conditions in capillares, few large molecules can cause marked increase the total osmotic pressure. Dextran-70 (70 kDa) and BSA (68 kDa) were widely used as colloids in previous *in vitro* and *in vivo* microdialysis studies (Ao et al., 2006; Garvin & Dabrosin, 2008) due to their high molecular weight and the relative inactivity.

In this study, the fluid recover olny significant decreased after adding PER/0.2% Dextran-70 or PER/0.4% Dextran-70 in PER at flow rates of 0.5 µL/min in rats with bone defect. For other cases in *in vitro* and *in vivo* study, after adding Dextran-70 or BSA in PER the fluid recovery increased slightly though without a statistically significant enhancement (Fig. 7). In a previous *in vivo* study the use of 1.5–4% Dextran-70 Krebs–Henseleit bicarbonate buffer at a flow rate of 0.335 µL/min with a higher concentration of colloid prevented fluid loss due to

the increased colloid osmotic pressure (Rosdahl et al., 1997). According to Dahlin's *in vitro* study, the addition of 2–4% Dextran-60 to the crystalloid perfusate enhanced the fluid recovery with increased concentrations of Dextran-60. However, the highest fluid recovery occurred when using 3% Dextran-60 (Dahlin et al., 2010). Compared with their studies, low concentrations of Dextran-70 (0.01–0.4%) were used in this study. This implied that at low range of the Dextran-70 concentration, the effect of Dextran-70 concentration on fluid recovery was small.

Although the flow rate did not significantly affect the fluid recovery in this study, at a higher flow rate of 2.0 µL/min the fluid recovery was over 90% when using colloid perfusates. The present results confirmed the findings in the literature. Trickler et al. have used a 100 kDa probe to investigate the fluid loss at flow rates between 0.5–5.0 µL/min when perfusing PBS and PBS/3.5–10% BSA. They revealed that when using a certain perfusate, a higher flow rate induced a greater absolute amount of fluid loss due to the increased hydrostatic pressure while fluid recovery was not affected by the flow rate (Trickler & Miller 2003).

Both Dextran-70 and BSA had an identical potency to enhance fluid recovery. But Hillman et al. have reported 3% Dextran-60 in ringer's solution to be more powerful on the fluid recovery than 3.5% albumin when using microdialysis in humans (Hillman et al., 2005). It is speculated that BSA may potentially increase the permeability of the membrane by reducing the water barriers around the membrane (Trickler & Miller 2003). However, because this study used different types and concentrations of Dextran and BSA, the discrepancy between Dextran-70 and BSA did not become obvious.

During 24 h after creating a bone defect or soft tissue defect in rats, the fluid recovery did not significantly change with perfusing either PER/0.01% Dextran-70 or PER/1% BSA. Furthermore, since 9 h after injury, the fluid recovery was above 95%. Some researchers have revealed that the *in vivo* fluid loss differed according to the different types of tissues like brain/catheter *vs.* cerebrospinal fluid/catheter or muscle/catheter *vs.* adipose/catheter (Rosdahl et al., 1997; Helmy et al., 2011). However, in the present study, different types of injury between bone defect and soft tissue defect did not alter the fluid recovery.

6.2 Influence of the crystalloid perfusate on relative recovery

Three crystalloid perfusates (0.9% NaCl, PBS or PER) were compared on the basis of relative recovery (RR) in this *in vitro* study. These 3 solutions are common solutions used in clinical or biological research because of their identical crystalloid pressure to the blood plasma or cells in mammals. Previous *in vitro* studies have suggested that the physiological properties of the perfusates might correlate with the RR. The pH of the perfusates would

interact with the pI of the molecules and the charges on the probe membrane (Zhao et al., 1995; Helmy et al., 2009). The farther the difference between the pI of cytokine or growth factor and the pH of the perfusate, the stronger the hydrophility of the cytokine and thus the better the recovery which can be achieved (Helmy et al., 2009). However, in this study, the pH of crystalloid perfusates adding BSA were not measured. Therefore, it is impossible to determine the reason for the individual detection of IL-6 on the aspect of relationship of pI and RR when using the same perfusate to sample TGF-β1 with pI 8.61 and IL-6 with a pI of 7.7. Nevertheless, for TGF-β1 sampling, the pH of different crystalloid perfusates seems not to affect the RR. Similarly Kjellström et al. reported that there were no significant differences in the RR when using different crystalloid perfusates (Ringer at pH 7.4 and 9.4, and PBS at pH 5.4 and 7.4) *in vitro* (Kjellström et al., 1999). Therefore 0.9% NaCl, PER and PBS were all acceptable crystalloid perfusates.

6.3 Relative recovery of cytokines and growth factors *in vitro*

In vitro, the recovery of TGF-β1, VEGF and IL-6 was investigated using different perfusates and flow rates to optimize the conditions for *in vivo* microdialysis. Neither the used crystalloid perfusates nor the addition of Dextran-70 resulted in a reproducible detection of these proteins. However, addition of 1% BSA led to detectable IL-6 and TGF-β1 concentrations (Fig. 9, Fig. 10). Consistent with previous findings, the colloids enhanced cytokine RR (Hillman et al., 2005; Helmy et al., 2009). Furthermore, apart from the effect of the increasing colloid osmotic pressure, BSA can potentially serve as a blocking agent to prevent the non-specific binding of proteins to the inner wall of the tube or the membrane (Ao et al., 2006). In addition, being a negatively charged protein, it generates an ionic gradient across the probe membrane. Via binding with the charged proteins, a BSA-protein complex is formed and consequently prohibits the reflux of the proteins. However, the neutrally charged Dextran is unable to do so (Trickler & Miller, 2003; Helmy et al., 2009). Moreover BSA could reduce the water boundary surrounding the membrane to maintain the permeability of the membrane, although this potentially would increase the fluid loss (Trickler & Miller, 2003). Nevertheless, the discrepancy between BSA effects on sampling TGF-β1 and IL-6 in this *in vitro* study was probably due to the different pI and molecular weights. In PER (pH 6.0), TGF-β1 possesses more positive charges (pI 8.6) than IL-6 (pI 7.7). This suggests that the BSA was able to bind with TGF-β1 rather than IL-6. The smaller size of TGF-β1 compared to IL-6 (12.5 kDa *vs.* 21.6 kDa) may also have partially accounted for the superior passing. On the other hand, compared to previous studies, the individual detection of IL-6 may be ascribe to multiple factors: the different concentrations of IL-6 in the external fluid, the different lengths of the probe, the different temperatures or the different additives in the perfusates

(Ao et al., 2005; Ao et al., 2006; Wang & Stenken, 2009). Although it is known that RR depends on the concentration of the colloid, Hemly et al. have indicated the higher concentration of colloid might bring more external fluid into the microdialysate which induced a low RR compared with a lower concentration of colloid (Helmy et al., 2009). In this *in vitro* study, the low concentration (0.01–0.04%) of Dextran-70 might explain the missing correlation between colloid concentration and RR.

It is known that an increasing flow rate reduces the RR for cytokines *in vitro* (Ao et al., 2004; Ao et al., 2005; Duo & Stenken, 2011). Many researchers used an ultraslow flow rate to achieve a higher RR (Kjellström et al., 1999; Rosenbloom et al., 2005; Helmy et al., 2009). Although at a slow flow rate some additives like BSA have sufficient time to bind with the target, the negative effects on recovery, like evaporation and limited sample volume, led to using flow rates of 0.5, 1.0 and 2.0 µL/min in this study based on the previous literature (Li & Cui, 2008). Similar with the results from Ao et al. who found a decreasing RR for some cytokines including IL-6 with increasing flow rate (0.5–2.0 µL/min) (Ao et al., 2005), the present *in vitro* study showed that RR of TGF-β1 decreased with increasing flow rate, but IL-6 did not constantly follow this principle according to the individual detection. The discrepancy may be explained by the fact that Ao et al. have used a longer probe (10 mm) and higher concentration of IL-6 in the standard external fluid (Ao et al., 2005). Furthermore, Waelgaard et al. also reported that some molecules like chemokines and anaphylatoxins would break the inverse relation between RR and the flow rate. It was assumed that these molecules easily bind with the inner surface of the membrane. Thus the higher flow rate could flush and resolve them into the microdialysates (Waelgaard et al., 2006).

VEGF was below the detection limit of ELISA in all *in vitro* microdialysates. It was found that the recovery efficiency decreased with an increased molecular weight of the protein (Schutte et al., 2004; Helmy et al., 2009). The larger molecular weight of the rat recombinant VEGF homodimer with 50 kDa might restrict crossing of the 100 kDa membrane. It is known that only proteins with one third to one fourth of the MWCO have a good recovery (Plock & Kloft, 2005). However, many *in vitro* and *in vivo* studies proved the recoverability of VEGF by using 100 kDa probe (Dabrosin et al., 2002; Helmy et al., 2011; Åberg et al., 2011). The RR of VEGF *in vitro* was found 4% at a flow rate of 2.0 µL/min at room temperature using 10 mm length of 100 kDa probe, but the concentration and composition of the protein solution were not reported (Dabrosin et al., 2002). One interpretation might be the different parameters used in previous experiments, e.g. the longer probe (10 or 20 mm probe), higher concentration of colloid (3.5% human albumin solution), or slower flow rate (0.3 µL/min). Furthermore, the cytokine concentration in external fluid linearly correlated with the RR (Folkersma et al., 2008). Hence, low concentration of VEGF in external fluid probably also lead to the missing detection of VEGF in *in vitro* microdialysates.

6.4 *In vivo* microdialysis

6.4.1 Total protein concentration

By perfusing PER, 0.9% NaCl or PER/0.01% Dextran-70 during microdialysis in rats with bone defect, the total protein concentration in the microdialysates ranged from 0.14 to 0.36 mg/mL which is similar to the concentration of total protein measured in microdialysates from the brain (Maurer et al., 2003; Hillman et al., 2005). For 2 h- or 3 h-intervals, the highest concentration of the total protein occurred in the first interval. This was related to the initial burst when starting microdialysis without equilibration. To get a steady-state for sampling, it is required to perfuse until the concentration gradient in external fluid becomes steady (Benveniste et al., 1989). Rosdahl et al. have used ultraslow flow rates to test the equilibration time in human muscle and adipose tissue. They found that time of equilibration for molecules, like glucose, lactate and glycerol took 90 min after probe insertion to get to a steady-state, whereas urea was faster (Rosdahl et al., 1998). As seen in this *in vivo* study, after the burst during the first interval, the total protein concentrations were constant. It could be shown that microdialysate collection from a bone defect was possible for 24 h continuously without substance loss.

6.4.2 Annotation of proteins in hematoma identified by HPLC-MS/MS

1) Overview of the detected proteins

HPLC-MS/MS was used to profile the recovered proteins in the microdialysates and the proteins absorbed on the probes. In the microdialysates collected for 8 h from creation of the bone defect, 36 proteins were identified. However, various proteins were blocked due to the adsorption on the outer surface of the probe. In total, 884 proteins were found to be adsorbed on the probes which were implanted in rats with a bone defect within 48 h after surgery, while 1063 proteins were identified on the probes from rats with a soft tissue defect (Fig. 19). In accordance with the statement that molecules smaller than one third to one fourth of MWCO are readily recovered, among the proteins identified in the microdialysates the median molecular weight was 32.8 kDa and 78.4% of the recovered proteins were below MWCO (Plock & Kloft, 2005). However, among the proteins found on the probe, 87.9% proteins were below MWCO due to their strong adsorption. The replacement of the proteins on the probe and the limited availability of binding sites on the probes could explain the missing detection of some proteins. Nevertheless, analyzing the proteins on the membrane provided additional useful information to understand the process of bone healing apart from the proteins in microdialysates.

Among those proteins identified in the bone defect only 11.1–13.6 % derived from the

extracellular region. These results demonstrated that in the interstitial space of the hematoma, cellular proteins from lysed cells were predominant at the early stage of wound healing, while secreted proteins, ECM proteins or blood proteins only occupied a small part.

2) Biological processes

Biological processes and the overrepresented signaling pathways were analyzed to reveal the underlying healing mechanism. Based on the proteins identified in the 8 h microdialysates, no biological processes or pathways specifically associated with bone healing were found. In contrast with few information concluded from microdialysates, the adsorbed proteins suggested that both the bone defect and the soft tissue defect displayed a similar biological response and that the “response of the immune system” and “response to stimulus” were the predominant processes during at early stage of healing. “Blood coagulation” as the child term of “response to stimulus” contained 17 and 9 proteins from probes in bone and soft tissue defects, respectively. On the other hand, among the overrepresented pathways, 4 of 9 and 3 of 11 were found to be significantly overrepresented during the early healing period. “Blood coagulation”, “integrin signaling” and “inflammation mediated by chemokine and cytokine signaling” were overrepresented for both the bone defect and soft tissue defect. In addition, the “FGF signaling” pathway was specifically overrepresented in bone defect only. These results were different from that of a previous study using the entire fractured rat femur for analysis of gene expression. The authors reported that “IGF-1 signaling”, “cell cycle: G1/S checkpoint regulation”, “PDGF signaling”, “insulin receptor signaling”, “nuclear factor ‘kappa-light-chain-enhancer’ of activated B cell (NF-κB) signaling” and “ERK/MAPK signaling” were significantly upregulated within 24 h after the fracture (Li et al., 2007b). Moreover, they suggested the “cell cycle” pathway was the central theme within 24 h after fracture. However, in the present study this signaling pathway was not identified as being overrepresented. Nevertheless, as a biological process it was found after the injury but not among the top processes. This discrepancy may be attributed to the different sample sources and methods of analysis (gene expression vs. *in vivo* microdialysis).

Li et al. found “integrin signaling” was unregulated during the stage of fracture remodeling (Li et al. 2007b). In this study, this pathway was revealed to be overrepresented as early as in the inflammatory stage. Integrin signaling improves cell migration, mediates the cellular adherence to the ECM and affects the cell cycle specifically for neutrophils, macrophages and MSCs (Berton & Lowell, 1999; Docheva et al., 2007). Moreover, via integrin signaling the phagocytosis was actuated in neutrophils and macrophages, and damaged ECM facilitated the migration of cells (Docheva et al., 2007). Concerning the present results, it is concluded that the damaged ECM potentially modulates the progress of

healing at an early stage via the “integrin signaling” pathway.

The specifcally overrepresented pathway of “FGF signaling” revealed that during bone defect healing, the proportion of proteins involved in the “FGF signaling” over the total protein was significantly higher than the reference data in database of Panther. In soft tissue defects the proteins of “FGF signaling” were not increased significantly. This pathway can regulate a variety of basic cellular processes. But the response to FGF signaling is both cell type-specific and stage-specific (Dailey et al., 2005). FGF signaling is controlled by the glycosaminoglycan heparan sulfate with the aid from other mediators (Jackson et al., 2006). FGF signaling is thought to be crucial in bone development (Naski & Ornitz, 1998). As a part of FGF signaling pathway, FGF-1, FGF-2 and FGF-5 were upregulated at 24 h after bone injury (Schmid et al., 2009). However, in this study neither FGF nor the key of this pathway, FGF receptor substrate 2α was identified within 24 h after injury. The limitation of proteins collection, which depended on the absorption of probe membrane and the properties of proteins (e.g the size or pI of the proteins), may induce the missing detection.

6.4.3 Identification of cytokines and bone related proteins

When comparing the proteins adsorbed to the probe and the proteins identified in the microdialysate by HPLC-MS/MS, 6 proteins were found exclusively in the microdialysates. Among them only musculoskeletal embryonic nuclear protein 1 was associated with bone and muscle tissue. It is reported to be expressed and acutely upregulated in callus at 3 days after femur fracture in rats (Lombardo et al., 2004). In this study its immediate production corresponded to the regenerative response of bone and muscle within 8 h after bone defect.

Among the 7 selected cytokines and growth factors (IL-6, IL-1β, TNF-α, TGF-β1, VEGF, PDGF-BB and BMP-2), none was detected in 8 h microdialysates via HPLC-MS/MS. However, by ELISA IL-6 and TGF-β1 could be detected and monitored constantly in microdialysates for 24 h after both bone and soft tissue defects.

IL-6 was recoverable in microdialysates either by perfusing 0.9% NaCl, PER, PER/0.01% Dextran-70 or PER/1% BSA. However, without BSA IL-6 was only detected in individual samples. This confirmed that BSA in PER had a better performance than Dextran-70. After creating a bone defect and soft tissue defect, the concentration of IL-6 peaked at 12–15 h and 6–9 h, respectively. Within 24 h, there were no significant changes of the IL-6 concentration in bone defect. But after a soft tissue defect has been created, the concentrations of IL-6 significantly increased until the interval of 9–12 h. Then in both types of injury, the concentration of IL-6 declined to baseline at 21–24 h (Fig. 15). These results correspond with a study, where IL-6 was recovered by microdialysis from ultraviolet B (UVB)-irradiated skin. The IL-6 concentration ascended within the first 8–16 h and decreased to

baseline after 24 h (Averbeck et al., 2006). The production of IL-6 accompanies an acute injury (Farnebo et al., 2009). The present study revealed that at 6–9 h the concentration of IL-6 in the soft tissue defect was significantly higher than in the bone defect. The recovered IL-6 may have been released from PMNs, monocytes, microphages and endothelial cells (Cicco et al., 1990; Leeuwenberg et al., 1990; Terebuh et al., 1992). Because of the predominance of PMNs in wounds within 24 h, the PMNs might be tha main source of the production of IL-6.

Although previous *in vivo* and clinical studies found TGF-β1 expression and concentration to be elevated in hematoma within 2 weeks after fracture, the dynamic changes of the production within 24 h after bone defect has not been determined yet (Steinbrech et al., 2000; Sarahrudi et al., 2011b). TGF-β1 gene was expressed constantly in fractured bone from mice during the whole repair process with a sharp upregulation between 12 and 24 h after fracture, and then returned to the pre-surgery high baseline (Ito et al., 1999; Cho et al., 2002). In this study, the concentration of TGF-β1 in the microdialysates remained relatively constant over 24 h both in both bone and soft tissue defects. The concentration of TGF-β1 in microdialysates from human UVB-irradiated skin also displayed a similar pattern within the first 24 h (Averbeck et al., 2006). Moreover, a previous *in vivo* study demonstrated that the first peak of the active TGF-β was generated at 1 h after injury and the second peak occurred 5 days later in rat wound model (Yang et al., 1999). The initial release from the platelets would be sustained by release from the ECM (Werner & Grose, 2003). Although macrophages can produce TGF-β1 (Bourque et al., 1993), they usually occur in the fracture hematoma after 48–96 h, which was confirmed by the histological results of this study. Thus, a higher content of TGF-β1 might be obtained when prolonging the time of sample collection.

Comparing with the consistent detection of IL-6 and TGF-β1 in microdialysates, IL-1β and TNF-α as the predominant proinflammatory cytokines were detected only rarely within the microdialysates. The difficulty of IL-1β and TNF-α detection was also reported in fracture hematoma serum in a clinical trial by Hauser et al., who detected IL-1β sporadically but did not detect the soluble TNF-α (Hauser et al., 1997). Different studies showed that the mRNA of IL-1β and TNF-α were strongly expressed within 24 h after bone fracture in mice and their productions was increased in monocytes (Kon et al., 2001; Cho et al., 2002). Of them, TNF-α was weakly produced at 24 h in the bone marrow space or periosteum nearest to the fracture in mice (Kon et al., 2001). In a rat limb trauma model, the secreted TNF-α was consistently detected via microdialysis throughout 3 h without a significant increase using a probe with 100 kDa MWCO (Farnebo et al., 2009). Compared with their results, the occasional recovery in this study might be attributed to the higher flow rate and shorter probe membrane especially for the large molecular weight of TNF-α (51 kDa). While Farnebo et al. used a flow rate of 0.3 μL/min and the length of membrane was 30 mm (Farnebo et al., 2009), in this

study the flow rate was 2.0 µL/min and the probe length was 4 mm. Platelets as well as monocytes and macrophages are the major sources of IL-1β and TNF-α (Dinarello, 1984; Broughton et al., 2006). The low infiltration of monocytes and macrophages and release from activated platelets within 24 h after surgery probably induced the low concentration of these cytokines being insufficient for consistent recovery and detection via microdialysis.

Instead of detecting IL-1β in the fracture hematoma, IL-1R2 and IL-1ra were found to be adsorbed on the probe membranes within 48 h after surgery. IL-1R2 was found 24 h after creating the bone defect while IL-1ra was found 48 h after bone defect and 24 h after soft tissue defect creation. Both proteins inhibit the IL-1 signaling transduction, downregulate IL-1β level and inhibit the IL-1β activity *in vitro* (Carter et al., 1990; Giri et al., 1994). Neutrophils are the major source of soluble IL-1R2 after the response to TNF or endotoxin (Giri et al., 1994). After bone fracture in mice the expression of IL-1R2 increased within 24 h and peaked at day 3 (Kon et al., 2001). Overall, these results indicate that IL-1R2 and IL-1ra play a role in regulation of IL-1β levels and the subsequent healing cascade.

Previously it was reported that the concentration of PDGF and VEGF in local human hematoma supernatant was above 4 ng/mL within 24 h after bone fracture with a 2.5 fold and 10 fold increase compared to the circulation level respectively (Street et al., 2001). However, they were undetectable locally at the site of injury by microdialysis. The pI of PDGF-BB and VEGF (9.3 for VEGF and 9.4 for PDGF-BB) seems not to be a barriers to their recovery, however, their molecular weights (40 kDa for VEGF and 30 kDa for PDGF-BB) were close to the optimal threshold for the 100 kDa membrane (Plock & Kloft, 2005). So far there is no report on PDGF-BB recovery with microdialysis, while VEGF has been recovered in several clinical microdialysis studies (Helmy et al., 2011; Åberg et al., 2011). However, in this *in vivo* study, VEGF and PDGF-BB were not detected in the microdialysates. The missing detection of VEGF was in agreement with the results of a present *in vitro* study, and the potential reasons were discussed above. Hence, the missing detection of VEGF and PDGF-BB suggested the difficulty of their recovery at a sufficient concentration by using a CMA 20 probe in rats with either bone or soft tissue defects.

Another undetectable growth factor throughout the study was BMP-2. The BMP-2 gene is an early response gene for bone fractures and is highly expressed within 24 h after tibia fractures in mice (Cho et al., 2002). However, the unexpectedly low concentration within 24 h after bone defect creation in rats may lead to the missing detection of BMP-2 in microdialysates.

The release of chemokines is a marker of early inflammation (Klapperich & Bertozzi, 2004). After creation of bone and soft tissue defects, CXCL-1, CXCL-5 and CXCL-7 were detected and monitored in 3 h-intervals for 6 h in microdialysates by proteome profiler^{TM} array (Fig. 17). Throughout 6 h after the fracture, the release of CXCL-1 increased in bone

defects, while CXCL-1 was secreted steadily after creating a soft tissue defect. Additionally CXCL-1 was also detected between 24 to 48 h after the bone defect by HPLC-MS/MS. An *in vivo* study showed the degree of infiltration of neutrophils to be dependent on the concentration of CXCL-1 (Shibata et al., 1996). Meanwhile CXCL-2 and CXCL-3 have an amino acid sequence homology with CXCL-1 of 67% and 63%, respectively, in rats and they have an identical activity for neutrophil chemotaxis (Nakagawa et al., 1994). But the release of CXCL-2 and CXCL-3 within 6 h after bone defect was undetectable by proteome profiler™ array in the microdialysates. Nevertheless, they were detected on the probe by HPLC-MS/MS at 24 h after bone defect. It is therefore suggested that CXCL-1 plays a predominant role during the very early reaction to injury compared with CXCL-2 and CXCL-3.

Besides CXCL-1, the other 2 chemokines recovered by microdialysis were CXCL-5 and CXCL-7 within 6 h after surgery. CXCL-5 responded immediately but the production slightly decreased within 6 h after bone defect creation. However, in soft tissue defects it was just released during 3–6 h. It can be expressed by monocytes and released from platelets (Rihl et al., 2009; Nurden, 2011). An *in vivo* study demonstrated that CXCL-5 is a potent neutrophil chemoattractant. Nevertheless, CXCL-5 also mediates the release of other cytokines like IL-1β and TNF-α (Chandrasekar et al., 2003). Considering to the relatively low concentration of IL-1β and TNF-α within 24 h in bone defect hematoma, it can be assumed that there is a relative weak ability of CXCL-5 to induce IL-1β and TNF-α *in vivo*. Apart from the role in inflammatory response, it also chemoattractes BM-MSCs, seems to be involved in regulating angiogenesis and mitogenesis, and may be involved in the maintenance of hematopoietic stem cells (Choong et al., 2004; Nedeau et al., 2008). Hence, the production of CXCL-5 in bone defects may potentially influence those aspects that contribute to bone healing.

Compared to CXCL-1 and CXCL-5, CXCL-7 was abundantly released within 6 h in bone and soft tissue defects. During the first 3 h the release of CXCL-7 displayed a similar immediate response both in the bone and soft tissue defect. However, in the bone defect, the release of CXCL-7 only slightly increased, while in the soft tissue defect it decreased to about 50%. The vascular injury and the release of high concentrations of CXCL-7 from platelets (von Hundelshausen et al., 2007; Shi & Morrell, 2011) was associated with the intensive detection after bone and soft tissue defects in rats. This chemokine might be associated with injury due to its properties of neutrophils chemotaxis, mediation of neutrophils transendothelial migration and angiogenesis (Schenk et al., 2002; Romagnani et al., 2004). Moreover, in an *in vitro* study, CXCL-7 was reported to be able to recruit MSCs (Kalwitz et al., 2009; Kalwitz et al., 2011). Further, exogenous CXCL-7 enhanced the differentiation of IGF-2 treated mouse bone marrow cells into osteoclasts (Nakao et al., 2009). Hence compared to the other cytokines plotted on the array, the intensive and steady production of CXCL-7 implies its diverse and important roles during bone defect healing

especially at the initial 6 h after injury.

As an important negative regulator for CXCL-7, CXCL-4, also known as platelet factor 4, was identified in bone defect at 12 h after surgery. CXCL-4 is synthesized in megakaryocytes and released by activated platelets. It was also expressed in smooth muscle cells, monocytes or macrophages (Schaffner et al., 2005; Schiemann et al., 2006; Lasagni et al., 2007). CXCL-4 plays a role in inflammation and wound repair. In contrast to other CXC chemokines, CXCL-4 lacks chemotactic properties for neutrophils (Petersen et al., 1996). Moreover, CXCL-4 is a high affinity heparin-binding tetramer (Ruoslahti & Yamaguchi, 1991). Due to these characteristics it affects the coagulation via neutralizing the anticoagulant factor heparin during injury (Eitzman et al., 1994). Moreover, in an *in vitro* study it activated PMNs by binding chondroitin sulfate on the cellular membrane (Petersen et al., 1998). On the other hand, CXCL-4 is an inhibitor of angiogenesis by inhibiting the proliferation of endothelial cells (Maione et al., 1990; Bikfalvi, 2004). An *in vitro* study in bone showed that CXCL-4 can inhibit collagenase and ensue the significant inhibition of osteoclastic bone resorption (Horton et al., 1980). In addition, as a component of platelet-rich plasma (PRP), which is widely used in bone tissue engineering, CXCL-4 potentially contributes to enhancing the bone regeneration together with other mediators (Plachokova et al., 2007).

Apart from those chemokines and cytokines, many complement components were also detected within 48 h after the injury. These components conducted the inflammatory and immune response. Apart from their effects on the immune and inflammatory response, for instance C5 and C3 were potentially associated with bone tissue regeneration with respect to chemotaxis for osteoprogenitors and the formation of osteoblasts and osteoclasts (Sato et al., 1993; Ignatius et al., 2011; Schoengraf et al., 2013). Among the identified complete components, CRP is a major acute phase protein that can regulate the complement system (Schultz & Arnold, 1990). It is synthesized by hepatocytes. Normally it is only present in a trace amount in human serum under physiological conditions, but following a fracture it is acutely increased and peaks at day 2 in the patients' blood (Yoon et al., 1993; Neumaier et al., 2006; Gottlieb et al., 2011). Therefore, in this study it likely derived from the bleeding blood vessels. In clinical applications, it was used to monitor the progress of fracture treatment as a marker of inflammation, especially acute infection (Kallio et al., 1990; Uzel et al., 2010). In an *in vivo* study on bone tissue engineering it also served as the marker of immune response (Niemeyer et al., 2010). Besides of local complement activation it can also interact with PMNs and leukocytes (Schultz & Arnold, 1990). Therefore, it is an important protein during bone healing, but the specfic role of circulating or local CRP in bone defect healing need to be further eludicated.

Among the proteins which were specifically present in the bone defect according to the HPLC-MS/MS analysis, some possess the properties of growth factors. Chitinase-3-like

protein 1 is a biomarker of inflammation (Rathcke et al., 2006) and was found in bone defects at 17 h and 24 h after surgery. The biological function of this protein is unclear, but so far it was found to be associated with wound healing and tissue remodeling (Gottlieb et al., 2011). It can modulate type I collagen fibril formation, proliferation and differentiation of cells and angiogenesis by enhancing the migration of endothelial cells (Nishikawa & Millis, 2003; Stoffel et al., 2007; Gottlieb et al., 2011). Although it played a central role in chondrogenesis, according to data from clinical studies, the circulating Chitinase-3-like protein 1 increased within 24 h and then declined at 3 days after tibia fracture (Stoffel et al., 2007; Gottlieb et al., 2011). Hence, the potential source of Chitinase-3-like protein 1 might be the blood during bleeding. Moreover, the circulating level depended on the fracture type and the amount of the osseous injury (Gottlieb et al., 2011). Nevertheless in accordance with the qualitative results in this study, more information about this protein at the site of injury during the early stage of bone healing is needed.

Although IGF-1 was not detected in the hematoma by microdialysis or on microdialysis probes within 48 h after creating the bone defect, a 15 kDa IGF-1 isoform A preproprotein, was found in the bone defect at 48 h after surgery. It was cleaved to IGF-1 (Chen et al., 2001). Although IGF-1 mainly functions at the soft callus stage, during the very early inflammatory stage macrophages and periosteum cells might produce the preproprotein (Bourque et al., 1993; Okazaki et al., 2003). In an *in vivo* mandibular osteotomy model, the mRNA expression of IGF-1 decreased at day 3 after surgery (Steinbrech et al., 1999). However, Li et al. have demonstrated that IGF-1 signaling pathways were upregulated according to genetic analysis within 24 h after a rat femoral fracture (Li et al., 2007b). Therefore, the presence of IGF-1 isoform A preproprotein in bone defects indicates that the synthesis of IGF-1 corresponds with early defect healing.

Finally, RoBo-1 is a bone specific protein, which was identified both in bone and soft tissue defects. It was firstly reported in rats as a novel cDNA in 1998 and was found to be abundant specifically in the growth plate during endocartilagineous bone healing (Noel et al., 1998). Hence, this protein may be derived from the injured matrix. In an *in vivo* study it was found that during rat tibia regeneration the RoBo-1 gene expression responded to PTH treatment (Horesovsky et al., 2003). Moreover, it also responded to an estrogen treatment in bone tissue (Noel et al., 1998). However, considering the limited information that s available so far about this protein, the relationship between the protein and early bone healing needs to be further eludicated.

6.5 The humoral inflammatory response

A systemic response to bone and soft tissue injury is induced by specific proteins, and it

is accompanied by a local response to recruit angiogenic cells and MSCs (Marsell & Einhorn, 2009). For some proteins, it is assumed that the circulating levels are related to the fracture healing process (Zimmermann et al., 2005). The present study revealed the temporal pattern of circulating concentrations of IL-6, IL-1β, TNF-α, TGF-β1, VEGF, PDGF-BB and BMP-2 in rats with bone or soft tissue defect. The observations were made up to 24 h after the injury. Among those cytokines, only TGF-β1, VEGF and PDGF were consistently detected in the blood plasma. IL-6 was detected in individual samples.

Circulating TGF-β1 was suggested to be a biomarker of delayed/nonunion fracture (Zimmermann et al., 2005). The increasing plasma concentration of TGF-β1 lasted for about 8 h with a sharp increase at 2 h, followed by a decrease at 24 h in bone defects. This trend was not reproduced locally with microdialysis that showed a constant production of TGF-β1 for 24 h at the site of injury. Compared with the bone defect, the plasma concentration of TGF-β1 decreased in the soft tissue defect without any increase before 21 h. The acute increase might be ascribed to the uptake of TGF-β1 from the local site of injury into the blood stream which usually takes hours to days (Giannoudis et al., 2008). Moreover, the systemic TGF-β1 did not correspond to the local release.

Within 8 h of bone defect creation, the concentration of circulating PDGF-BB showed an inconsistent trend with an immediate increase after the injury. This may be attributed to a constant release from platelets and the plasma levels of PDGF-BB seems not to be affected by the injury within 8 h. Furthermore, the concentrations of VEGF in the circulation were below the detection limit of ELISA before and after surgery. A 24 week observation in patients with fractures revealed increasing levels of circulating TGF-β1 accompanied by increased concentrations of the circulating PDGF, VEGF and M-CSF which indicated the systemic response to fracture (Sarahrudi et al., 2011a; Sarahrudi et al., 2011b). However, no such correlation was seen in 8 h after bone defect or soft tissue defect in rats. Moreover, elevation of circulating PDGF and VEGF concentrations has been observed within 24 h and 1 week after the trauma (Street et al., 2001; Sarahrudi et al., 2009). Street et al. found that together with the local response to bone injury, the systemic response of PDGF and VEGF culminated following fracture revascularization (Street et al. 2001). Within 8 h after the injury, no angiogenesis was noticeable, which corresponds to the fact tha the plasma levels of PDGF-BB and VEGF were not affected by the injury.

Other than in previous animal or clinical studies which found the circulating concentrations of IL-6, TNF-α and IL-1β to be increased during the initial stages of fracture healing (Kobbe et al., 2008; Lee et al., 2009a; Sears et al., 2010), this study revealed that IL-6 concentration in the blood plasma was only measurable in individual samples and that TNF-α as well as IL-1β were not detectable in blood plasma neither before nor after surgery with ELISA. This result implied that although the inflammatory cytokines played a role locally,

the systemic inflammatory cytokine response in rat may not be significant immediately after a local bone or soft tissue defect.

The concentrations of circulating BMP-2 were below the detection limit in all blood plasma samples in this study. BMP-2 was reported to be detectable in the circulation of healthy human volunteers and healthy rats (Park et al., 2008; Choi et al., 2012; Günary et al., 2013). In Zimmermann's study, the circulating BMP-2 was not detected for 72 weeks after bone fracture in patients (Zimmermann et al., 2005). However, no information is available about the plasma BMP-2 in rats with either a fracture or bone defect. This study suggests for first time that BMP-2 does not respond systemically in rats during the early phase after bone injury in detectable concentrations.

6.6 Cellular response

In this study, at 9-12 h after bone defect creation, PMNs and mononuclear cells were found to be scattered in the bone defect hematoma and their amount peaked at 24 h. Meanwhile the monocytes were seen since 24 h after bone defect and the macrophages appeared at 45 h (Fig. 27). The PMN infiltration was in agreement with a previous *in vivo* study which demonstrated that the infiltration of inflammatory cells scattered throughout the site of bone injury during the early stages of fracture healing (Andrew et al., 1994). Moreover, in this study several cytokines including IL-6, CXCL-1, CXCL-2, CXCL-3, CXCL-4, CXCL-5, CXCL-7 and TGF-β1 were identified to be associated with the chemotaxis of inflammatory cells into the hematoma. In a sheep fracture model, the PMNs in the fracture hematoma increased over 1–4 h and then decreased due to the short life span. Subsequently, the percentage of lymphocytes was elevated. The same study revealed that the number of monocytes was increased within 4 h (Schmidt-Bleek et al., 2009). The discrepancy to this study might be due to the different analysis methods and the different experimental models. Moreover, many *in vivo* studies have demonstrated that after a fracture few monocytes are transformed into macrophages within 24 h and macrophages become predominant after 48 h (Bourque et al., 1993; Andrew et al., 1994; Kon et al., 2001).

An abundant fibrin network was seen in the fracture hematoma beginning 24 h after bone defect creation in the present study. At 45 h after surgery, the fibrin network formation increased and became looser. This primitive fibrin network helps to recruit more cells including bone progenitors thus being beneficial for the bone healing progress. In a study on rats a cranial bone defect was flled with connective tissue, endothelial cells and clots within one day after the injury (Itagaki et al., 2008). However, in this study, endothelial cells were not identified in the hematoma by H&E staining within 45 h after surgery. This result was in agreement with Bourque et al. who identified the endothelial cells beyond day 5 after tibial

fractures in mice (Bourque et al., 1993). The different bone types, animals and bone defect models may be responsible for the different results.

7 Conclusions

In the present study microdialysis could be established to monitor the local early response to bone and soft tissue injury in rats with a critical-size bone defect. Among the different conditions for microdialysis, adding the colloids BSA or Dextran-70 to the crystalloid perfusates slightly enhanced the fluid recovery. The crystalloid perfusates did not significantly affect the recovery of cytokines and growth factors. Nevertheless, 1% BSA had a slightly better performance with respect to enhancing cytokine and growth factor recovery. The flow rates did not significantly affect the protein recovery *in vitro* or *in vivo*, but at a flow rate of 2.0 µL/min the total amount of protein was higher and larger sample volumes were obtained which was beneficial for multiple analysis.

During 24 h after surgery, among 7 cytokines and growth factors involved in early wound healing, only IL-6 and TGF-β1 were detectable consistently in bone or soft tissue defects with microdialysis. The concentration of IL-6 peaked during 12–15 h in microdialysates from bone defects whereas the concentration of TGF-β1 remained relatively constant for 24 h. However, the concentrations of TNF-α, IL-1β, VEGF, PDGF-BB and BMP-2 were below the detection limits of the ELISA. Furthermore, several chemokines like CXCL-1, CXCL-5 and CXCL-7 were released in bone defects within 6 h after surgery, and CXCL-2, CXCL-3, CXCL-4, RoBo-1, IGF-1 isoform A preproprotein and Chitinase-3-like protein 1 were identified on the probe membrane implanted in bone and soft tissue defects. Taking all detected proteins from bone detect hematoma into account, it was revealed that during 48 h after bone defect the pathways of “nicotinic acetylcholine receptor signaling”, “blood coagulation”, “integrin signaling”, “inflammation mediated by chemokine and cytokine signaling” were overrepresented bone and soft tissue defects. In addition, the “FGF signaling” pathway was specifically overrepresented in bone defects and s therefore thought to have a particular role in bone healing.

When looking at the systemic reaction to bone and soft tissue injury, only PDGF-BB and TGF-β1 were constantly detected in the blood plasma within 24 h. This finding suggests that during the response to bone defects in rats different mediators are expressed systemically and locally.

In the histological analysis, polymorphonuclear leucocytes and mononuclear cells infiltrated into the bone defect hematoma immediately after surgery and peaked at 24 h.

The experiments used in this study may serve as a baseline for further investigations of the acute response to osseous and soft tissue trauma with microdialysis. The detected proteins like CXCL-1, CXCL-2, CXCL-3, CXCL-4, CXCL-5, CXCL-7, RoBo-1, Chitinase-3-like protein 1 or IGF-I should be monitored further to enhance our understanding of the complex process of bone defect healing and to develop novel strategies for bone regeneration.

8 References

Åberg UWN, Saarinen N, Abrahamsson A, Nurmi T, Engblom S, Dabrosin C (2011). Tamoxifen and flaxseed alter angiogenesis regulators in normal human breast tissue in vivo. PLoS One 6: e25720.

Aksamit RR, Falk W, Leonard EJ (1981). Chemotaxis by mouse macrophage cell lines. J. Immunol. 126: 2194–9.

Andrew J, Andrew S, Freemont A, Marsh D (1994). Inflammatory cells in normal human fracture healing. Acta Orthop. Scand. 65: 462–6.

Ao X, Rotundo R, Loegering D, Stenken J (2005). In vivo microdialysis sampling of cytokines produced in mice given bacterial lipopolysaccharide. J. Microbiol. Methods 62: 327–36.

Ao X, Sellati T, Stenken J (2004). Enhanced microdialysis relative recovery of inflammatory cytokines using antibody-coated microspheres analyzed by flow cytometry. Anal. Chem. 76: 3777–84.

Ao X, Stenken JA (2006). Microdialysis sampling of cytokines. Methods 38: 331–41.

Ao X, Wang X, Lennartz M, Loegering D, Stenken J (2006). Multiplexed cytokine detection in microliter microdialysis samples obtained from activated cultured macrophages. J. Pharm. Biomed. Anal. 40: 915–21.

Assoian R, Komoriya A, Meyers C, Miller D, Sporn M (1983). Transforming growth factor-beta in human platelets. Identification of a major storage site, purification, and characterization. J. Biol. Chem. 258: 7155–60.

Averbeck M, Beilharz S, Bauer M, Gebhardt C, Hartmann A, Hochleitner K, Kauer F, Voith U, Simon J, Termeer C (2006). In situ profiling and quantification of cytokines released during ultraviolet B-induced inflammation by combining dermal microdialysis and protein microarrays. Exp. Dermatol. 15: 447–54.

Bais M, Wigner N, Young M, Toholka R, Graves D, Morgan E, Gerstenfeld LC, Einhorn T (2009). BMP2 is essential for post natal osteogenesis but not for recruitment of osteogenic stem cells. Bone 45: 254–66.

Barnes GL, Kostenuik PJ, Gerstenfeld LC, Einhorn TA (1999). Growth factor regulation of fracture repair. J. Bone Miner. Res. 14: 1805–15.

Baum CL, Arpey CJ (2005). Normal cutaneous wound healing: clinical correlation with cellular and molecular events. Dermatol. Surg. 31: 674–86; discussion 686.

Bautista C, Mohan S, Baylink D (1990). Insulin-like growth factors I and II are present in the skeletal tissues of ten vertebrates. Metabolism 39: 96–100.

Beamer B, Hettrich C, Lane J (2010). Vascular endothelial growth factor: an essential component of angiogenesis and fracture healing. HSS J. 6: 85–94.

Benveniste H, Hansen AJ, Ottosen NS (1989). Determination of brain interstitial concentrations by microdialysis. J. Neurochem. 52: 1741–50.

Berton G, Lowell CA (1999). Integrin signalling in neutrophils and macrophages. Cell. Signal. 11: 621–35.

Bevilacqua MP, Stengelin S, Gimbrone MA, Seed B (1989). Endothelial leukocyte adhesion molecule 1: an inducible receptor for neutrophils related to complement regulatory proteins and lectins. Science 243: 1160–5.

Bikfalvi A (2004). Platelet factor 4: an inhibitor of angiogenesis. Semin. Thromb. Hemost. 30: 379–85.

Bøgehøj M, Emmeluth C, Overgaard S (2007). Blood flow and microdialysis in the human femoral head. Acta Orthop. 78: 56–62.

Bolander ME (1992). Regulation of fracture repair by growth factors. Proc. Soc. Exp. Biol. Med. 200: 165–70.

Bostrom M (1998). Expression of bone morphogenetic proteins in fracture healing. Clin. Orthop. Relat. Res. 355 Suppl: S116–23.

Bostrom M, Lane J, Berberian W, Missri A, Tomin E, Weiland A, Doty S, Glaser D, Rosen V (1995). Immunolocalization and expression of bone morphogenetic proteins 2 and 4 in fracture healing. J. Orthop. Res. 13: 357–67.

Bourque W, Gross M, Hall B (1993). Expression of four growth factors during fracture repair. Int. J. Dev. Biol. 37: 573–9.

Brighton C, Hunt R (1991). Early histological and ultrastructural changes in medullary fracture callus. J. Bone Joint Surg. Am. 73: 832–47.

Broughton G, Janis JE, Attinger CE (2006). The basic science of wound healing. Plast. Reconstr. Surg. 117: 12S–34S.

Brown SA, Mayberry AJ, Mathy JA, Phillips TM, Klitzman B, Levin LS (2000). The effect of muscle flap transposition to the fracture site on TNFalpha levels during fracture healing. Plast. Reconstr. Surg. 105: 991–8.

Bungay P, Morrison P, Dedrick R (1990). Steady-state theory for quantitative microdialysis of solutes and water in vivo and in vitro. Life Sci. 46: 105–19.

Calori GM, Albisetti W, Agus A, Iori S, Tagliabue L (2007). Risk factors contributing to fracture non-unions. Injury 38 Suppl 2: S11–8.

Caplan AI (1991). Mesenchymal stem cells. J. Orthop. Res. 9: 641–50.

Caplan AI, Correa D (2011). PDGF in bone formation and regeneration: new insights into a novel mechanism involving MSCs. J. Orthop. Res. 29: 1795–803.

Carter D, Deibel M, Dunn C, Tomich C, Laborde A, Slightom J, Berger A, Bienkowski M, Sun F, McEwan R (1990). Purification, cloning, expression and biological characterization of an interleukin-1 receptor antagonist protein. Nature 344: 633–8.

Chandrasekar B, Melby P, Sarau H, Raveendran M, Perla R, Marelli-Berg F, Dulin N, Singh I (2003). Chemokine-cytokine cross-talk. The ELR+ CXC chemokine LIX (CXCL5) amplifies a proinflammatory cytokine response via a phosphatidylinositol 3-kinase-NF-kappa B pathway. J. Biol. Chem. 278: 4675–86.

Chen MH-C, Lin G-H, Gong H-Y, Weng C-F, Chang C-Y, Wu J-L (2001). The characterization of prepro-Insulin-like growth factor-1 Ea-2 expression and Insulin-like growth factor-1 genes (devoid 81 bp) in the zebrafish (Danio rerio). Gene 268: 67–75.

Chiba S, Okada K, Lee K, Segre G, Neer R (2001). Molecular analysis of defect healing in rat diaphyseal bone. J. Vet. Med. Sci. 63: 603–8.

Cho T, Gerstenfeld LC, Einhorn T (2002). Differential temporal expression of members of the transforming growth factor beta superfamily during murine fracture healing. J. Bone Miner. Res. 17: 513–20.

Choi Y, Kim S, Park K, Oh S, Seo J, Shin S, Kim J, Kim Y (2012). The serum bone morphogenetic protein-2 level in non-small-cell lung cancer patients. Med. Oncol. 29: 582–8.

Choong M, Yong Y, Tan A, Luo B, Lodish H (2004). LIX: a chemokine with a role in hematopoietic stem cells maintenance. Cytokine 25: 239–45.

Chu AJ (2010). Blood coagulation as an intrinsic pathway for proinflammation: a mini review. Inflamm. Allergy Drug Targets 9: 32–44.

Cicco NA, Lindemann A, Content J, Vandenbussche P, Lübbert M, Gauss J, Mertelsmann R, Herrmann F (1990). Inducible production of interleukin-6 by human polymorphonuclear neutrophils: role of granulocyte-macrophage colony-stimulating factor and tumor necrosis factor-alpha. Blood 75: 2049–52.

Clauss M, Gerlach M, Gerlach H, Brett J, Wang F, Familletti PC, Pan YC, Olander J V, Connolly DT, Stern D (1990). Vascular permeability factor: a tumor-derived polypeptide that induces endothelial cell and monocyte procoagulant activity, and promotes monocyte migration. J. Exp. Med. 172: 1535–45.

Clough G (2005). Microdialysis of large molecules. AAPS J. 7: E686–92.

Dabrosin C, Chen J, Wang L, Thompson L (2002). Flaxseed inhibits metastasis and decreases extracellular vascular endothelial growth factor in human breast cancer xenografts. Cancer Lett. 185: 31–7.

Dahlin AP, Wetterhall M, Caldwell KD, Larsson A, Bergquist J, Hillered L, Hjort K (2010). Methodological aspects on microdialysis protein sampling and quantification in biological fluids: an in vitro study on human ventricular CSF. Anal. Chem. 82: 4376–85.

Dailey L, Ambrosetti D, Mansukhani A, Basilico C (2005). Mechanisms underlying differential responses to FGF signaling. Cytokine Growth Factor Rev. 16: 233–47.

Deschaseaux F, Sensébé L, Heymann D (2009). Mechanisms of bone repair and regeneration. Trends Mol. Med. 15: 417–29.

Deuel T, Senior R, Chang D, Griffin G, Heinrikson R, Kaiser E (1981). Platelet factor 4 is chemotactic for neutrophils and monocytes. Proc. Natl. Acad. Sci. U. S. A. 78: 4584–7.

Deuel T, Senior R, Huang J, Griffin G (1982). Chemotaxis of monocytes and neutrophils to platelet-derived growth factor. J. Clin. Invest. 69: 1046–9.

Dimitriou R, Tsiridis E, Giannoudis P (2005). Current concepts of molecular aspects of bone healing. Injury 36: 1392–404.

Dinarello CA (1984). Interleukin-1 and the pathogenesis of the acute-phase response. N. Engl. J. Med. 311: 1413–8.

Docheva D, Popov C, Mutschler W, Schieker M (2007). Human mesenchymal stem cells in contact with their environment: surface characteristics and the integrin system. J. Cell. Mol. Med. 11: 21–38.

Drosse I, Volkmer E, Seitz S, Seitz H, Penzkofer R, Zahn K, Matis U, Mutschler W, Augat P, Schieker M (2008). Validation of a femoral critical size defect model for orthotopic evaluation of bone healing: a biomechanical, veterinary and trauma surgical perspective. Tissue Eng. Part C. Methods 14: 79–88.

Duo J, Stenken J (2011). In vitro and in vivo affinity microdialysis sampling of cytokines using heparin-immobilized microspheres. Anal. Bioanal. Chem. 399: 783–93.

Ehrnthaller C, Ignatius A, Gebhard F, Huber-Lang M (2011). New insights of an old defense system: structure, function, and clinical relevance of the complement system. Mol. Med. 17: 317–29.

Einhorn TA (1998). The cell and molecular biology of fracture healing. Clin. Orthop. Relat. Res. 355 Suppl: S7–21.

Eitzman DT, Chi L, Saggin L, Schwartz RS, Lucchesi BR, Fay WP (1994). Heparin neutralization by platelet-rich thrombi. Role of platelet factor 4. Circulation 89: 1523–9.

Farnebo S, Lars-Erik K, Ingrid S, Sjögren F, Folke S (2009). Continuous assessment of concentrations of cytokines in experimental injuries of the extremity. Int. J. Clin. Exp. Med. 2: 354–62.

Fiedler J, Röderer G, Günther K-P, Brenner RE (2002). BMP-2, BMP-4, and PDGF-bb stimulate chemotactic migration of primary human mesenchymal progenitor cells. J. Cell. Biochem. 87: 305–12.

Folkersma H, Brevé JJP, Tilders FJH, Cherian L, Robertson CS, Vandertop WP (2008). Cerebral microdialysis of interleukin (IL)-1beta and IL-6: extraction efficiency and production in the acute phase after severe traumatic brain injury in rats. Acta Neurochir. 150: 1277–84.

Frost HM (1989). The biology of fracture healing. An overview for clinicians. Part I. Clin. Orthop. Relat. Res. 248: 283–93.

Garvin S, Dabrosin C (2008). In vivo measurement of tumor estradiol and vascular endothelial growth factor in breast cancer patients. BMC Cancer 8: 73.

Gasteiger E, Hoogland C, Gattiker A, Duvaud S, Wilkins M, Appel R, Bairoch A (2005). Protein Identification and Analysis Tools on the ExPASy Server.In: John M. Walker (Ed) The Proteomics Protocols Handbook. Humana Press, New Jersey, P.571–607.

Gerstenfeld LC, Alkhiary YM, Krall EA, Nicholls FH, Stapleton SN, Fitch JL, Bauer M, Kayal R, Graves DT, Jepsen KJ, Einhorn TA (2006). Three-dimensional reconstruction of fracture callus morphogenesis. J. Histochem. Cytochem. 54: 1215–28.

Gerstenfeld LC, Cho T, Kon T, Aizawa T, Cruceta J, Graves B, Einhorn T (2001). Impaired intramembranous bone formation during bone repair in the absence of tumor necrosis factor-alpha signaling. Cells Tissues Organs 169: 285–94.

Gerstenfeld LC, Cho T, Kon T, Aizawa T, Tsay A, Fitch J, Barnes G, Graves D, Einhorn T (2003). Impaired fracture healing in the absence of TNF-alpha signaling: the role of TNF-alpha in endochondral cartilage resorption. J. Bone Miner. Res. 18: 1584–92.

Giannoudis P, Pountos I, Morley J, Perry S, Tarkin H, Pape H (2008). Growth factor release following femoral nailing. Bone 42: 751–7.

Giri J, Wells J, Dower S, McCall C, Guzman R, Slack J, Bird T, Shanebeck K, Grabstein K, Sims J (1994). Elevated levels of shed type II IL-1 receptor in sepsis. Potential role for type II receptor in regulation of IL-1 responses. J. Immunol. 153: 5802–9.

Gottlieb H, Klausen TW, Boegsted M (2011). A clinical study of circulating cellular and humoral biomarkers involved in bone regeneration following traumatic lesions. J. Stem Cell Res. Ther. 3: 1–10.

Grosskreutz C, Anand-Apte B, Dupláa C, Quinn TP, Terman B, Zetter B, D'Amore P (1999). Vascular endothelial growth factor-induced migration of vascular smooth muscle cells in vitro. Microvasc. Res. 58: 128–36.

Gruber R, Karreth F, Frommlet F, Fischer MB, Watzek G (2003). Platelets are mitogenic for periosteum-derived cells. J. Orthop. Res. 21: 941–8.

Günay M, Amanvermez R, Keleş G (2013). Ankaferd Blood Stopper: Does it have a role in fracture healing? Turkish J. Med. Sci. 43: 733–8.

Hamrin K, Rosdahl H, Ungerstedt U, Henriksson J (2002). Microdialysis in human skeletal muscle: effects of adding a colloid to the perfusate. J. Appl. Physiol. 92: 385–93.

Han R, Buch S, Freeman B, Post M, Tanswell A (1992). Platelet-derived growth factor and growth-related genes in rat lung. II. Effect of exposure to 85% O2. Am. J. Physiol. 262: L140–6.

Hauser C, Joshi P, Zhou X, Kregor P, Hardy KJ, Devidas M, Scott P, Hughes J (1996). Production of interleukin-10 in human fracture soft-tissue hematomas. Shock 6: 3–6.

Hauser C, Zhou X, Joshi P, Cuchens M, Kregor P, Devidas M, Kennedy R, Poole G, Hughes J (1997). The immune microenvironment of human fracture/soft-tissue hematomas and its relationship to systemic immunity. J. Trauma 42: 895–903; discussion 903–4.

Hauser CJ, Desai N, Fekete Z, Livingston DH, Deitch EA (1999). Priming of neutrophil $[Ca^{2+}]i$ signaling and oxidative burst by human fracture fluids. J. Trauma 47: 854–8.

Hazuda D, Strickler J, Simon P, Young P (1991). Structure-function mapping of interleukin 1 precursors. Cleavage leads to a conformational change in the mature protein. J. Biol. Chem. 266: 7081–6.

Helmy A, Carpenter K, Menon D, Pickard J, Hutchinson P (2011). The cytokine response to human traumatic brain injury: temporal profiles and evidence for cerebral parenchymal production. J Cereb Blood Flow Metab. 31: 658–70.

Helmy A, Carpenter K, Skepper J, Kirkpatrick P, Pickard J, Hutchinson P (2009). Microdialysis of cytokines: methodological considerations, scanning electron microscopy, and determination of relative recovery. J. Neurotrauma 26: 549–61.

Hietbrink F, Koenderman L, Rijkers G, Leenen L (2006). Trauma: the role of the innate immune system. World J. Emerg. Surg. 1: 15.

Hill C, Flyvbjerg A, Grønbaek H, Petrik J, Hill D, Thomas C, Sheppard M, Logan A (2000). The renal expression of transforming growth factor-beta isoforms and their receptors in acute and chronic experimental diabetes in rats. Endocrinology 141: 1196–208.

Hillman J, Aneman O, Anderson C, Sjögren F, Säberg C, Mellergård P (2005). A microdialysis technique for routine measurement of macromolecules in the injured human brain. Neurosurgery 56: 1264–8; discussion 1268–70.

Horesovsky GJ, Staton NL, Raha D (2003). Method of identifying osteoregenerative agents using differential gene expression. US Patent 2003/0091973 A1.

Horowitz MC, Lorenzo JA (2008). Local regulators of bone: IL-1, TNF, lymphotoxin, interferon-γ, the LIF/IL-6 family, and additional cytokines.In: Bilezikian JP, Raisz LG, Martin TJ (Eds) Principles of Bone Biology.3rd ed Academic Press, San Diego, P.1209–34.

Horton J, Harper J, Harper E (1980). Platelet factor 4 regulates osteoclastic bone resorption in vitro. Biochim. Biophys. Acta 630: 459–62.

Hübner G, Brauchle M, Smola H, Madlener M, Fässler R, Werner S (1996). Differential regulation of pro-inflammatory cytokines during wound healing in normal and glucocorticoid-treated mice. Cytokine 8: 548–56.

Huinink KD, Lambooij B, Jansen-van Zelm K, Cremers TIFH, van Oeveren W, Bakker PL, Venema K, Westerink BHC, Korf J (2010). Microfiltration sampling in rats and in cows:

toward a portable device for continuous glucocorticoid hormone sampling. Analyst 135: 390–6.

Von Hundelshausen P, Petersen F, Brandt E (2007). Platelet-derived chemokines in vascular biology. Thromb. Haemost. 97: 704–13.

Ignatius A, Ehrnthaller C, Brenner RE, Kreja L, Schoengraf P, Lisson P, Blakytny R, Recknagel S, Claes L, Gebhard F, Lambris JD, Huber-Lang M (2011). The anaphylatoxin receptor C5aR is present during fracture healing in rats and mediates osteoblast migration in vitro. J. Trauma 71: 952–60.

Itagaki T, Honma T, Takahashi I, Echigo S, Sasano Y (2008). Quantitative analysis and localization of mRNA transcripts of type I collagen, osteocalcin, MMP 2, MMP 8, and MMP 13 during bone healing in a rat calvarial experimental defect model. Anat. Rec. 291: 1038–46.

Ito H, Akiyama H, Shigeno C, Iyama K, Matsuoka H, Nakamura T (1999). Hedgehog signaling molecules in bone marrow cells at the initial stage of fracture repair. Biochem. Biophys. Res. Commun. 262: 443–51.

Jackson R, Nurcombe V, Cool S (2006). Coordinated fibroblast growth factor and heparan sulfate regulation of osteogenesis. Gene 379: 79–91.

Janssens K, ten Dijke P, Janssens S, Van Hul W (2005). Transforming growth factor-beta1 to the bone. Endocr. Rev. 26: 743–74.

Joyce M, Jingushi S, Bolander M (1990). Transforming growth factor-beta in the regulation of fracture repair. Orthop. Clin. North Am. 21: 199–209.

Kaipel M, Schützenberger S, Schultz A, Ferguson J, Slezak P, Morton T, Van Griensven M, Redl H (2012). BMP-2 but not VEGF or PDGF in fibrin matrix supports bone healing in a delayed-union rat model. J. Orthop. Res. 10: 1563–9.

Kallio P, Michelsson JE, Lalla M, Holm T (1990). C-reactive protein in tibial fractures. Natural response to the injury and operative treatment. J. Bone Joint Surg. Br. 72: 615–7.

Kalwitz G, Endres M, Neumann K, Skriner K, Ringe J, Sezer O, Sittinger M, Häupl T, Kaps C (2009). Gene expression profile of adult human bone marrow-derived mesenchymal stem cells stimulated by the chemokine CXCL7. Int. J. Biochem. Cell Biol. 41: 649–58.

Kalwitz G, Neumann K, Ringe J, Sezer O, Sittinger M, Endres M, Kaps C (2011). Chondrogenic differentiation of human mesenchymal stem cells in micro-masses is impaired by high doses of the chemokine CXCL7. J. Tissue Eng. Regen. Med. 5: 50–9.

Kaplanski G, Marin V, Montero-Julian F, Mantovani A, Farnarier C (2003). IL-6: a regulator of the transition from neutrophil to monocyte recruitment during inflammation. Trends Immunol. 24: 25–9.

Kirker-Head C, Karageorgiou V, Hofmann S, Fajardo R, Betz O, Merkle HP, Hilbe M, von Rechenberg B, McCool J, Abrahamsen L, Nazarian A, Cory E, Curtis M, Kaplan D,

Meinel L (2007). BMP-silk composite matrices heal critically sized femoral defects. Bone 41: 247–55.

Kitaori T, Ito H, Schwarz EM, Tsutsumi R, Yoshitomi H, Oishi S, Nakano M, Fujii N, Nagasawa T, Nakamura T (2009). Stromal cell-derived factor 1/CXCR4 signaling is critical for the recruitment of mesenchymal stem cells to the fracture site during skeletal repair in a mouse model. Arthritis Rheum. 60: 813–23.

Kjeldsen L, Bjerrum OW, Askaa J, Borregaard N (1992). Subcellular localization and release of human neutrophil gelatinase, confirming the existence of separate gelatinase-containing granules. Biochem. J. 287: 603–10.

Kjellström S, Appels N, Ohlrogge M, Laurell T, Marko-Varga G (1999). Microdialysis—a membrane based sampling technique for quantitative determination of proteins. Chromatographia 50: 539–46.

Klapperich C, Bertozzi C (2004). Global gene expression of cells attached to a tissue engineering scaffold. Biomaterials 25: 5631–41.

Klein E, Holland F, Eberle K (1979). Comparison of experimental and calculated permeability and rejection coefficients for hemodialysis membranes. J. Memb. Sci. 5: 173–88.

Kobbe P, Vodovotz Y, Kaczorowski D, Mollen K, Billiar T, Pape H (2008). Patterns of cytokine release and evolution of remote organ dysfunction after bilateral femur fracture. Shock 30: 43–7.

Kolar P, Schmidt-Bleek K, Schell H, Gaber T, Toben D, Schmidmaier G, Perka C, Buttgereit F, Duda GN (2010). The early fracture hematoma and its potential role in fracture healing. Tissue Eng. Part B. Rev. 16: 427–34.

Kon T, Cho TJ, Aizawa T, Yamazaki M, Nooh N, Graves D, Gerstenfeld LC, Einhorn TA (2001). Expression of osteoprotegerin, receptor activator of NF-kappaB ligand (osteoprotegerin ligand) and related proinflammatory cytokines during fracture healing. J. Bone Miner. Res. 16: 1004–14.

Kurkinen M, Vaheri A, Roberts PJ, Stenman S (1980). Sequential appearance of fibronectin and collagen in experimental granulation tissue. Lab. Invest. 43: 47–51.

Lacey D, Simmons P, Graves S, Hamilton J (2009). Proinflammatory cytokines inhibit osteogenic differentiation from stem cells: implications for bone repair during inflammation. Osteoarthritis Cartilage 17: 735–42.

Lange J, Sapozhnikova A, Lu C, Hu D, Li X, Miclau T, Marcucio R (2010). Action of IL-1beta during fracture healing. J. Orthop. Res. 28: 778–84.

Lasagni L, Grepin R, Mazzinghi B, Lazzeri E, Meini C, Sagrinati C, Liotta F, Frosali F, Ronconi E, Alain-Courtois N, Ballerini L, Netti G, Maggi E, Annunziato F, Serio M, Romagnani S, Bikfalvi A, Romagnani P (2007). PF-4/CXCL4 and CXCL4L1 exhibit

distinct subcellular localization and a differentially regulated mechanism of secretion. Blood 109: 4127–34.

Lee J, Ryu C, Moon N, Kim S, Park S, Suh K (2009a). Changes in serum levels of receptor activator of nuclear factor-kappaB ligand, osteoprotegerin, IL-6 and TNF-alpha in patients with a concomitant head injury and fracture. Arch. Orthop. Trauma Surg. 129: 711–8.

Lee S, Bowrin K, Hamad AR, Chakravarti S (2009b). Extracellular matrix lumican deposited on the surface of neutrophils promotes migration by binding to beta2 integrin. J. Biol. Chem. 284: 23662–9.

Leeuwenberg JF, von Asmuth EJ, Jeunhomme TM, Buurman WA (1990). IFN-gamma regulates the expression of the adhesion molecule ELAM-1 and IL-6 production by human endothelial cells in vitro. J. Immunol. 145: 2110–4.

Li J, Chen J, Kirsner R (2007a). Pathophysiology of acute wound healing. Clin. Dermatol. 25: 9–18.

Li X, Wang H, Touma E, Rousseau E, Quigg R, Ryaby J (2007b). Genetic network and pathway analysis of differentially expressed proteins during critical cellular events in fracture repair. J. Cell. Biochem. 100: 527–43.

Li YP, Stashenko P (1992). Proinflammatory cytokines tumor necrosis factor-alpha and IL-6, but not IL-1, down-regulate the osteocalcin gene promoter. J. Immunol. 148: 788–94.

Li Z, Cui Z (2008). Application of microdialysis in tissue engineering monitoring. Prog. Nat. Sci. 18: 503–11.

Lombardo F, Komatsu D, Hadjiargyrou M (2004). Molecular cloning and characterization of Mustang, a novel nuclear protein expressed during skeletal development and regeneration. FASEB J. 18: 52–61.

Louzada-Júnior P, Dias J, Santos W, Lachat J, Bradford H, Coutinho-Netto J (1992). Glutamate release in experimental ischaemia of the retina: an approach using microdialysis. J. Neurochem. 59: 358–63.

Maione T, Gray G, Petro J, Hunt A, Donner A, Bauer S, Carson H, Sharpe R (1990). Inhibition of angiogenesis by recombinant human platelet factor-4 and related peptides. Science 247: 77–9.

Marsell R, Einhorn TA (2011). The biology of fracture healing. Injury 42: 551–5.

Marsell R, Einhorn TA (2009). The role of endogenous bone morphogenetic proteins in normal skeletal repair. Injury 40 Suppl 3: S4–7.

Marzona L, Pavolini B (2009). Play and players in bone fracture healing match. Clin. Cases Miner. Bone Metab. 6: 159–62.

Maurer MH, Berger C, Wolf M, Fütterer CD, Feldmann RE, Schwab S, Kuschinsky W (2003). The proteome of human brain microdialysate. Proteome Sci. 1: 7.

Menacherry S, Hubert W, Justice J (1992). In vivo calibration of microdialysis probes for exogenous compounds. Anal. Chem. 64: 577–83.

Mountziaris PM, Mikos AG (2008). Modulation of the inflammatory response for enhanced bone tissue regeneration. Tissue Eng. Part B. Rev. 14: 179–86.

Nakagawa H, Komorita N, Shibata F, Ikesue A, Konishi K, Fujioka M, Kato H (1994). Identification of cytokine-induced neutrophil chemoattractants (CINC), rat GRO/CINC-2 alpha and CINC-2 beta, produced by granulation tissue in culture: purification, complete amino acid sequences and characterization. Biochem. J. 301: 545–50.

Nakagawa M, Kaneda T, Arakawa T, Morita S, Sato T, Yomada T, Hanada K, Kumegawa M, Hakeda Y (2000). Vascular endothelial growth factor (VEGF) directly enhances osteoclastic bone resorption and survival of mature osteoclasts. FEBS Lett. 473: 161–4.

Nakamura T, Hara Y, Tagawa M, Tamura M, Yuge T, Fukuda H, Nigi H (1998). Recombinant human basic fibroblast growth factor accelerates fracture healing by enhancing callus remodeling in experimental dog tibial fracture. J. Bone Miner. Res. 13: 942–9.

Nakao K, Aoyama M, Fukuoka H, Fujita M, Miyazawa K, Asai K, Goto S (2009). IGF2 modulates the microenvironment for osteoclastogenesis. Biochem. Biophys. Res. Commun. 378: 462–6.

Nandi P, Lunte SM (2009). Recent trends in microdialysis sampling integrated with conventional and microanalytical systems for monitoring biological events: a review. Anal. Chim. Acta 651: 1–14.

Naski MC, Ornitz DM (1998). FGF Signaling in Skeletal Development. Fetal Pediatr. Pathol. 18: 355–79.

Nedeau A, Bauer R, Gallagher K, Chen H, Liu Z, Velazquez O (2008). A CXCL5- and bFGF-dependent effect of PDGF-B-activated fibroblasts in promoting trafficking and differentiation of bone marrow-derived mesenchymal stem cells. Exp. Cell Res. 314: 2176–86.

Neumaier M, Metak G, Scherer M (2006). C-reactive protein as a parameter of surgical trauma: CRP response after different types of surgery in 349 hip fractures. Acta Orthop. 77: 788–90.

Niemeyer P, Szalay K, Luginbühl R, Südkamp NP, Kasten P (2010). Transplantation of human mesenchymal stem cells in a non-autogenous setting for bone regeneration in a rabbit critical-size defect model. Acta Biomater. 6: 900–8.

Nishikawa KC, Millis AJT (2003). gp38k (CHI3L1) is a novel adhesion and migration factor for vascular cells. Exp. Cell Res. 287: 79–87.

Noel LS, Champion BR, Holley CL, Simmons CJ, Morris DC, Payne JA, Lean JM, Chambers TJ, Zaman G, Lanyon LE, Suva LJ, Miller LR (1998). RoBo-1, a novel member of the

urokinase plasminogen activator receptor/CD59/Ly-6/snake toxin family selectively expressed in rat bone and growth plate cartilage. J. Biol. Chem. 273: 3878–83.

Nurden AT (2011). Platelets, inflammation and tissue regeneration. Thromb. Haemost. 105 Suppl: S13–33.

Nwomeh BC, Liang HX, Diegelmann RF, Cohen IK, Yager DR (1998). Dynamics of the matrix metalloproteinases MMP-1 and MMP-8 in acute open human dermal wounds. Wound Repair Regen. 6: 127–34.

Oe K, Miwa M, Sakai Y, Lee S, Kuroda R, Kurosaka M (2007). An in vitro study demonstrating that haematomas found at the site of human fractures contain progenitor cells with multilineage capacity. J. Bone Joint Surg. Br. 89: 133–8.

Okazaki K, Jingushi S, Ikenoue T, Urabe K, Sakai H, Iwamoto Y (2003). Expression of parathyroid hormone-related peptide and insulin-like growth factor I during rat fracture healing. J. Orthop. Res. 21: 511–20.

Opal SM (2000). Phylogenetic and functional relationships between coagulation and the innate immune response. Crit. Care Med. 28: S77–80.

Osborn L, Hession C, Tizard R, Vassallo C, Luhowskyj S, Chi-Rosso G, Lobb R (1989). Direct expression cloning of vascular cell adhesion molecule 1, a cytokine-induced endothelial protein that binds to lymphocytes. Cell 59: 1203–11.

Ozaki A, Tsunoda M, Kinoshita S, Saura R (2000). Role of fracture hematoma and periosteum during fracture healing in rats: interaction of fracture hematoma and the periosteum in the initial step of the healing process. J. Orthop. Sci. 5: 64–70.

Park Y, Kim JW, Kim D, Kim E, Park S, Park JY, Choi W, Song J, Seo H, Oh S, Kim B, Park JJ, Kim Y, Kim JS (2008). The Bone Morphogenesis Protein-2 (BMP-2) is associated with progression to metastatic disease in gastric cancer. Cancer Res. Treat. 40: 127–32.

Peerschke EIB, Yin W, Grigg SE, Ghebrehiwet B (2006). Blood platelets activate the classical pathway of human complement. J. Thromb. Haemost. 4: 2035–42.

Petersen F, Bock L, Flad H, Brandt E (1998). A chondroitin sulfate proteoglycan on human neutrophils specifically binds platelet factor 4 and is involved in cell activation. J. Immunol. 161: 4347–55.

Petersen F, Ludwig A, Flad HD, Brandt E (1996). TNF-alpha renders human neutrophils responsive to platelet factor 4. Comparison of PF-4 and IL-8 reveals different activity profiles of the two chemokines. J. Immunol. 156: 1954–62.

Phillips AM (2005). Overview of the fracture healing cascade. Injury 36 Suppl 3: S5–7.

Plachokova AS, van den Dolder J, Stoelinga PJ, Jansen JA (2007). Early effect of platelet-rich plasma on bone healing in combination with an osteoconductive material in rat cranial defects. Clin. Oral Implants Res. 18: 244–51.

Plock N, Kloft C (2005). Microdialysis--theoretical background and recent implementation in applied life-sciences. Eur. J. Pharm. Sci. 25: 1–24.

Pohlman TH, Stanness KA, Beatty PG, Ochs HD, Harlan JM (1986). An endothelial cell surface factor(s) induced in vitro by lipopolysaccharide, interleukin 1, and tumor necrosis factor-alpha increases neutrophil adherence by a CDw18-dependent mechanism. J. Immunol. 136: 4548–53.

Rathcke C, Johansen J, Vestergaard H (2006). YKL-40, a biomarker of inflammation, is elevated in patients with type 2 diabetes and is related to insulin resistance. Inflamm. Res. 55: 53–9.

Ray P, Estrada-Hernandez T, Sasaki H, Zhu L, Maulik N (2000). Early effects of hypoxia/reoxygenation on VEGF, ang-1, ang-2 and their receptors in the rat myocardium: implications for myocardial angiogenesis. Mol. Cell. Biochem. 213: 145–53.

Recknagel S, Bindl R, Kurz J, Wehner T, Schoengraf P, Ehrnthaller C, Qu H, Gebhard F, Huber-Lang M, Lambris JD, Claes L, Ignatius A (2012). C5aR-antagonist significantly reduces the deleterious effect of a blunt chest trauma on fracture healing. J. Orthop. Res. 30: 581–6.

Rihl M, Barthel C, Klos A, Schmidt RE, Tak PP, Zeidler H, Kuipers JG (2009). Identification of candidate genes for susceptibility to reactive arthritis. Rheumatol. Int. 29: 1519–22.

Romagnani P, Lasagni L, Annunziato F, Serio M, Romagnani S (2004). CXC chemokines: the regulatory link between inflammation and angiogenesis. Trends Immunol. 25: 201–9.

Romano M, Sironi M, Toniatti C, Polentarutti N, Fruscella P, Ghezzi P, Faggioni R, Luini W, van Hinsbergh V, Sozzani S, Bussolino F, Poli V, Ciliberto G, Mantovani A (1997). Role of IL-6 and its soluble receptor in induction of chemokines and leukocyte recruitment. Immunity 6: 315–25.

Rosdahl H, Hamrin K, Ungerstedt U, Henriksson J (1998). Metabolite levels in human skeletal muscle and adipose tissue studied with microdialysis at low perfusion flow. Am. J. Physiol. 274: E936–45.

Rosdahl H, Ungerstedt U, Henriksson J (1997). Microdialysis in human skeletal muscle and adipose tissue at low flow rates is possible if dextran-70 is added to prevent loss of perfusion fluid. Acta Physiol. Scand. 159: 261–2.

Rosen C, Niu T (2008). Insulin-like Growth Factors and the IGF Binding Proteins: Implications for Bone Biology.In: Bilezikian J, Raisz L, Martin T (Eds) Principles of Bone Biology.3rd ed Academic Press, San Diego, P.1069–94.

Rosenbloom A, Sipe D, Weedn V (2005). Microdialysis of proteins: performance of the CMA/20 probe. J. Neurosci. Methods 148: 147–53.

Ruoslahti E, Yamaguchi Y (1991). Proteoglycans as modulators of growth factor activities. Cell 64: 867–9.

Sarahrudi K, Thomas A, Braunsteiner T, Wolf H, Vécsei V, Aharinejad S (2009). VEGF serum concentrations in patients with long bone fractures: a comparison between impaired and normal fracture healing. J. Orthop. Res. 27: 1293–7.

Sarahrudi K, Thomas A, Heinz T, Krumböck A, Vécsei V, Aharinejad S (2011a). Growth factor release in extra- and intramedullary osteosynthesis following tibial fracture. Injury 42: 772–7.

Sarahrudi K, Thomas A, Mousavi M, Kaiser G, Köttstorfer J, Kecht M, Hajdu S, Aharinejad S (2011b). Elevated transforming growth factor-beta 1 (TGF-β1) levels in human fracture healing. Injury 42: 833–7.

Sato T, Abe E, Jin C, Hong M, Katagiri T, Kinoshita T, Amizuka N, Ozawa H, Suda T (1993). The biological roles of the third component of complement in osteoclast formation. Endocrinology 133: 397–404.

Schaffner A, Rhyn P, Schoedon G, Schaer D (2005). Regulated expression of platelet factor 4 in human monocytes--role of PARs as a quantitatively important monocyte activation pathway. J. Leukoc. Biol. 78: 202–9.

Schenk BI, Petersen F, Flad H, Brandt E (2002). Platelet-derived chemokines CXC chemokine ligand (CXCL)7, connective tissue-activating peptide III, and CXCL4 differentially affect and cross-regulate neutrophil adhesion and transendothelial migration. J. Immunol. 169: 2602–10.

Schiemann F, Grimm T, Hoch J, Gross R, Lindner B, Petersen F, Bulfone-Paus S, Brandt E (2006). Mast cells and neutrophils proteolytically activate chemokine precursor CTAP-III and are subject to counterregulation by PF-4 through inhibition of chymase and cathepsin G. Blood 107: 2234–42.

Schmid GJ, Kobayashi C, Sandell LJ, Ornitz DM (2009). Fibroblast growth factor expression during skeletal fracture healing in mice. Dev. Dyn. 238: 766–74.

Schmidt-Bleek K, Schell H, Kolar P, Pfaff M, Perka C, Buttgereit F, Duda G, Lienau J (2009). Cellular composition of the initial fracture hematoma compared to a muscle hematoma: a study in sheep. J. Orthop. Res. 27: 1147–51.

Schmidt-Bleek K, Schell H, Schulz N, Hoff P, Perka C, Buttgereit F, Volk H, Lienau J, Duda G (2012). Inflammatory phase of bone healing initiates the regenerative healing cascade. Cell Tissue Res. 347: 567–73.

Schoengraf P, Lambris JD, Recknagel S, Kreja L, Liedert A, Brenner RE, Huber-Lang M, Ignatius A (2013). Does complement play a role in bone development and regeneration? Immunobiology 218: 1–9.

Schraufstatter IU, Discipio RG, Zhao M, Khaldoyanidi SK (2009). C3a and C5a are chemotactic factors for human mesenchymal stem cells, which cause prolonged ERK1/2 phosphorylation. J. Immunol. 182: 3827–36.

Schultz DR, Arnold PI (1990). Properties of four acute phase proteins: C-reactive protein, serum amyloid A protein, alpha 1-acid glycoprotein, and fibrinogen. Semin. Arthritis Rheum. 20: 129–47.

Schutte R, Oshodi S, Reichert W (2004). In vitro characterization of microdialysis sampling of macromolecules. Anal. Chem. 76: 6058–63.

Sears B, Volkmer D, Yong S, Himes R, Lauing K, Morgan M, Stover M, Callaci J (2010). Correlation of measurable serum markers of inflammation with lung levels following bilateral femur fracture in a rat model. J. Inflamm. Res. 2010: 105–14.

Shapiro F (2008). Bone development and its relation to fracture repair. The role of mesenchymal osteoblasts and surface osteoblasts. Eur. Cell. Mater. 15: 53–76.

Shi G, Morrell CN (2011). Platelets as initiators and mediators of inflammation at the vessel wall. Thromb. Res. 127: 387–90.

Shibata F, Kato H, Konishi K, Okumora A, Ochiai H, Nakajima K, Al-Mokdad M, Nakagawa H (1996). Differential changes in the concentrations of cytokine-induced neutrophil chemoattractant (CINC)-1 and CINC-2 in exudate during rat lipopolysaccharide-induced inflammation. Cytokine 8: 222–6.

Shibata F, Konishi K, Nakagawa H (2002). Chemokine receptor CXCR2 activates distinct pathways for chemotaxis and calcium mobilization. Biol. Pharm. Bull. 25: 1217–9.

Shubayev V, Myers R (2001). Axonal transport of TNF-alpha in painful neuropathy: distribution of ligand tracer and TNF receptors. J. Neuroimmunol. 114: 48–56.

Simpson DM, Ross R (1972). The neutrophilic leukocyte in wound repair a study with antineutrophil serum. J. Clin. Invest. 51: 2009–23.

Steinbrech DS, Mehrara BJ, Rowe NM, Dudziak ME, Luchs JS, Saadeh PB, Gittes GK, Longaker MT (2000). Gene expression of TGF-beta, TGF-beta receptor, and extracellular matrix proteins during membranous bone healing in rats. Plast. Reconstr. Surg. 105: 2028–38.

Steinbrech DS, Mehrara BJ, Rowe NM, Dudziak ME, Saadeh PB, Gittes GK, Longaker MT (1999). Gene expression of insulin-like growth factors I and II in rat membranous osteotomy healing. Ann. Plast. Surg. 42: 481–7.

Stenken JA (2006). Microdialysis Sampling.In: Webster JG (Ed) Encyclopedia of Medical Devices and Instrumentation.2nd ed Wiley, New York, P.1–67.

Stoffel K, Engler H, Kuster M, Riesen W (2007). Changes in biochemical markers after lower limb fractures. Clin. Chem. 53: 131–4.

Stolle L, Arpi M, Holmberg-Jørgensen P, Riegels-Nielsen P, Keller J (2004). Application of microdialysis to cancellous bone tissue for measurement of gentamicin levels. J. Antimicrob. Chemother. 54: 263–5.

Street J, Wang J, Wu Q, Wakai A, McGuinness A, Redmond H (2001). The angiogenic response to skeletal injury is preserved in the elderly. J. Orthop. Res. 19: 1057–66.

Street J, Winter D, Wang J, Wakai A, McGuinness A, Redmond H (2000). Is human fracture hematoma inherently angiogenic? Clin. Orthop. Relat. Res. 278: 224–37.

Sutherland D, Bostrom M (2005). Grafts and Bone Graft Substitutes.In: Lieberman J, Friedlaender G (Eds) Bone Regeneration and Repair: Biology and Clinical Applications. Humana Press, New Jersey, P.133–56.

Takeda S, Sato N, Ikimura K, Nishino H, Rakugi H, Morishita R (2011). Novel microdialysis method to assess neuropeptides and large molecules in free-moving mouse. Neuroscience 186: 110–9.

Tanaka H, Liang C (1995). Effect of platelet-derived growth factor on DNA synthesis and gene expression in bone marrow stromal cells derived from adult and old rats. J. Cell. Physiol. 164: 367–75.

Terebuh PD, Otterness IG, Strieter RM, Lincoln PM, Danforth JM, Kunkel SL, Chensue SW (1992). Biologic and immunohistochemical analysis of interleukin-6 expression in vivo. Constitutive and induced expression in murine polymorphonuclear and mononuclear phagocytes. Am. J. Pathol. 140: 649–57.

Thorsen K, Kristoffersson A, Lerner U, Lorentzon R (1996). In situ microdialysis in bone tissue. Stimulation of prostaglandin E2 release by weight-bearing mechanical loading. J. Clin. Invest. 98: 2446–9.

Timlin M, Toomey D, Condron C, Power C, Street J, Murray P, Bouchier-Hayes D (2005). Fracture hematoma is a potent proinflammatory mediator of neutrophil function. J. Trauma 58: 1223–9.

Torto N, Bång J, Richardson S, Nilsson G, Gorton L, Laurell T, Marko-Varga G (1998). Optimal membrane choice for microdialysis sampling of oligosaccharides. J. Chromatogr. A 806: 265–78.

Trickler W, Miller D (2003). Use of osmotic agents in microdialysis studies to improve the recovery of macromolecules. J. Pharm. Sci. 92: 1419–27.

Tsuji K, Bandyopadhyay A, Harfe B, Cox K, Kakar S, Gerstenfeld LC, Einhorn T, Tabin C, Rosen V (2006). BMP2 activity, although dispensable for bone formation, is required for the initiation of fracture healing. Nat. Genet. 38: 1424–9.

Uzel A-P, Lemonne F, Casoli V (2010). Tibial segmental bone defect reconstruction by Ilizarov type bone transport in an induced membrane. Orthop. Traumatol. Surg. Res. 96: 194–8.

Waelgaard L, Pharo A, Tønnessen T, Mollnes T (2006). Microdialysis for monitoring inflammation: efficient recovery of cytokines and anaphylotoxins provided optimal catheter pore size and fluid velocity conditions. Scand. J. Immunol. 64: 345–52.

Wahl SM, Hunt DA, Wakefield LM, McCartney-Francis N, Wahl LM, Roberts AB, Sporn MB (1987). Transforming growth factor type beta induces monocyte chemotaxis and growth factor production. Proc. Natl. Acad. Sci. U.S.A. 84: 5788–92.

Wallace A, Cooney T, Englund R, Lubahn J (2011). Effects of interleukin-6 ablation on fracture healing in mice. J. Orthop. Res. 29: 1437–42.

Wang X, Lennartz M, Loegering D, Stenken J (2007). Interleukin-6 collection through long-term implanted microdialysis sampling probes in rat subcutaneous space. Anal. Chem. 79: 1816–24.

Wang Y, Stenken J (2009). Affinity-based microdialysis sampling using heparin for in vitro collection of human cytokines. Anal. Chim. Acta 651: 105–11.

Werner S, Grose R (2003). Regulation of wound healing by growth factors and cytokines. Physiol. Rev. 83: 835–70.

Winn SR (2005). The Manipulation of Mesenchymal Stem Cells for Bone Repair.In: Lester LB (Ed) Stem Cells in Endocrinology. Humana Press, New Jersey, P.183–206.

Witte MB, Barbul A (1997). General principles of wound healing. Surg. Clin. North Am. 77: 509–28.

Yang L, Qiu C, Ludlow A, Ferguson M, Brunner G (1999). Active transforming growth factor-beta in wound repair: determination using a new assay. Am. J. Pathol. 154: 105–11.

Yoon SI, Lim SS, Rha JD, Kim YH, Kang JS, Baek GH, Yang KH (1993). The C-reactive protein (CRP) in patients with long bone fractures and after arthroplasty. Int. Orthop. 17: 198–201.

Zhao Y, Liang X, Lunte CE (1995). Comparison of recovery and delivery in vitro for calibration of microdialysis probes. Anal. Chim. Acta 316: 403–10.

Zimmermann G, Henle P, Küsswetter M, Moghaddam A, Wentzensen A, Richter W, Weiss S (2005). TGF-beta1 as a marker of delayed fracture healing. Bone 36: 779–85.

9 Appendix

9.1 Figure index

9.2 Table index

III. Eidesstattliche Erklärung

Technische Universität Dresden
Medizinische Fakultät Carl Gustav Carus
Promotionsordnung vom 24. Juli 2011

Erklärungen zur Eröffnung des Promotionsverfahrens

1. Hiermit versichere ich, dass ich die vorliegende Arbeit ohne unzulässige Hilfe Dritter und ohne Benutzung anderer als der angegebenen Hilfsmittel angefertigt habe; die aus fremden Quellen direkt oder indirekt übernommenen Gedanken sind als solche kenntlich gemacht.

2. Bei der Auswahl und Auswertung des Materials sowie bei der Herstellung des Manuskripts habe ich Unterstützungsleistungen von folgenden Personen erhalten:

Prof. Dr. med. Stefan Rammelt
Dr. rer. nat. Yvonne Förster

3. Weitere Personen waren an der geistigen Herstellung der vorliegenden Arbeit nicht beteiligt. Insbesondere habe ich nicht die Hilfe eines kommerziellen Promotionsberaters in Anspruch genommen. Dritte haben von mir weder unmittelbar noch mittelbar geldwerte Leistungen für Arbeiten erhalten, die im Zusammenhang mit dem Inhalt der vorgelegten Dissertation stehen.

4. Die Arbeit wurde bisher weder im Inland noch im Ausland in gleicher oder ähnlicher Form einer anderen Prüfungsbehörde vorgelegt.

5. Die Inhalte dieser Dissertation wurden in folgender Form veröffentlicht:

Publizierte Abstracts:
Förster Y, Gao W, Betz V, Zwipp H, Kalkhof S, von Bergen M, Hempel U, Rammelt S. Microdialysis as a method to describe the molecular events in the early phase of bone healing. Biomaterialien 11: 177, 2010
Förster Y, Gao W, Rentsch C, Hofbauer L, Gelinsky M, Rammelt S. Microdialysis as a method to characterize the fracture hematoma. Biomaterialien 12: 171, 2011

Publikation:
Förster Y, Gao W, Demmrich A, Hempel U, Hofbauer LC, Rammelt S (2013). Monitoring of the first stages of bone healing with microdialysis. Acta Orthop 84: 76-81

6. Ich bestätige, dass es keine zurückliegenden erfolglosen Promotionsverfahren~~/ erfolglose Promotionsverfahren~~ gab*.
*unzutreffendes bitte streichen

7. Ich bestätige, dass ich die Promotionsordnung der Medizinischen Fakultät der Technischen Universität Dresden anerkenne.

Dresden, 20.12.2013

Unterschrift des Doktoranden

Hiermit bestätige ich die Einhaltung der folgenden aktuellen gesetzlichen Vorgaben im Rahmen meiner Dissertation

☐ das zustimmende Votum der Ethikkommission bei Klinischen Studien, epidemiologischen Untersuchungen mit Personenbezug oder Sachverhalten, die das Medizinproduktegesetz betreffen
Aktenzeichen der zuständigen Ethikkommission ……..…

■ die Einhaltung der Bestimmungen des Tierschutzgesetzes
Aktenzeichen der Genehmigungsbehörde zum Vorhaben/zur Mitwirkung

AZ: 24-9168.11-1/2010-22

☐ die Einhaltung des Gentechnikgesetzes

Projektnummer ……..……..……
….

die Einhaltung von Datenschutzbestimmungen der Medizinischen Fakultät und des Universitätsklinikums Carl Gustav Carus.

Dresden, 20.12.2013

Unterschrift des Doktoranden

IV. Selbständigkeitserklärung

Hiermit erkläre ich, dass mir die Promotionsordnung der Medizinischen Fakultät Carl Gustav Carus der Technischen Universität Dresden bekannt ist.

Hiermit versichere ich eidesstattlich, dass ich die vorliegende Arbeit selbstständig und ohne fremde Hilfe verfasst und keine anderen als die angegebenen Hilfsmittel benutzt habe. Die Dissertation wurde in Dresden unter der wissenschaftlichen Betreuung von Prof. Dr. med. Stefan Rammelt, UniversitätsCentrum für Orthopädie und Unfallchirurgie, Dresden, angefertigt.

Folgende Personen haben mich bei der Auswahl und Auswertung des Materials sowie bei der Herstellung des Manuskripts unterstützt:
Prof. Dr. med. Stefan Rammelt,
Dr. rer. nat. Yvonne Förster

Ich versichere, dass die Dissertation nicht bereits in derselben oder einer ähnlichen Fassung an einer anderen Fakultät oder einem anderen Fachbereich zur Erlangung eines akademischen Grades eingereicht worden ist. Im Vorfeld habe ich noch keinen anderen Promotionsversuch eingereicht.

Declaration of Authorship

I am aware of the PhD regulations of the Medical Faculty Carl Gustav Carus of the Technische Universität Dresden. I hereby declare under oath that the thesis submitted is my own unaided work. All direct or indirect sources used are acknowledged as references. The thesis was completed in Dresden under the scientific supervision of Prof. Dr. Stefan Rammelt, in the University Center of Orthopaedic and Trauma Surgery at the Medical Faculty of the TU Dresden.

The following persons have supported me in the selection and assessment of materials and in the production of the manuscript:
Prof. Dr. med. Stefan Rammelt,
Dr. rer. nat. Yvonne Förster

I certify that the dissertation was not previously submitted in an identical or similar version to another faculty or another section in order to obtain an academic degree. Furthermore, I have not submitted any other promotion attempt previously.

Dresden, 20.12.2013

Unterschrift des Doktoranden

V. Acknowledgements

I would like to thank Prof. Dr. Stefan Rammelt who gave me the opportunity to work in his department, provided the outline of my thesis, and supervised the manuscript preparation. It was my immense privilege to work with Dr. Yvonne Förster who supported the experimental design and conduction, and supervised the manuscript preparation. Her insight and extraordinary supervision has led this project towards its goal. I deeply appreciate of the great support she has provided to this project during my stay in Germany. Moreover, I appreciate with the encouragement and the guidance from Dr. Claudia Rentsch who helped me a lot in my living since I came to Germany. I also would like to acknowledge Ms. Suzanne Manthey who made tireless efforts on the preparation of the histological samples and on the technical support.

I would like to extend my thanks to Dr. Stefan Kalkhof from the Department of Proteomics in the Helmholtz Centre for Environmental Research in Lepzig for the effective cooperation and for the conduction of HPLC-MS/MS and analysis of primary data. Furthermore, I also acknowledge Stefanie Kliemt, Stephan Müller and the technician, Ms. Jacqueline Kobelt, from his group who provided a great assistance during my lab rotation.

I would like to express my sincere thanks to Dr. Ute Hempel and their group for their scientific help with the SDS-PAGE experiment and the scanning of the membranes of proteome profile array.

I particularly acknowledge the generous help from Dr. Kathrin Spekl and Dr. Roland Jung in animal laboratory during this animal experiment.

I sincerely thank the Transregio 67, supported by the DFG (Deutsche Forschungsgemeinschaft), which provided the favourable circumstances of getting to know so many outstanding scientists and students. Meanwhile it offered me a great opportunity to expand my multidisciplinary knowledge and to cooperate with so many brilliant people.

Finally, I will thank my friend Juliane Salbach who gave a plenty of advice for my work and shared a lot experiences of work and life.

Wenling Gao